1-1-2004

Dynamic analysis of particle adhesion and removal in the micro/nano scale

Satya Seetharaman
Iowa State University

Dynamic analysis of particle adhesion and removal in the micro/nano scale

by

Satya Seetharaman

A thesis submitted to the graduate faculty

in partial fulfillment of the requirements for the degree of

MASTER OF SCIENCE

Major: Mechanical Engineering

Program of Study Committee:

Abhijit Chandra, Co-major Professor

Sriram Sundararajan, Co-major Professor

Thomas Rudolphi

Iowa State University

Ames, Iowa

2004

Graduate College

Iowa State University

This is to certify that the master's thesis of

Satya Seetharaman

has met the thesis requirements of Iowa State University

Signatures have been redacted for privacy

TABLE OF CONTENTS

ABSTRACT v

ACKNOWLEDGEMENTS vii

CHAPTER 1. INTRODUCTION 1

Adhesion in MEMS 1

Types of adhesive forces 2

Electrostatic Forces 3

Capillary Forces 5

Van Der Waal Forces 9

Particle Removal – Existing Theories 13

Objectives of Research 16

Model Development 16

CHAPTER 2. REMOVAL BY LONGITUDINAL VIBRATIONS 19

Introduction 19

Assumptions 19

System Characterization 20

System Dynamics 22

Stability Analysis by Evaluating the Eigen Values 28

Stability Analysis by Lyapunov's Direct Method 35

Lyapunov's Stability Theorem for Non – Autonomous Systems 36

Simulation of the Linearized System Based on Stability Analysis 41

Parameters for Simulation 43

CHAPTER 3. LATERAL REMOVAL METHODS 54

Introduction 54

Lateral Force Model 54

Forces Involved in the Lateral Removal Model 60

Moment Balance at O 64

Removal by Opposing the Shear Force 66

Removal by Considering Stiffness of Fluid Layer 66

Determination of Stiffness of Fluid Layer 67

CHAPTER 4. REMOVAL BY COUPLED VIBRATIONS 69

Introduction 69

Formulation of the Dynamic System for Coupled Vibrations 70

Stability Criteria Based on Steady State Solutions of the Coupled Vibrations 72

Simulation of the Coupled System Based on the Stability Criterion 77

Equilibrium Points for Various Particle Sizes 80

Simulations for the Lateral System 81

Phenomenon of Beat Frequency 84

CHAPTER 5. DISCUSSION AND CONCLUSION 95

Introduction 95

Longitudinal Vibrations Model 95

Lateral Removal Model 99

Coupled Vibrations Model 101

Future Work 103

REFERENCES CITED 106

ABSTRACT

Adhesion of particles to surfaces is one of the major problems encountered in Micro Electro Mechanical Systems (MEMS). Typically, this problem affects gripping of micro/nano particles. The particle gets stuck to the surface and removal becomes a crucial issue. It is also encountered in Chemical Mechanical Polishing (CMP), wherein sub -micron particles adhere to the silicon wafers after polishing, causing circuit defects and other possible damages to the electronic networks. The major contributors to adhesion force are the Van Der Waal and capillary forces, formed due to polarization between molecules and fluid film condensation due to humidity. The aim of this thesis is to investigate the issue of particle adhesion and propose effective means of particle removal.

The first method proposed, utilizes longitudinal vibrations to separate the particle from the substrate. Vibrations of any form (thermal/mechanical) have been found to be an effective method of particle removal. The longitudinal model determines a stability criterion based on eigenvalue analysis and Lyapunov's stability theorems. Simulations to verify the stability conditions are carried out using Matlab. The dynamic system is formulated and simulations are carried out on the linearized system and also on the fully non – linear system. Results are compared and the effectiveness of this method is evaluated from the numerical results obtained. The phenomenon of negative damping, which causes an unstable limit cycle behavior, is encountered during the numerical simulations.

The second method, which is a more effective one, proposes the use of lateral removal moments to separate the particle from the surface. Different lateral removal

techniques are discussed and the criterion for separation is established. Separation is induced, once the lateral removal - moments overcome the adhesion resisting moment. It is found that friction plays an important role during separation. Contrary to existing beliefs that friction hinders motion, friction is actually found to aid particle separation, during the lateral removal - moment technique. Comparisons of the lateral model are made with the longitudinal removal technique and the conclusions prove the effectiveness of the lateral removal model, over the previous technique, in that, a lower removal force is required when particle separation is brought about, by the lateral - removal method.

The third method studies the effect of coupled vibrations. Coupled vibrations refer to the coupling enforced between lateral and longitudinal directions of motion, during the formulation of the dynamic system, through the relationship between the adhesion and friction forces. A characteristic matrix is postulated, which comes up with a stability criterion for the equilibrium points and lateral stiffness. Enforcing the stability criteria makes the system stable. The numerical simulations carried out, on solving the longitudinal system analytically and inserting the solution into the lateral system, prove that the stability conditions are true. During the simulation, the interesting phenomenon of beating frequency is observed and important conclusions are made, on exciting the dynamic system with a combination of the excitation and beating frequency. Separation is found to be enhanced by a combination of the beating and excitation frequency along with an increase in the amplitude of vibration.

ACKNOWLEDGEMENTS

I would first like to thank my advisors, Prof. Abhijit Chandra and Dr. Sriram Sundararajan for their unstinted encouragement and valuable guidance. I must certainly say that I have learnt the qualities of patience and discretion from them and gained confidence in my work, from the numerous interactions I have had in discussing my research problem, with them. Research means continuous improvement. I certainly understood what that meant, during the course of my thesis work at Iowa State University, over the past two years. I would like to express my heart felt gratitude to my committee member, Prof. Thomas Rudolphi for his invaluable advice and timely tips. It certainly was a pleasure, discussing my research work with him. I would also like to thank Dr. Li Cao, for her financial support during Fall and Spring 2003.

The help and technical expertise of Prof. Michael Smiley and Prof. Roger Alexander of the Mathematics Department at Iowa State University helped me tide over certain impossible situations in my research work. I am indebted to them for their valuable guidance on Perturbation techniques, Lindstedt–Poincare' Method and Lyapunov's Stability theorems. I would also like to express my sincere thanks to Dr. Abu Sebastian of the Electrical Engineering Department at Iowa State University, for his patience in going through my research work and finding out the critical issues in the initial stages of my model development.

I would like to thank my parents and sisters, who were the driving force behind me, all these twenty three years of my life. Without their love and encouragement, I would not be

what I am today. I am sure that if words were deeds, even then I would be indebted to them throughout life. I would also like to thank my friends and lab mates, for the various interesting technical arguments and discussions we have had over the past two years. Last, but not the least, I would like to thank my very special friend, whose virtual presence, made my stay at Iowa State University, a very memorable one. These have been two wonderful years, and without your presence, life would have been very bland.

CHAPTER 1

INTRODUCTION

1.1 ADHESION IN MICRO ELECTRO MECHANICAL SYSTEMS

One of the common problems encountered in micro electro mechanical systems (MEMS) is the adhesion of particles to the substrate. Often, it is required to grip a particle by means of a MEMS gripper and move it from one point to another, but then the particle might get stuck to the substrate due to adhesion forces in which case, separation becomes difficult if not impossible.

This poses a very challenging problem in the field of chemical mechanical polishing (CMP). Typically CMP involves the polishing of silicon wafers by means of a rotating polish pad, soaked with slurry. The slurry consists of abrasive particles in a medium of chemical reagents. Polishing is due to the combined action of the slurry and the abrasive particles. After CMP, some of the abrasive particles such as submicron silica or alumina adhere to the wafer surface. Hence, this can cause circuit defects during operation of the wafer in semiconductor devices. Considering the atomic force microscope (AFM), the tip jumps into contact with the surface, whose properties are being measured due to the adhesion forces. If the adhesion forces are large, then it might cause the tip to break off. This might cause substantial damage if the adhesion forces aren't reduced. Hence it is necessary, to first understand the physics of such forces and then determine a means to reduce the adhesion forces. There are a lot of existing models and the aim would be to come up with a unique and effective model based on the existing theories

Another area, where particle adhesion becomes a relevant issue is in the field of Bio-MEMS. During cell transfer the cell, which is fragile and can be modeled as a microstructure, can get stuck to the tweezers by means of the adhesion forces and, in such cases, separation becomes a critical issue. Also, during bio-medical device transfers, adhesion poses a critical problem. Thus, adhesion or stiction is a key problem affecting the reliability of most MEMS devices.

There is a need to differentiate between adhesion and surface forces and understand the behavior of the various forces causing adhesion. Surface forces are those forces present when two bodies are brought together. Adhesion forces are those, which work to hold two bodies in contact with each other. Surface forces are generally attractive in nature, but can be repulsive at times (such as electrical double layer forces). On the other hand, adhesion forces, as their definition implies, are always attractive and tend to hold two bodies together. If a process between two bodies is perfectly elastic, i.e., there is no energy dissipated during their interaction, the adhesive and surface forces are equal, in such a case. Generally, adhesion is greater than any initial attraction, which gives rise to adhesion hysteresis (Burnham and Kulik, 1997).

1.2 TYPES OF ADHESIVE FORCES

The various adhesion forces of importance are explained below. Critically important are the Van Der Waal (VDW), Electrostatic and Capillary forces. Analysis is done as to which of them are most relevant to the proposed particle removal model. Also, expressions for the most pertinent of them all are derived, as regards to the work being proposed.

1.2.1 ELECTROSTATIC FORCES

Electrostatic forces include those due to charges, image charges and dipoles. Electric fields polarize the molecules and atoms, so that there exist forces which act between the electric field and the polarized object. Electric fields can purposefully be applied between object and substrate, or may exist due to differences in the work function between them. Moreover, electric fields may surround the object and/or substrate due to variations in the work function over their surfaces (Burnham and Kulik, 1997).

Two types of electrostatic forces are important in the issue of particle adhesion. These forces may act to hold particles to surfaces. The first is due to bulk excess charges present on the surface and/or particle, which produces a classical Coulombic attraction known as an electrostatic image force. This electrostatic image force F(i) is given as:

$$F_i = \frac{q^2}{4\pi Eel^2}, \textbf{(1.2.1.1)}$$

where, e is the dielectric constant of the medium between the particle and the surface, E is the permittivity of the free space, q is the charge and l is the distance between the charge centers. The distance between the charge centers can be approximately taken to be equal to 2r, where r is the particle radius and q can be expressed as a function of the particle radius by the expression:

$$q = CU = 4\pi ErU, \textbf{(1.2.1.2)}$$

where C is the capacitance and U is the potential in volts.

The capacitance can be expressed as a function of the particle radius via an approximation of the *Euler* equation. The expression for the total image force then reduces as

a function of the particle diameter d, in approximation to the expression given below. The particle diameter is in microns and hence the force is obtained in milli dynes. This equation assumes a charge density of 10 electronic charges per square micron, what might be considered a typical large charge (Bowling, 1988):

$$F(i) = 3\times10^{-2} d^2 mdyn \text{ , } \textbf{(1.2.1.3)}$$

The more important electrostatic force for very small particles is the electrostatic contact potential induced double layer forces. They can be explained as follows. Two different materials in contact develop a contact potential caused by differences in the local energy states and work functions. Electrons are transferred from one solid to another, until equilibrium is reached and the current flow in both directions is equal. The resulting potential difference is called a contact potential difference U, which generally ranges from zero to about 0.5 volts. It sets up a so called double layer charge region. In the case of two metals in contact, only the surfaced layer carries contact charges. For a particle on a surface, the electrostatic double layer force, F(el), can be calculated as:

$$F(el) = \frac{nErU^2}{z} dynes \text{ , } \textbf{(1.2.1.4)}$$

this reduces in approximation to:

$$F(el) = 4dU^2 mdyn \text{ , } \textbf{(1.2.1.5)}$$

where d is in microns and U is in volts. For a maximum potential difference of 0.5 volts, F(el) is approximately equal to d mdyn.

Double layer electrostatic forces generally dominate the imaging forces for small particles. It is to be noted that all these equations have been derived, considering the interaction between a spherical particle and a flat surface (Bowling, 1988). Typically for

other interactions, there might be other forces which dominate the electrostatic forces or vice-versa.

1.2.2 CAPILLARY FORCES

Due to high humidity or to an adhered particle/surface system having been immersed and then withdrawn from a liquid, a liquid film will be formed due to the phenomenon of capillary condensation or capillary action between the particle and the surface. The resulting capillary force can make a large contribution to the total adhesion force. The capillary force is generally a function of the particle radius and the liquid surface tension between the particle and the surface (Bowling, 1988).

If a thin uniform layer of water or any other liquid covers the interface between the particle and the surface, then the following events occur. The particle approaches the surface first and due to the presence of the liquid layer, when the liquid on either surfaces touch, the system tries to minimize the fluid surface area. The liquid suddenly draws the particle towards the surface and hence adhesion takes place. Thus there is a capillary bridge formed between the particle and the surface and on separation, the bridge would thin out, until the waist of the capillary were of atomic dimensions. It is usually broken by mechanical or thermal vibrations. The overall magnitude of the capillary forces can be large enough to surpass the other adhesion forces and obscure their effects. The liquid films make significant contributions to any damping measurements performed in the interface (Burnham and Kulik, 1997).

Thus, mechanical and adhesive properties are very sensitive to change, in many materials, even if there remains a trace of such liquid bridges or vapor in the atmosphere. The

derivation of the expression for capillary forces involves the use of the *Kelvin equation* and *Laplace pressure distribution.* Liquids that wet or have small contact angle on surfaces will condense from vapor into cracks and pores as bulk liquids. The meniscus curvature or the equivalent curvature is defined based on the following figure. *Figure 1.2.2.1* gives the capillary bridge formed between a sphere and a flat surface. Thus in this case, the analogy is between the sphere and a particle stuck on a surface.

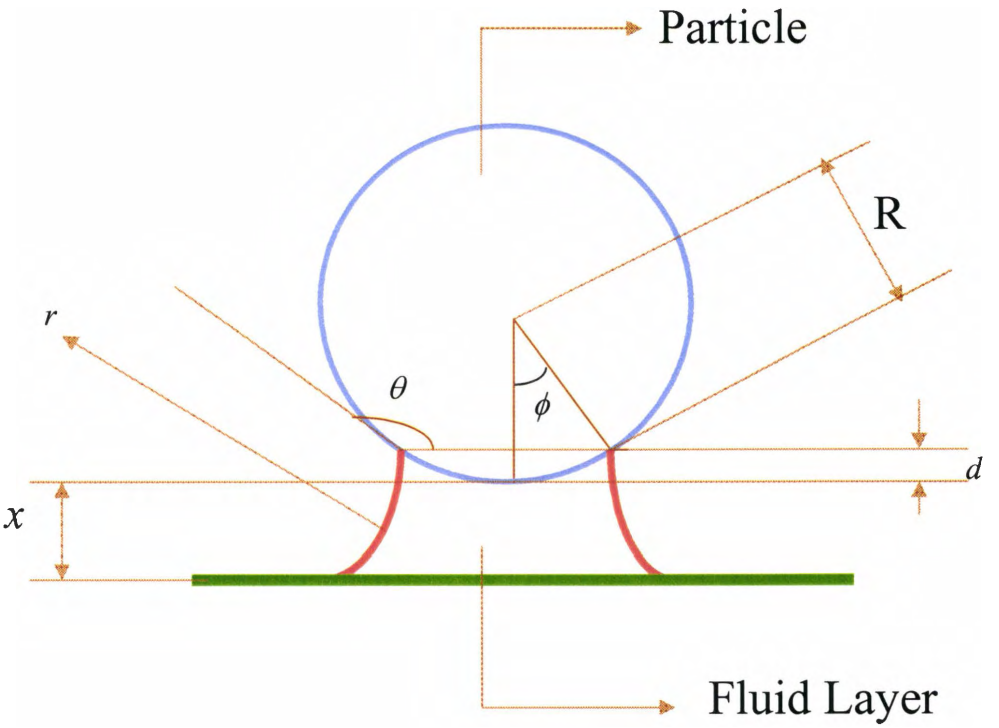

***Figure 1.2.2.1*: Schematic Representation of Particle on Substrate under the Action of Capillary forces**

Here θ is the contact angle, usually assumed to be zero degrees, R is the particle radius, x is the distance between the particle and the surface measured from the bottom end of the particle, r is the contact radius and d is the distance between the meniscus and the bottom of the particle. Hence the meniscus curvature is defined as follows:

$$\text{Meniscus Curvature} = \left(\frac{1}{r_1}+\frac{1}{r_2}\right)^{-1}, \textit{(1.2.2.1)}$$

At equilibrium, the meniscus curvature is related to the relative vapor pressure by *Kelvin's equation*:

$$\left(\frac{1}{r_1}+\frac{1}{r_2}\right)^{-1} = r_k = \frac{\gamma V}{RT\log(p/p_s)}, \textit{(1.2.2.2)}$$

where, $\gamma V / RT = 0.54nm$ for water at 20 C, V is the molar volume, p/p_s is the relative vapour pressure. For a spherical concave water meniscus: - $r_1 = r_2 = r$.

Now there is a need to find the effect of a liquid condensate on the adhesion force between a sphere and a surface as shown above. The derivation is to consider the *Laplace pressure* in the liquid:

$$P = \gamma_l\left(\frac{1}{r_1}+\frac{1}{r_2}\right) \approx \frac{\gamma_l}{r_1}, \textit{(1.2.2.3)}$$

This is generally true when r_2 is greater than r_1. The *Laplace pressure* acts on an area $\pi x^2 = 2\pi Rd$ between the two surfaces thus pulling them together with a force equal to:

$$F \approx \left(\gamma_l / r_1\right) 2\pi Rd, \textit{(1.2.2.4)}$$

For small $\phi, d \approx 2r_1\cos\theta$. So the above equation becomes

$$F \approx 4\pi\gamma_l R\cos\theta, \textit{(1.2.2.5)}$$

The additional force arising from surface tension around the circumference of the particle is always going to be small when compared to the Laplace pressure distribution, except when the contact angle is 90 degrees. An alternative way to derive this is to consider the change of the total surface free energy with separation x.

$$-W_{tot} \approx 2\pi R^2 \sin^2\phi\left(\gamma_{sl}-\gamma_{sv}\right)+C$$

$$-W_{tot} \approx 2\pi R^2\phi^2\left(\gamma_{sl}-\gamma_{sv}\right)+C \text{ (for small } \phi\text{)}, \textbf{(1.2.2.6)}$$

$$-W_{tot} \approx 2\pi R^2\phi^2\gamma_l\cos\theta+C$$

so that

$$F=-dW_{tot}/dx=4\pi R^2\,\phi\gamma_l\cos\theta\,d\phi/dx, \textbf{(1.2.2.7)}$$

Now if the liquid volume V remains constant, then

$$\begin{aligned} V &\approx \pi R^2\sin^2\phi(x+d)-(\pi R^3/3)(1-\cos\phi)^2(2+\cos\phi) \\ &\rightarrow\approx \pi R^2 x\phi^2+\pi R^3\phi^4/3, \text{ for small } \phi \end{aligned}, \textbf{(1.2.2.8)}$$

Thus, dV/dx = 0, which gives

$$\frac{d\phi}{dx}=-\frac{1}{\left(R\phi+2x/\phi\right)}, \textbf{(1.2.2.9)}$$

Thus the attractive force between the particle modeled as a sphere and the flat surface due to the presence of a capillary bridge is given as

$$F=\frac{4\pi\gamma_l R\cos\theta}{\left(1+x/d\right)}, \textbf{(1.2.2.10)}$$

The maximum value for this force occurs, when x = 0. Thus,

$$F_{\max}=F_{x=0}=4\pi R\gamma_l\cos\theta, \textbf{(1.2.2.11)}$$

Thus, it is found that, the capillary force not only depends on the radius of the particle and the liquid surface tension, but also depends on the distance between the particle and the surface (Israelachvili, 1985). This fact, in the form of the above equation, can be exploited when modeling the phenomenon of particle adhesion as a nonlinear dynamic system.

1.2.3 VAN DER WAAL (VDW) FORCES

Sometimes, even at absolute zero temperature, solids can contain local electric fields, which originate from polarizations of the constituent atoms and molecules. Above zero temperature, additional contributions are made by the thermal excitations. By quantum theory, the electrons of an electrically neutral solid does not occupy fixed states of a sharply defined minimum energy, which results in spontaneous electric and magnetic polarizations, varying quickly with time. VDW forces include forces between molecules possessing dipoles and quadrapoles caused by polarization of the atoms and molecules. This can include natural dipoles as well as induced dipoles. Hence VDW forces are often classified as either orientation, induced or dispersion type forces. The VDW forces also include non polar attractive forces. These non polar forces are referred to as the *London – VDW* dispersion forces as they were associated with optical dispersion, i.e. spontaneous polarizations (Bowling, 1988). The dominant contribution is by the dispersion or the *London forces*, due to the non-zero instantaneous dipole moments of all atoms and molecules. The second contribution to VDW forces is by the *Keesom Force*, which originates from the attraction produced by permanent dipoles. The interaction between the rotating permanent dipoles of all atoms and molecules and the polarizability of the atoms and molecules generates the third type of VDW force, called the *Debye Force*. This dispersion force is the most important, because all materials are polarizable. But the *Keesom* and *Debye forces* must have a permanent dipole to be present for them to be induced (Burnham and Kulik, 1997).

Essentially, there are two theories to predict the VDW forces. One of them is the *Microscopic Hamaker theory*, which starts from interactions between individual molecules or atoms and calculates the attraction between larger bodies as integration over all pairs of

atoms or molecules. This method uses the so called *Hamaker Constant*. The *Hamaker constant* (A) reflects the strength of the VDW interactions and depends on the type of material used for the particle and the surface. The shortcoming of this approach is that linear additivity doesn't hold, as there might be interactions between neighboring atoms, which might have been neglected when integrated over the entire pair of atoms or molecules. A more satisfactory theory was derived by *Lifshitz*, called the *Macroscopic Lifshitz theory*, which started directly from the bulk optical properties of the interacting bodies. In this method, the decisive material value is the *Lifshitz-VDW constant* h, which is defined as an integral function of the imaginary parts of the dielectric constants of the adhering materials. The *Lifshitz* and *Hamaker constants*, under certain conditions, are related as follows (Bowling, 1988):

$$h = 4\pi A / 3 \text{ , } \textbf{(1.2.3.1)}$$

It is now required to derive the expression for the VDW force, based on the interaction between a sphere and a flat surface. It is achieved by making use of the Lennard-Jones potential between two molecules (only the attractive part of the L-J potential). The entire potential, considering the attractive and repulsive parts is given as follows:

$$w(r) = \frac{c_1}{r^{12}} + \frac{c_2}{r^6} = 4\beta\left[\left(\frac{\sigma}{r}\right)^{12} + \left(\frac{\sigma}{r}\right)^{6}\right], \textbf{(1.2.3.2)}$$

This in turn reduces to the following form when the attractive part is considered. Here r is the distance between the molecules, σ is the molecular diameter, c_1 and c_2 are interaction constants and $-\beta$ is the minimum of the potential. Hence:

$$w(r) = -\frac{c}{r^6} = -4\beta\left[\frac{\sigma}{r}\right]^6 \textbf{(1.2.3.3)}$$

Now, consider the interaction between a sphere and a flat surface. Initially, the interaction between a single molecule placed at a particular distance z from the surface is evaluated. If the surface has γ_1 molecules per unit volume and the sphere has γ_2 molecules per unit volume, then the total number if molecules in an annular region in the surface, of thickness dy and width dx, at a distance y is given by $2\pi\ \gamma_2 y\ dx\ dy$. Then the interaction energy is given by:

$$w(z) = \int_{y=0}^{\infty}\int_{x=z}^{\infty} 2\pi\gamma_2 y\left(-\frac{c}{\left(x^2+y^2\right)^3}\right)dydx$$

$$w(z) = -2\pi\gamma_2 c\int_{x=z}^{\infty} dx\int_{y=0}^{\infty}\frac{ydy}{\left(x^2+y^2\right)^3} \qquad \textbf{, (1.2.3.4)}$$

$$w(z) = -2\pi\gamma_2 c\int_{x=z}^{\infty} -\frac{dx}{4x^4}$$

$$\Rightarrow w(z) = \frac{-2\pi\gamma_2 c}{12z^3}$$

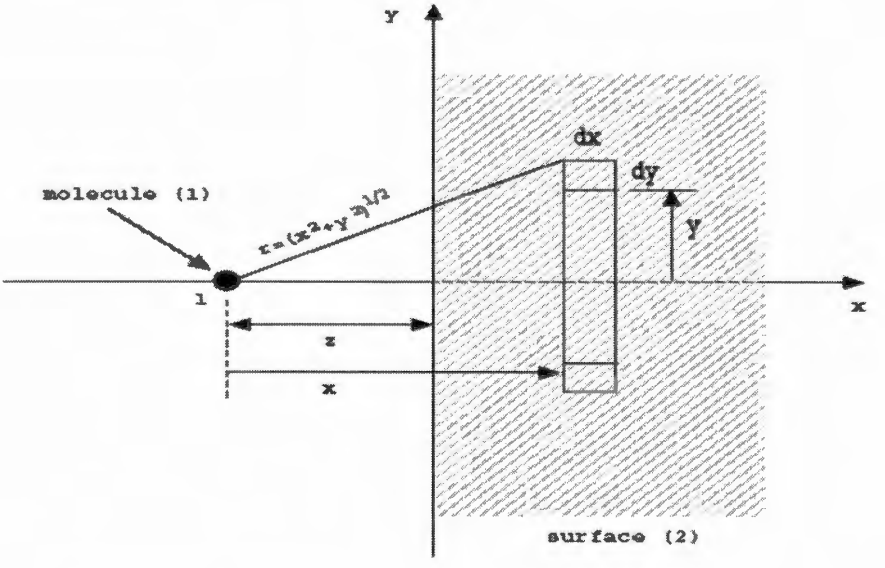

***Figure 1.2.3.1*: Molecule – Flat Surface Interaction**

Now, the sphere – surface interaction energy is computed. As shown in *Figure 1.2.3.2*, all the molecules which are at a distance of (x + d) from the surface (d = D_{ss}), lie in a circular region of area πy^2 and thickness dx. Hence, the number of molecules in this section is $\gamma_1 \pi y^2 dx = \gamma 1 \pi (2R - x) x\, dx$. Hence the interaction energy is given as,

$$W(d) = \int_{x=0}^{x=2R} \gamma_1 \pi (2R - x) x \left(-\frac{2\pi\gamma_2 c}{12(x+d)^3} \right) dx \quad , \textbf{(1.2.3.5)}$$

Typically, the particle radius, R is much greater than d (Hutter and Bechhoefer, 1993). By this assumption, $2Rx$ is much greater than x^2. Hence the equation for the main interaction potential between the sphere and the surface can be written as:

$$W(d) = -\frac{2A}{12} \int_{x=0}^{\infty} \frac{2Rx}{(x+d)^3} dx$$

$$W(d) = -\frac{AR}{6d} \quad , \textbf{(1.2.3.6)}$$

$$\Rightarrow V(x,z) = -\frac{AR}{6(x+z)}$$

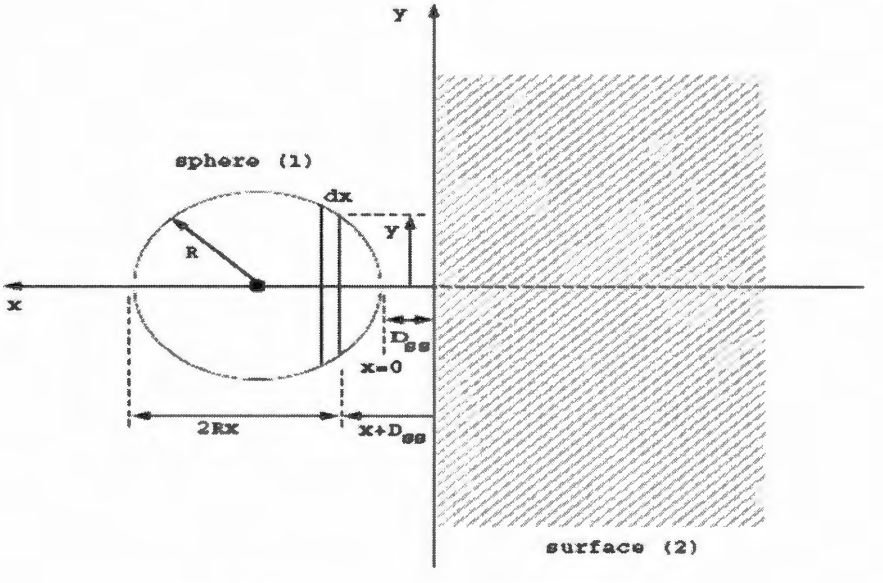

***Figure 1.2.3.2*: Sphere – Flat Surface Interaction**

Thus, by integrating the potential (interaction), the expression for VDW force can be obtained. Hence:

$$F = \frac{dV}{dx} = \frac{AR}{6(x+z)^2}, \quad \textit{(1.2.3.7)}$$

where z is the initial distance between the sphere and surface (Ashhab, Salapaka, Dahleh, Mezic, 1999).

Thus, expression for VDW forces is derived in the above manner. Let A be the *Hamaker Constant* and given as $A = \pi^2 \gamma_1 \gamma_2 c$. The VDW force has an inverse dependence on the square of the distance between the sphere and the surface, and along with the Capillary force, forms the major adhesion force which causes stiction between the sphere and surface.

1.3 PARTICLE REMOVAL: - EXISTING THEORIES

Removal of micro/nano particles is an ever present problem, as explained before. There are several removal methods, some successful and some not so successful. But all these methods have paved the way for future work, like the present one, postulated in the following chapters, utilizing the basic principles of dynamics and vibration.

One of the important removal methods was proposed by Busnaina et al. in 2002 (Busnaina, 2002). The method was applied to remove submicron silica and alumina particles on polished silicon wafers. Three types of removal mechanisms: contact, non-contact and partial-contact brush cleaning were proposed. The idea utilized here was that, brush cleaning could be an effective method, if applied properly by optimizing the water flow, brush rotational speed and brush pressure. The water flow induces drag forces and there will also be the presence of electrical double layer forces, and if the sign of the zeta potential of the

particle and the surface is the same, then repulsion occurs. So, these two forces, namely drag and electrical double layer forces, act against the adhesion forces (VDW and chemical bonding), to bring about particle removal. The particle can be removed by sliding or rolling. Typically, rolling requires less energy to remove the particle than sliding. The following figure depicts the full contact mode particle rolling removal mechanism (Busnaina, 2002).

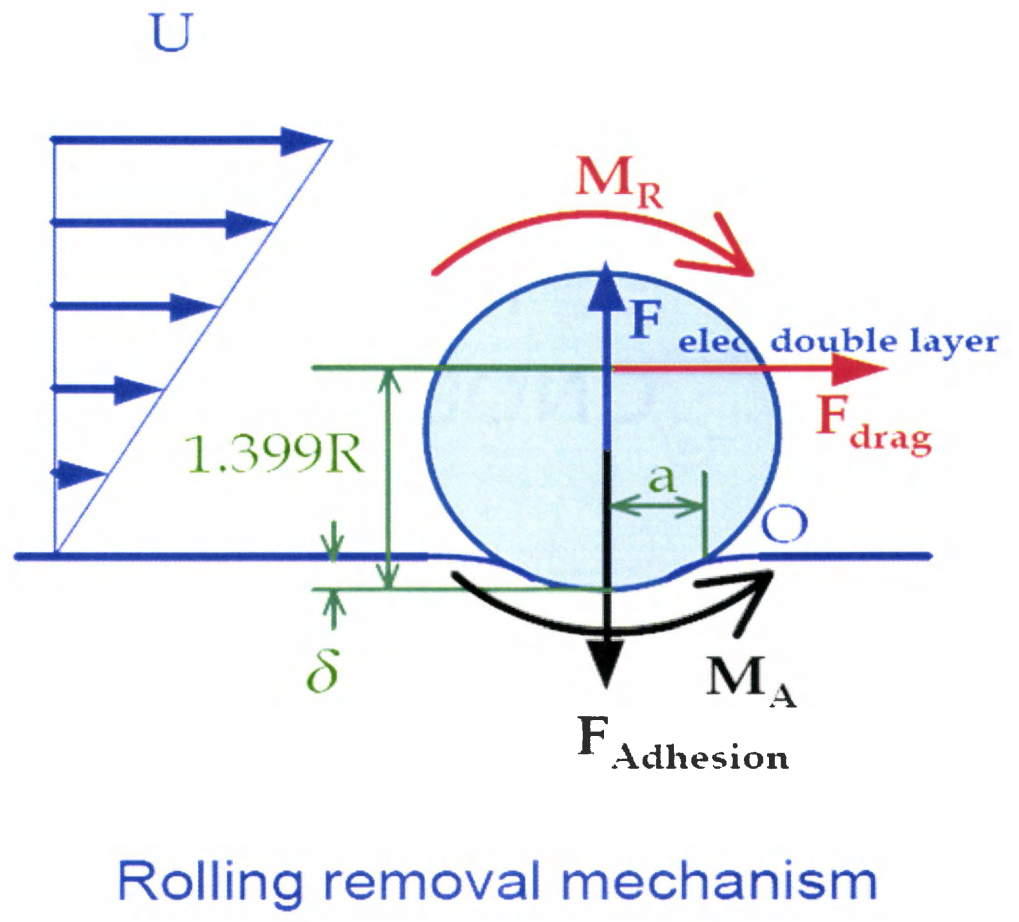

***Figure 1.3.1*: Rolling Removal Mechanism in Brush Cleaning**

In *Figure 1.3.1* (Busnaina, 2002) for contact brush cleaning U is the drag velocity, R is the particle radius, and a, the contact radius. The drag force, electrical double layer force and

adhesion force are considered during removal. When removal force overcomes the adhesion force, i.e. when,

$$RF = \frac{\text{Removal Force}}{\text{Adhesion force}} \geq 1, \textit{(1.3.1)}$$

then, the particle is removed by sliding. But when the removal moment overcomes the adhesion resisting moment, i.e. when,

$$RM = \frac{\text{Removal Moment}}{\text{Adhesion Resisting Moment}} \geq 1, \textit{(1.3.2)}$$

then, the particle is removed by rolling. For contact brush cleaning, the contact removal moment is a function of Power (I_b) and the rotating speed (w_b).

$$M_r = \frac{I_b}{\omega_b}, \textit{(1.3.3)}$$

When, the brush engulfs the particle without contacting the wafer surface, the contact removal moment overcomes the adhesion resisting moment. Hence,

$$RM = \frac{\left(\frac{I_b}{\omega_b} + F_{el}.a\right)}{\left(F_a.a\right)}, \textit{(1.3.4)}$$

Thus, when RM is greater than 1, the particle is removed by rolling. Similarly, non-contact and partial-contact brush cleaning can also be explained. This was a pioneer work in particle removal methods, and serves as an important tool, when removing particles by lateral vibration.

Other papers on particle removal concentrate on the nano manipulation of particles and achieve motion of a particle from one point to another, against the adhesion forces holding it, by means of the AFM tip. This work was proposed by Junno et.al. (Junno,

Deppert, Montelius and Samuelson, 1995) and was further developed, to obtain controlled pushing of nano particles by Metin Setti and Hideki Hashimoto (Setti and Hashimoto, 2000). There are different other methods proposed and studied and the aim of the present work is to improve on the existing ones, by devising a unique model that will require an optimal force to remove the particle from the surface without substantial damage.

1.4 OBJECTIVES OF RESEARCH

The objectives of this research are: -

1) To investigate the phenomenon of particle adhesion and the various adhesive forces which impede particle removal.
2) To understand existing theories on particle removal and to evaluate their effectiveness.
3) To propose a unique theoretical model which can predict conditions for particle separation from the substrate.
4) To establish framework for experimental verification of the theoretical model. This can be left as future work, considering the restricted time frame for the model.

1.5 MODEL DEVELOPMENT

The model is divided into three parts: Longitudinal, Lateral and Coupled Vibrations. In the longitudinal case, the particle and surface are treated as a single system, and separation is made possible by exciting the system with sufficient amplitudes and excitation frequency as a fraction of the natural frequency of the system.

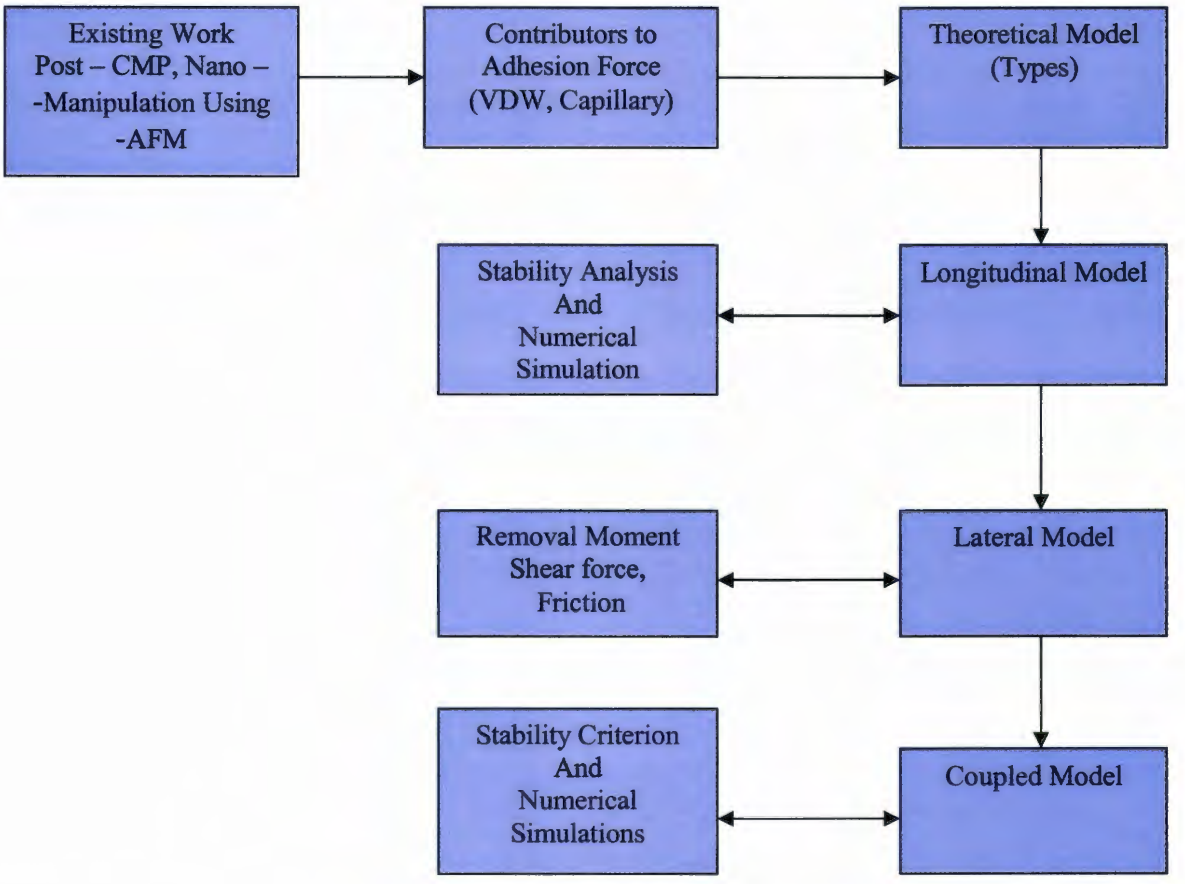

***Figure 1.5.1*: Model Development Flow Chart**

Results, which will be discussed in the subsequent chapters point out that separation, might not be possible if the amplitudes are small. Hence, there is a possibility that the system might fail if excited at very large amplitudes. In the lateral case, the particle is made to move from one point to the other by means of lateral removal moments. This is similar to the work done by Busnaina (Busnaina, 2002). The coupled case, presents a whole plethora of opportunities for particle removal. The lateral and longitudinal vibrations are coupled, with a feedback term provided into the lateral case and separation is possible by means of coupled excitation. Chapter 2 deals with the longitudinal vibrations. A stability analysis is carried out for the homogenous as well as the non-autonomous system, by means of eigenvalue and Lyapunov methods. Simulations are carried at various amplitudes and excitation frequencies on the

non-linear system. Chapter 3 describes the lateral vibration model. Following the pattern of Busnaina's work, a model is postulated and particle separation is brought about by utilizing this model. Chapter 4 deals with the Coupled model. A stability criterion is sought and the dynamic system is formulated and numerically simulated.

The conclusions of the various models are summarized in Chapter 5. Also this chapter throws light on future possibilities and work in progress in the area particle removal and separation.

CHAPTER 2

REMOVAL BY LONGITUDINAL VIBRATION

2.1 INTRODUCTION

This chapter focuses on particle removal by longitudinal vibrations. It is divided into five parts. The first part focuses on the assumptions around which the model revolves. Model development is described in the second part. The third part describes the notion of stability by eigenvalue analysis and Lyapunov's direct method. The stability analysis is carried out after linearizing the system around the equilibrium point. Based on the stability analysis, simulations are carried out and compared with the analytical solution in part four. The simulation results are compared with the results obtained by numerical solutions based on the Runge-Kutta fourth order method, for the complete nonlinear system. The final part summarizes the results obtained and predicts the possibility of particle removal by longitudinal vibrations.

2.2 ASSUMPTIONS

1. Interaction between a spherical particle and a flat surface is considered, while formulating the system dynamics.
2. The entire dynamic system is to be considered to be operating in the micro/nano region.

3. Effect of electrostatic imaging forces, electrical double layer forces and hydration forces are neglected (as explained in *Table 2.3.1*). It is assumed that the major adhesive forces contributing to stiction are the VDW and capillary forces.
4. There is a thin film of fluid (water), between the surface and the particle, which constitutes the basis for capillary adhesion. This is due to the presence of high humidity (70 % to 90 %). The thickness of the fluid layer is taken to be 1.5 nm, from standard studies (Israelachvili, 1985).
5. The particle is assumed to be made of silica/alumina and the flat surface made of silicon. The respective material properties are taken into account while calculating the parameters for the dynamic system. Various particle sizes are considered in the micro/nano regime.

2.3 SYSTEM CHARACTERISATION

Before launching into the system dynamics, a brief note on the selection of the relevant adhesive forces, causing adhesion, is required. Typically, the different forces involved in adhesion of particle to surface are VDW, capillary, electrostatic forces, imaging forces and gravity. The expressions for the various forces are as follows:

$$\text{Van Der Waal Force -: } F_{VDW} = \frac{AR}{6(x+x_0)^2}$$

$$\text{Capillary Force -: } F_{CAPS} = \frac{4\pi\gamma R\cos\theta}{(1+\frac{x}{x_0})} \quad , \textbf{(2.3.1)}$$

$$\text{Electrostatic Force -: } F_{ELEC} = \frac{\pi\Sigma RU^2}{(x+x_0)}$$

$$\text{Imaging Force -: } F_{IMAG} = 0.03D^2 \text{ milli dynes}$$

$$\text{Gravity -: } mg = \frac{4\pi R^3 \rho g}{3} \quad \textit{(2.3.2)}$$

Here, A is the Hamaker constant, R is the particle radius, x is the separation between the particle and the surface, x_0 is the initial separation and is equal to 1.5 nm, U represents the potential on the particle, D is the particle diameter, γ represents the surface tension of the interfacial fluid, Σ is the charge density and ρ represents the density of the particle. A study of the various different forces is carried out for a range of $(x + x_0) = 0.5$ to 2.5 nm and *Table 2.3.1* illustrates the dominant as well as weak forces.

***Table 2.3.1*: Table Illustrating the Strength of Various Adhesive Forces and also Gravity**

R (m)	R-CNTCT (m)	F-VDW (N)	F-CAPS (N)	F-ELEC (N)	F-IMAG (N)	F-GRAV (N)
1.00E-07	5.00E-09	3.11E-11	9.17E-08	2.00E-15	1.20E-23	9.45E-17
1.00E-06	5.00E-08	2.09E-09	9.17E-07	2.00E-14	1.20E-21	9.45E-14
1.00E-05	5.00E-07	1.29E-07	9.17E-06	2.00E-13	1.20E-19	9.45E-11
1.00E-04	5.00E-06	1.14E-05	9.17E-05	2.00E-12	1.20E-17	9.45E-08
1.00E-03	5.00E-05	1.12E-03	9.17E-04	2.00E-10	1.20E-15	9.45E-05

Here, R represents the particle radius; R-Cntct represents the contact radius, whose value is 5 % of the actual particle radius. F-VDW represents the VDW force; F-CAPS represent the

capillary force; F-ELEC represents the electrostatic double layer force; F-IMAG represents the imaging force and F-GRAV represents the gravity force due to the weight of the particle. The material considered here is alumina for the particle and silicon for the surface. Depending on the radius of the particle and its density, we can calculate the mass, considering it to be spherical in nature. Note that, these are all static values and not dynamic force values. Based on *Table 2.3.1*, it is found that the VDW and capillary forces dominate during adhesion, whereas the electrostatic force, though an integral part of the adhesion process, is comparatively weak. Gravity can be neglected completely (except for the inertial force due to acceleration, during dynamic system formulation). Thus while formulating the dynamic system, only VDW and capillary forces contribute to the adhesion phenomenon and hence they are taken into account.

2.4 SYSTEM DYNAMICS

When the capillary forces are taken into account, the distance between the tip of the particle and the meniscus, which is a dynamic distance, and marked as 'd' in *Figure 2.4.1*, is taken to be equal to the initial separation between the particle and the object. This seems to be a valid approximation in the range of distances operated upon. If 'd' was left as a dynamic distance, then the system would be more non-linear and hence difficult to solve. This is the reason for such an approximation.

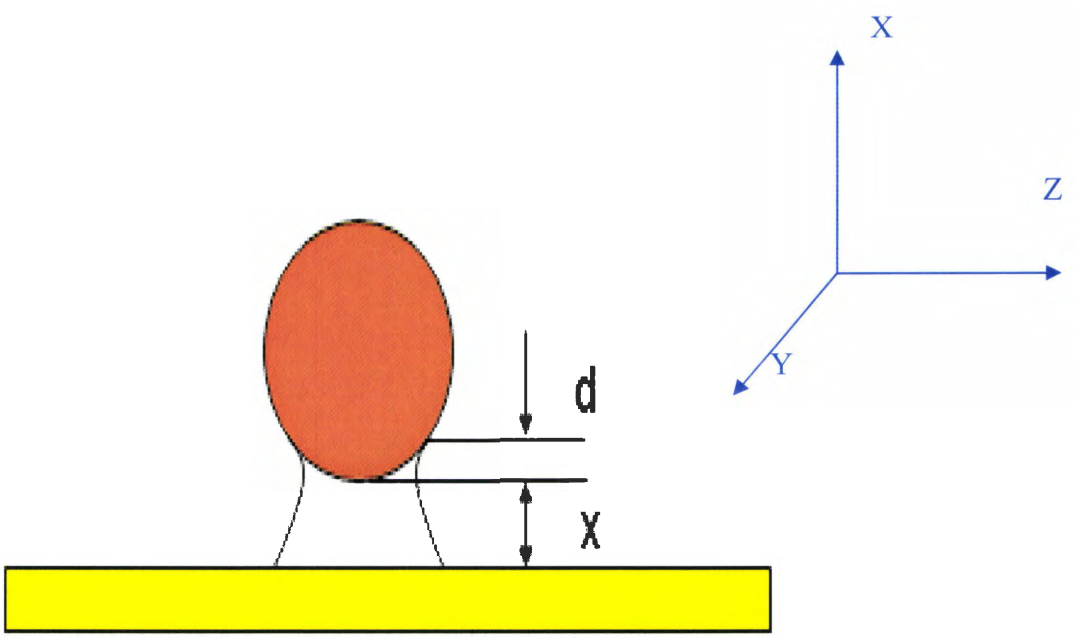

***Figure 2.4.1*: Schematic Representation of Particle on Substrate**

The system consisting of the particle attached to the substrate, and the film of fluid formed by capillary condensation, is modeled as a spring – mass – damper system. The spring and damper comes from the fluid film between the particle and substrate. The stiffness of the spring is taken to be equal to the contact stiffness between the particle and substrate. The damping coefficient is considered to be the result of the fluid viscosity. The mass of the particle is calculated, knowing the density and particle radius, from volume considerations. The damping can either be independent of distance (but dependant on velocity) or can be related to the distance, through one of the model assumptions. This is because, when the particle is near the substrate, the damping is strong and when the particle is away from the substrate, the damping weakens. This only goes to show that damping is related to the distance in a non-dimensional way. The following equations hold good, while evaluating the system parameters.

1) Mass of the particle = m = $\frac{4}{3}\pi R^3 \rho$; (ρ is the density of the particle)

2) Damping Coefficient = c = $6\pi\eta R$; (η is the kinematic viscosity

3) Static Load = L = $\frac{AR}{6z_0^2} + 4\pi\gamma R\cos\theta$; (Load at t = 0)

4) Contact radius = a = $\sqrt[3]{\frac{3RL}{4E^*}}$

5) Effective Elastic Modulus = $E^* = \left[\frac{1-\nu_1^2}{E_1} + \frac{1-\nu_2^2}{E_2}\right]^{-1}$

6) Longitudinal Stiffness = $k_1 = 2aE^*$

7) Damping Force = cx' (Independent of distance)

$= c\left(1 - \frac{x}{x_0}\right)x'$ (Dependent on distance in a non-dimensionalised manner)

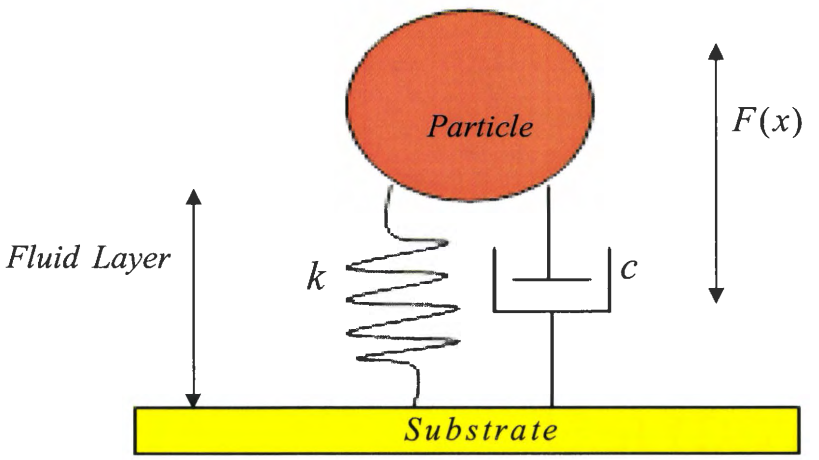

***Figure 2.4.2*: Formulation of System Dynamics**

When the system is given a displacement downwards, the inertial, spring and damping forces will try to counter the effects of the capillary and VDW forces. Thus if x is the displacement of the particle from its static position, due to a forcing function $f\cos(\omega t)$, then the system equation is given as follows:

$$mx'' + cx' + k(x + x_0) = \frac{AR}{6(x + x_0)^2} + \frac{4\pi\gamma R x_0}{(x + x_0)} + f\cos(\omega t), \text{ wherein d} = x_0 \text{ and } \omega < \omega_n$$

If we write $\bar{\Gamma}_1 = \frac{AR}{6}$ and $\bar{\Gamma}_2 = 4\pi\gamma R x_0$, then

$$x'' + \frac{c}{m}x' + \frac{k}{m}(x + x_0) = \frac{\Gamma_1}{(x + x_0)^2} + \frac{\Gamma_2}{(x + x_0)} + \frac{f}{m}\cos(\omega t), \text{ where } \Gamma_1 = \frac{\bar{\Gamma}_1}{m} \text{ and } \Gamma_2 = \frac{\bar{\Gamma}_2}{m} \quad \textit{(2.4.1)}$$

Thus, the above second order system is written as a first order system

$$x_1' = x_2 \quad \textit{(2.4.2)}$$

$$x_2' = -\frac{k}{m}(x_1 + x_0) - \frac{c}{m}x_2 + \frac{\Gamma_1}{(x_1 + x_0)^2} + \frac{\Gamma_2}{(x_1 + x_0)} + \frac{f}{m}\cos(\omega t)$$

Since the system is nonlinear, there is a need to linearize the system around the equilibrium point. For the equilibrium point, $x_1' = 0$ and $x_2' = 0$.

Thus,

$$x_2 = 0 \text{ and } -\frac{k}{m}(x_1 + x_0) + \frac{\Gamma_1}{(x_1 + x_0)^2} + \frac{\Gamma_2}{(x_1 + x_0)} = 0 \quad \textit{(2.4.3)}$$

The equation in x_1 is a third order equation. Simplification of the above terms yield,

$$x_1^3 + x_1^2(3x_0) + x_1(3x_0^2 - \Gamma_2') + (x_0^3 - \Gamma_1' - x_0\Gamma_2') = 0;\ x_2 = 0;\ \Gamma_1' = \frac{\bar{\Gamma}_1}{k} \text{ and } \Gamma_2' = \frac{\bar{\Gamma}_2}{k}, \quad \textit{(2.4.4)}$$

The above equation is solved and the three roots of the equations obtained. One of the roots might be imaginary, or there may be a pair of imaginary roots which can be discarded.

On solving the third order system for a particle of radius one micro meter and stiffness 3.7412e3 N/m, the roots found are as follows -:

$$x_1(1) = -1.711e-9\ m$$

$$x_1(2) = -1.504e-9\ m\ ,\ \textbf{\textit{(2.4.5)}}$$

$$x_1(3) = 2.15e-10\ m$$

The system parameters for various particle sizes are given in *Table 2.4.1*. The same table can be found in the case of coupled vibrations as well, with the only difference coming from the fact that lateral stiffness is redundant in case of longitudinal vibrations.

The next step would involve evaluating the Jacobian matrix at the equilibrium point. In solving for the Jacobian, the equilibrium point considered would be the one that makes most sense, which is the third equilibrium point.

***Table 2.4.1*: List of System Parameters Based on Various Particle Sizes**

Particle Radius (m)	Mass (Kg)	Damping Coefficient (Ns/m)	Load (N)
1.0000E-03	1.6671E-05	2.7143E-05	9.2542E-04
1.0000E-04	1.6671E-08	2.7143E-06	9.2542E-05
1.0000E-05	1.6671E-11	2.7143E-07	9.2542E-06
1.0000E-06	1.6671E-14	2.7143E-08	9.2542E-07
1.0000E-07	1.6671E-17	2.7143E-09	9.2542E-08

Contact Radius (m)	Normal Stiffness (N/m)	Natural Frequency (Hz)	Lateral Stiffness (N/m)
1.9262E-06	3.7412E+05	1.4980E+05	3.5658E+05
4.1500E-07	8.0601E+04	2.1988E+06	7.6823E+04
8.9408E-08	1.7365E+04	3.2274E+07	1.6551E+04
1.9262E-08	3.7412E+03	4.7371E+08	3.5658E+03
4.1500E-09	806.0069	6.9532E+09	768.2298

The Jacobian matrix is given as follows -:

$$J = \begin{pmatrix} \frac{\partial f_1}{\partial x_1} & \frac{\partial f_1}{\partial x_2} \\ \frac{\partial f_2}{\partial x_1} & \frac{\partial f_2}{\partial x_2} \end{pmatrix}_{x=x_e} \quad , \textit{(2.4.6)}$$

Where $f_1 = x_2$ and $f_2 = -\frac{k}{m}(x_1 + x_0) - \frac{c}{m}x_2 + \frac{\Gamma_1}{(x_1 + x_0)^2} + \frac{\Gamma_2}{(x_1 + x_0)}$, with the equilibrium point being given as $x_e = (x_1, 0)$.

Hence, evaluation of the Jacobian at the equilibrium point, yields,

$$\frac{\partial f_1}{\partial x_1} = 0; \frac{\partial f_1}{\partial x_2} = 1; , \textbf{(2.4.7)}$$

$$\frac{\partial f_2}{\partial x_1} = -\frac{k}{m} - \frac{2\Gamma_1}{(x_1 + x_0)^3} - \frac{\Gamma_2}{(x_1 + x_0)^2} = \text{A (say, at } x_e); \frac{\partial f_2}{\partial x_2} = -\frac{c}{m} = b \text{ (say at } x_e), \textbf{(2.4.8)}$$

Thus, the Jacobian at x_e is J = $\begin{pmatrix} 0 & 1 \\ A & b \end{pmatrix}$, where A and b are evaluated at x_e

The system equation can be written thus, as

$$\begin{bmatrix} x_1' \\ x_2' \end{bmatrix} = \begin{pmatrix} 0 & 1 \\ A & b \end{pmatrix} \begin{bmatrix} x_1 \\ x_2 \end{bmatrix} + \begin{bmatrix} 0 \\ \frac{f}{m}\cos(\omega t) \end{bmatrix}$$

$$A = -\frac{k}{m} - \frac{2\Gamma_1}{(x_1 + x_0)^3} - \frac{\Gamma_2}{(x_1 + x_0)^2} \quad , \textbf{(2.4.9)}$$

$$b = -\frac{c}{m}$$

2.5 STABILITY ANALYSIS BY EVALUATING THE EIGEN VALUES

The next step involves evaluating the eigenvalues of the characteristic (system) matrix and understanding stability characteristics from the obtained eigen values. Here, more light must be thrown on the notion of stability.

1. Stability -: The system is considered stable if the particle remains stuck to the substrate.
2. Instability -: The system is considered unstable, if the particle is separated from the substrate.

Whether the system is stable or unstable depends on the eigen values obtained from solving the characteristic equation. For this, a broader notion of definition of stability and

instability is required. The following section shows how a system is characterized stable or unstable. The characteristic equation is given as follows, after evaluating the Jacobian (J) -: $|J - I\lambda| = 0$.

Definition of stability was first proposed by Lyapunov in a broad sense. Hence, motions are called Lyapunov stable, uniformly stable, or asymptotically stable. They can either refer to global stability or local stability. Note must be taken of the fact that stability means the stability of the equilibrium point. Since the system is linearized, the study of the system is limited to a small area near the equilibrium point. Solution curves are studied near the equilibrium point and stability notions are formed thereafter.

1. Equilibrium point -: Where the system comes to rest.
2. Real and Imaginary axes -: These axes plot the eigenvalues obtained from the solution of the characteristic equations. Real values are plotted along the Re – axis and imaginary values plotted along the Im – axes. The eigenvalues obtained from the solution of the characteristic equations, represent the solution curves and the stability of these solution curves can be better studied once they are plotted along the real and imaginary axes. Generally all solution curves, having an eigenvalue that has a positive real part, are considered unstable and otherwise.
3. Closed trajectories -: Also called cycles and refer to the trajectories of the solution curves. Isolated closed trajectories are also called limit cycles. Stable limit cycles mean that nearby solution curves could be spiraling towards them and unstable limit cycles mean that nearby solution curves could be spiraling away from them. A combination of stable and unstable limit cycles are formed due to dissipation and generation of energy. This is commonly observed in Van Der Pol oscillators where in

there is a change or alternation between positive and negative damping. This behavior or flip from positive to negative damping leads to the limit cycle behavior. Stable closed trajectories are also called centers, which mean that the system is just oscillating between its equilibrium positions. This generally happens when a spring mass system is considered without any damping to dissipate the energy.

4. Open trajectories -: Also called focus or spirals, they are formed when there is generally dissipation or generation of energy. A stable spiral or focus spirals towards the equilibrium point, after starting from its initial condition, whereas an unstable spiral or focus spirals away from the equilibrium point, after originating at the initial condition. Spirals or focus are generally found in systems which have a spring mass and damper combination, leading to the formulation of the dynamic system.
5. Saddles -: Saddles are generally unstable trajectories. A simple example would be two straight line trajectories, one entering the origin and the other exiting the origin. The other trajectories either approach or leave these two. Saddles have solution curves which start simultaneously from the positive and negative regions of the real axes, which mean that the system switches between stable and unstable behavior. Hence saddle points are considered unstable and detrimental to the system. If positive and negative damping occurs, the balance between energy loss and energy gain can result in self sustained oscillations (or limit cycles, as explained previously).

Figure 2.5.1 explains in better detail the various types of behaviors exhibited by the solution curves. For the system to go unstable, either there must be an unstable limit cycle, an unstable focus or a saddle point behavior (Marquez, 2003)

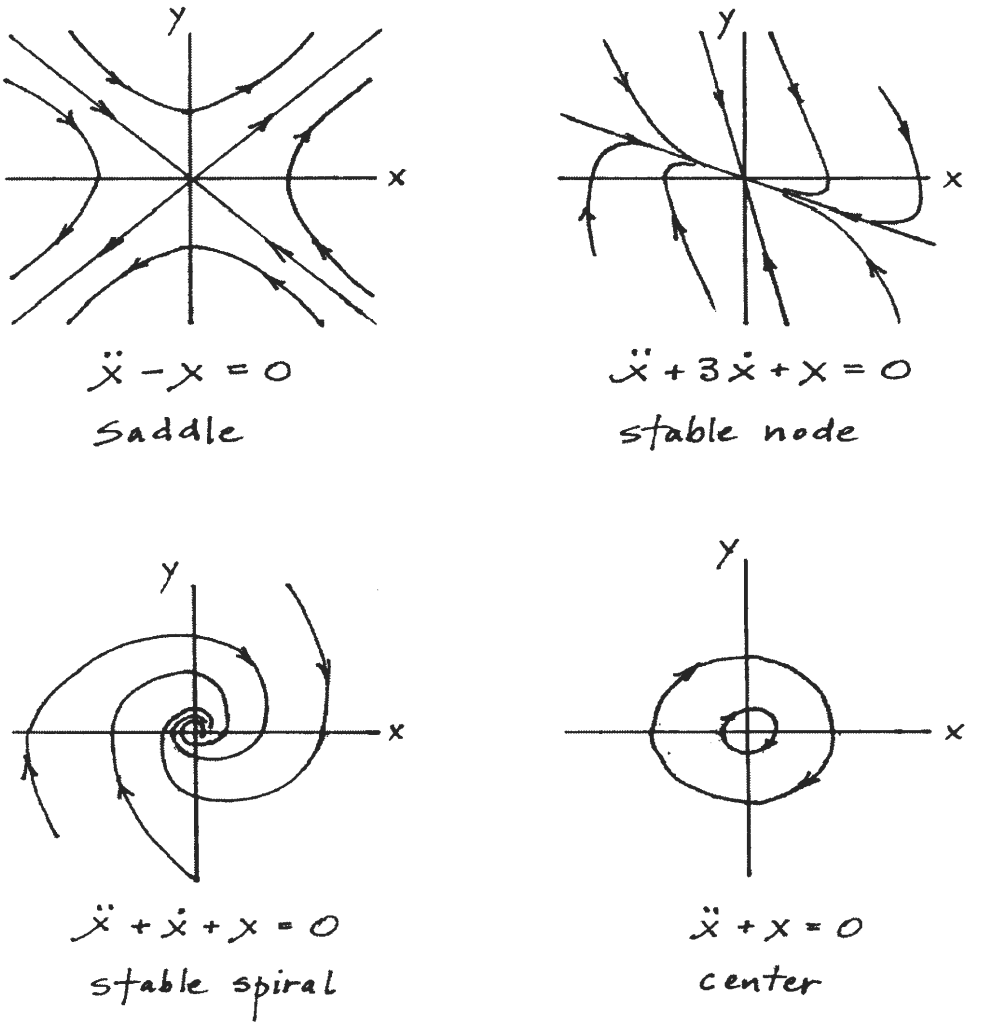

***Figure 2.5.1*: Various Stability Behaviors Depending on Eigen Values**

The above figures depict the notion of stability. The following definitions also hold well, when the factor of stability is defined (Rand, 2003).

Definition -: A motion M is said to be *Lyapunov stable*, if given any $\varepsilon > 0$, there exists a $\delta > 0$, such that, if N is any motion that starts out at t = 0 inside a δ – ball centered at M, then it stays in an ε – ball centered at M for all time t.

In particular, this means that an equilibrium point will be stable from the sense of Lyapunov, if the initial conditions are chosen sufficiently close to the equilibrium point so as to be able to keep all the ensuing motions inside an arbitrarily small neighborhood of the equilibrium point (inside an ε – ball). A motion is said to be Lyapunov unstable, if it is not Lyapunov stable. Refer *Figure 2.5.2* for Lyapunov Stability

Definition -: If in addition to being Lyapunov stable, all motions N which start at time t = 0 inside a δ – ball centered at M (for some δ), approach M asymptotically as t goes to infinity, then M is said to be *asymptotically Lyapunov stable (Figure 2.5.3)*

Definition -: An equilibrium point is said to be *Hyperbolic*, if all the eigen values of the linear variational equations have non – zero real parts.

In addition to the above definitions, the following theorems of Lyapunov also hold true.

Lyapunov theorems

1. **An equilibrium point in a nonlinear system is *asymptotically Lyapunov stable*, if all the eigenvalues of the linear variational equations have negative real parts.**
2. **An equilibrium point in a nonlinear system is said to be *Lyapunov unstable*, if there exists at least one eigenvalue of the linear variational equation which has a positive real part.**

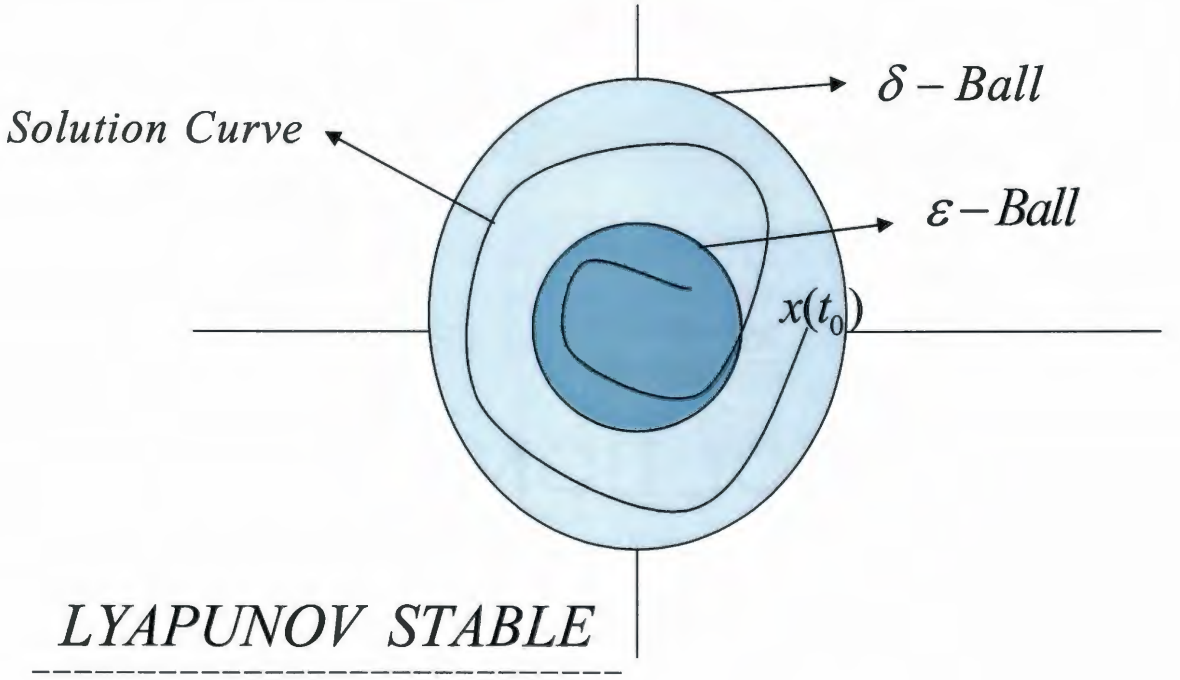

***Figure 2.5.2*: Uniform Lyapunov Stability**

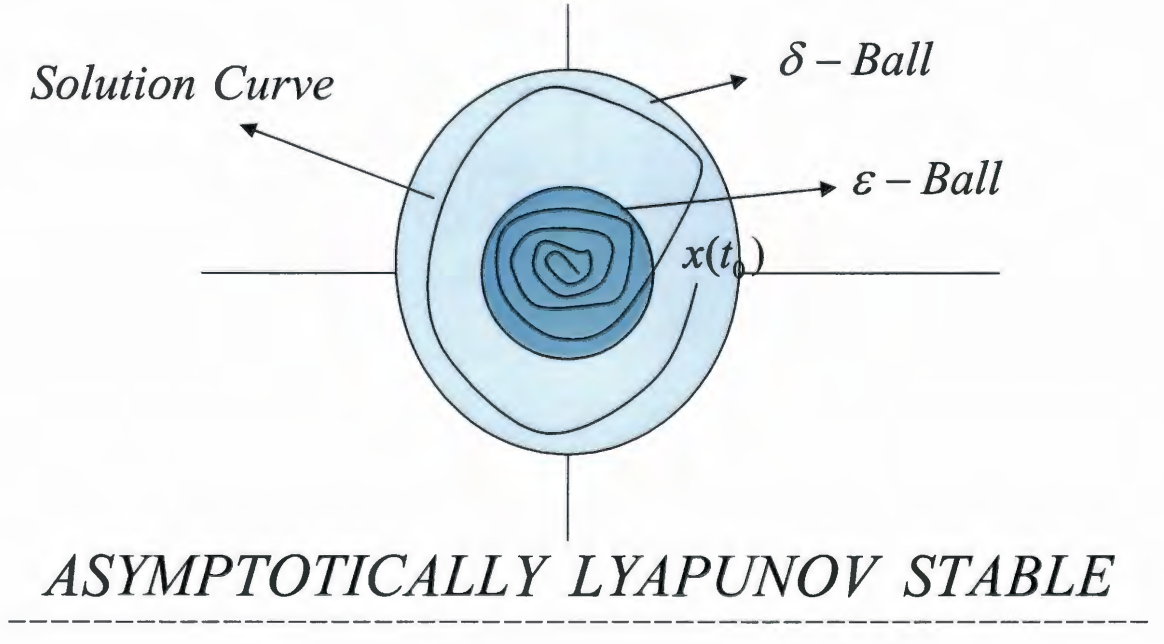

***Figure 2.5.3*: Asymptotic Lyapunov Stability**

Coming back to the eigenvalue analysis, the following procedure is carried out to evaluate the eigenvalues.

$|J - I\lambda| = 0 \rightarrow$

$$\begin{vmatrix} 0-\lambda & 1 \\ A & b-\lambda \end{vmatrix} = 0 \rightarrow \lambda^2 - b\lambda - A = 0, \textit{(2.5.1)}$$

Thus, $\lambda = \dfrac{b \pm \sqrt{b^2 + 4A}}{2}$

It is obvious that, whatever be the value for x_e, both A and b are negative.

Hence, $\lambda_1 = \dfrac{b + \sqrt{b^2 + 4A}}{2}$ and $\lambda_2 = \dfrac{b - \sqrt{b^2 + 4A}}{2}$, *(2.5.2)*

But, $\sqrt{b^2 + 4A}$ is an imaginary number and hence let $\sqrt{b^2 + 4A} = i\eta$.

Thus, $\lambda_{1,2} = -\mu \pm i\eta$.

So, according to the stability theory for eigenvalues, if the real part of the eigenvalue lies on the left side of the jω (imaginary axis), then the dynamic system is stable and it's unstable otherwise. More over, if the system contains an imaginary part, along with a real part which is negative i.e. $\lambda = -\mu \pm i\eta$, then such a behavior is called a stable focus, which was defined earlier. This is the case for the equilibrium point being taken as positive. It is seen that if other two values for the equilibrium points are considered, the behavior of the system remains the same (stable focus behavior). Hence, the eigenvalue analysis says that whatever be the equilibrium point, the system is going to be stable. This is somewhat contradictory because the forcing function does not play any role here and if it were taken into consideration then an increase in the amplitude and excitation frequency, would certainly render the system unstable, from an intuitive point. Thus, Lyapunov analysis of the

non – autonomous system is carried out and the uncertainties in the stability analysis are ironed out.

2.6 STABILITY ANALYSIS BY LYAPUNOV'S DIRECT METHOD

An intuitive view of Lyapunov's theory is given as follows. Consider a scalar potential function V (x), wherein there is no dependence on time (later on this can be taken into the scheme of things as well). Then V (x) = C defines a Lyapunov surface. A Lyapunov surface defines a region in the state space (where the velocity is plotted against the displacement vector) that encloses all Lyapunov functions of lesser value.

The condition $\dot{V}(x) \leq 0$ implies a trajectory crossing a Lyapunov surface V (x) = C and never coming out of it again. Thus a trajectory or a solution curve satisfying the above condition wherein the derivative is lesser than or equal to zero, is confined to a closed surface of limit C. Then such an equilibrium point is called stable and the derivative is negative semi - definite. If $\dot{V}(x) < 0$ then a trajectory can only move from inside a Lyapunov surface V (x) = C to an inner surface, for which, V (x) = C_1 where C > C_1. Thus C goes on decreasing as one goes deeper and deeper into the Lyapunov surface. Such a derivative is fully negative definite. This condition also ensures that we finally go on decreasing the limit of the Lyapunov surface and reach the origin or the equilibrium point. Hence, such a system is called asymptotically stable.

$$STABLE \Rightarrow V(0) = 0;\ V(x) > 0;\ \dot{V}(x) \leq 0$$

$$ASYMPTOTICALLY\ STABLE \Rightarrow V(0) = 0;\ V(x) > 0;\ \dot{V}(x) < 0$$

GLOBALLY ASYMPTOTICALLY STABLE $\Rightarrow V(0) = 0; V(x) > 0; \dot{V}(x) < 0$ *and* $V(x)$ *is radially unbounded.*

The following theorem explains Lyapunov's stability criterion following the intuitive ideas expressed earlier. Here the focus is more on the non – autonomous systems, which are time dependent, as the system under consideration is acted upon by a forcing function which depends on time as well.

2.6.1 Lyapunov's Stability Theorem for Non – Autonomous Systems

Consider a system

$$x' = f(x,t)\,, \textbf{\textit{(2.6.1.1)}}$$

With $f(x,t)$ being a continuous function of x and t. Suppose that this system has an equilibrium point at the origin (at x = 0), at a time t = 0 (if the equilibrium point isn't at the origin, the system can be shifted by suitable substitution, such that the new equilibrium point lies at the center).

The system's equilibrium state at the origin is said to be stable, if there exists an r > 0, and a scalar valued function V (x, t) such that, for all x, for which $\|x\| < r$ and $t \geq 0$:

1. $V(x,t)$ has continuous first partial derivatives
2. $V(x,t)$ is positive definite
3. $V'(x,t)$ is negative semi – definite along all of the system's state trajectories.

If, in (2), V (x, t) is positive definite and decresent, then the origin is uniformly stable.

If, in (2), V (x, t) is positive definite and decresent and in (3), $V'(x,t)$ is negative definite along all of the system's trajectories, then the origin is uniformly asymptotically stable.

There is also a Lyapunov's stability criterion for autonomous systems. But since we are dealing with time dependent systems (non – autonomous), the other method is not of much interest, though some of the criterions are similar to the above explained theory.

In order to apply Lyapunov's stability/instability criterion on the system under consideration, consider the system to be excited by a force dependent on the velocity of the system, scaled by a suitable constant. The damping is considered to be dependent on the distance, through a dimensionless constant. Thus, the system equation can be written as follows -:

$$mx'' + k(x + x_0) + c(1 - \frac{x}{x_0})x' = \bar{A}\, x' e^{-t} + \frac{\bar{\Gamma}_1}{(x + x_0)^2} + \frac{\bar{\Gamma}_2}{(x + x_0)}, \textbf{(2.6.1.2)}$$

Writing the above as a system of first order equations,

$$x_1' = x_2$$

$$x_2' = -\frac{k}{m}(x_1 + x_0) - \frac{c}{m}(1 - \frac{x_1}{x_0})x_2 + Ax_2 e^{-t} + \frac{\Gamma_1}{(x_1 + x_0)^2} + \frac{\Gamma_2}{(x_1 + x_0)}, \textbf{(2.6.1.3)}$$

The equilibrium point is calculated as before and it is found to remain the same, as the equilibrium point is calculated for the autonomous system and not the forced one. As usual, there will be three equilibrium points. The entire system can be shifted through the equilibrium point to the origin if necessary and hence the origin can become the equilibrium point. A particular equilibrium point is chosen (it is finally found that the behavior at all equilibrium points is the same).

The Jacobian gives the following values at x_e

$$\frac{\partial f_1}{\partial x_1} = 0; \quad \frac{\partial f_1}{\partial x_2} = 1;$$

$$\frac{\partial f_2}{\partial x_1} = -\frac{k}{m} - \frac{2\Gamma_1}{(x_1 + x_0)^3} - \frac{\Gamma_2}{(x_1 + x_0)^2} = -U \text{ (say, at } x_e) \qquad \textbf{(2.6.1.4)}$$

$$\frac{\partial f_2}{\partial x_2} = Ae^{-t} - \frac{c}{m}(1 - \frac{x_1}{x_0}) = Ae^{-t} - b \text{ (say, at } x_e), \text{ where } b = \frac{c}{m}(1 - \frac{x_1}{x_0})$$

The system equation can hence be written in the reduced manner as follows -:

$$\begin{aligned} x_1' &= x_2 \\ x_2' &= -Ux_1 - (b - Ae^{-t})x_2 \end{aligned} \qquad \textbf{(2.6.1.5)}$$

It has to be noted that, whatever be the equilibrium point, the value of U is always positive or –U is always negative. The case of positive damping where in (b - A) > 0, has to be considered while evaluating stability of the system. If (b - A) < 0, then that means the system possesses negative damping, which is tough to realize practically.

Considering the system after linearization, a particular scalar function V (x, t) of x and t is chosen.

$$V(x,t) = \frac{Ux_1^2}{2} + \frac{(b - Ae^{-t})x_2^2}{2}, \text{ where b} = \frac{c}{m}(1 - \frac{x_1}{x_0}), \textbf{(2.6.1.6)}$$

As $t \to 0$, $(b - Ae^{-t}) \to (b - A)$

As $t \to \infty$, $(b - Ae^{-t}) \to b$. **(2.6.1.7)**

Note that $b > (b - A)$.

A) So, $V(x,t)$ is positive definite because -:

1) $V(0,t) = 0$;

2) $\frac{Ux_1^2}{2} + \frac{(b - Ae^{-t})x_2^2}{2} \geq \frac{Ux_1^2}{2} + \frac{(b - A)x_2^2}{2} = V_0(x)$, provided, (b-A) > 0.

, ***(2.6.1.8)***

B) Also, $V(x,t)$ is decreasing because -:

1) $V(0,t) = 0$;

2) $\frac{Ux_1^2}{2} + \frac{(b - Ae^{-t})x_2^2}{2} \leq \frac{Ux_1^2}{2} + \frac{bx_2^2}{2} = V_1(x)$

Thus, $V_0(x) \leq V(x,t) \leq V_1(x)$. And since both the functions are positive definite, $V(x,t)$ is also positive definite and decreasing.

C) $V(x,t)$ is radially unbounded because -:

$$\frac{Ux_1^2}{2} + \frac{(b - Ae^{-t})x_2^2}{2} \to \infty \text{ as } \|x\| \to \infty, \forall\ t \geq 0 \quad \text{, ***(2.6.1.9)***}$$

Now, to take a look at the derivative of the scalar potential function.

$\dot{V}(x,t)$ is negative definite if,

1) $\dot{V}(x,t) = 0$, ***(2.6.1.10)***

2) A negative definite function $\dot{V}_0(x)$ exists such that $\dot{V}(x,t) \leq \dot{V}_0(x)\ \forall t \geq 0$

1) $\dot{V}(0,t) = \frac{d}{dt}\left[\frac{U}{2}0^2 + \frac{(b - Ae^{-t})}{2}0^2\right] = 0$

2) $\dot{V}(x,t) = \frac{d}{dt}\left[\frac{U}{2}x_1^{\,2} + \frac{(b - Ae^{-t})}{2}x_2^{\,2}\right]$, ***(2.6.1.11)***

$$\Rightarrow \dot{V}(x,t) = Ux_1\dot{x}_1 + (b - Ae^{-t})x_2\dot{x}_2 + \frac{Ae^{-t}}{2}x_2^{\,2}$$

Substituting for $\dot{x}_1$ and $\dot{x}_2$,

$$\dot{V}(x,t) = Ux_1x_2 + \frac{Ae^{-t}}{2}x_2^{\,2} + x_2(b - Ae^{-t})\left[-Ux_1 - (b - Ae^{-t})x_2\right]$$

$$\Rightarrow \dot{V}(x,t) = Ux_1x_2\left[1 - (b - Ae^{-t})\right] + x_2^{\,2}\left[\frac{Ae^{-t}}{2} - (b - Ae^{-t})^2\right] \quad , \textit{(2.6.1.12)}$$

$$\dot{V}(x,t) = \begin{bmatrix} x_1 & x_2 \end{bmatrix} \begin{pmatrix} 0 & \frac{U(1-b+Ae^{-t})}{2} \\ \frac{U(1-b+Ae^{-t})}{2} & \frac{Ae^{-t}}{2} - (b - Ae^{-t})^2 \end{pmatrix} \begin{bmatrix} x_1 \\ x_2 \end{bmatrix}$$

$$\Rightarrow \dot{V}(x,t) = x^T Q x, \text{ where } Q = \begin{pmatrix} 0 & \frac{U(1-b+Ae^{-t})}{2} \\ \frac{U(1-b+Ae^{-t})}{2} & \frac{Ae^{-t}}{2} - (b - Ae^{-t})^2 \end{pmatrix} \text{ and } x = \begin{bmatrix} x_1 \\ x_2 \end{bmatrix}$$

If it can be proven that for whatever the value of t, Q is negative definite, then stability can be attained.

$$\text{For t = 0; } Q = \begin{pmatrix} 0 & \frac{U(1-b+A)}{2} \\ \frac{U(1-b+A)}{2} & \frac{A}{2} - (b - A)^2 \end{pmatrix} \Rightarrow |Q| = -\frac{U^2(1-b+A)^2}{4} < 0$$

$$\text{For t = } \infty\text{; } Q = \begin{pmatrix} 0 & \frac{U(1-b)}{2} \\ \frac{U(1-b)}{2} & -b^2 \end{pmatrix} \Rightarrow |Q| = -\frac{U^2(1-b)^2}{4} < 0 \quad , \textit{(2.6.1.13)}$$

Thus, for whatever value of t, $|Q| < 0 \Rightarrow \dot{V}(x,t)$ is negative definite and hence the system is stable.

Hence, $\dot{V}(x,t) \le \dot{V}_0(x)$, where $\dot{V}_0(x)$ is also negative definite for all t.

Thus, the results can be summarized as follows -:

1) $V(x,t)$ is positive definite and decrescent for all t.

2) $V(x,t)$ is radially unbounded. , ***(2.6.1.14)***

3) $\dot{V}(x,t)$ is negative definite for all t.

For the case, where positive damping is considered, which means that (b - A) > 0, the system shows a stable behavior. This is reasonable and expected within the range of forcing functions considered. But if (b – A) < 0, then the system scalar function becomes negative definite. Hence the system therefore becomes unstable. It has to be understood that while Lyapunov's method is a rigorous method, wherein the forcing function is also taken into account, it is only a necessary criterion and is in no way a sufficient condition for stability. For whatever scalar potential function that has been chosen, there can always be a scalar potential function evaluated, which can show a different type of behavior then expected by the above analysis. Since the system itself is linearized and the area of concentration is a small region around the equilibrium point, it can be approximated that Lyapunov's method holds good for the range of values considered.

2.7 SIMULATION OF THE LINEARIZED SYSTEM BASED ON STABILITY ANALYSIS

The next step involves the simulation of the linearized dynamic system, based on the stability analysis, to prove that it holds good for the range of values considered in the micro/nano scale. There are two steps involved here. The first step lies in solving the linearized system analytically and then carrying out a numerical simulation based on the Runge – Kutta fourth order method. The solution of the linearized system is carried out as follows -:

Problem -: $mx'' + k(x + x_0) + cx' = \frac{AR}{6(x + x_0)^2} + \frac{4\pi\gamma R x_0}{(x + x_0)} + f\sin(\omega t)$, ***(2.7.1)***

Linearization is performed after evaluating the equilibrium point.

After linearization the system has the form, as show below

$x_1' = x_2$

$x_2' = -Ax_1 - bx_2$, where $-A = -\frac{k}{m} - \frac{2AR}{6m(x + x_0)^3} - \frac{4\pi\gamma R x_0}{m(x + x_0)^2}$; $-b = -\frac{c}{m}$, ***(2.7.2)***

Thus, $x'' + bx' + Ax = 0 \rightarrow (Homogenous)$

General solution for the linearized equation -:

Let, $x = e^{rt} \rightarrow x' = re^{rt}; x'' = r^2 e^{rt}$

So, $e^{rt}(r^2 + br + A) = 0 \rightarrow r = \frac{-b \pm \sqrt{b^2 - 4A}}{2}$, ***(2.7.3)***

Thus, $x = c_1 e^{r_1 t} + c_2 e^{r_2 t}$, where $r_1 = \frac{-b + \sqrt{b^2 - 4A}}{2}$; $r_2 = \frac{-b - \sqrt{b^2 - 4A}}{2}$

c_1 and c_2 can be found out from the initial conditions.

The next step is to find out the particular solution for the above system, after considering the forcing function to drive the system under scrutiny.

Thus, $x'' + bx' + Ax = f\sin(\omega t)$, ***(2.7.4)***

So, a good choice of x will help in solving the above equation.

$x = a\cos(\omega t) + c\sin(\omega t)$, ***(2.7.5)***

After inputting this into the system equation the solution scheme looks as follows -:

In solving the longitudinal vibration case -:

Initial conditions are -: $x(0) = x_0;\ x'(0) = 0;$

The solution form is -: $x(t) = c_1 e^{r_1 t} + c_2 e^{r_2 t} + a\cos(\omega t) + b\sin(\omega t),$ where

$$c_1 = -\frac{[cw + r_2(x_0 - a)]}{[r_1 - r_2]}$$

$$c_2 = \frac{[cw + r_1(x_0 - a)]}{[r_1 - r_2]}$$

$$r_1 = \frac{-b + \sqrt{b^2 - 4A}}{2}$$

$$r_2 = \frac{-b - \sqrt{b^2 - 4A}}{2}$$

$$a = -\frac{fbw}{[(A - \omega^2)^2 + (b\omega)^2]}$$

$$c = \frac{f(A - \omega^2)}{[(A - \omega^2)^2 + (b\omega)^2]} \qquad , \textit{(2.7.6)}$$

$$w = lw_n;\ l \le 1$$

2.7.1 PARAMETERS FOR SIMULATION

A = 3.3683e-020 J; **(HAMAKAR'S CONSTANT)**

K = 2.0167e+011 N/m^2; **(COMPOSITE YOUNG'S MODULUS)**

As = 3.9516e-023 m^2; **(CONTACT AREA)**

R = 16-6 m; **(PARTICLE RADIUS)**

Initial separation = 1.5 nm; **(MINIMUM SEPARATION DISTANCE)**

k = 3.7412e3 N/m; **(STIFFNESS)**

c = 2.733e-8 Ns/m; **(DAMPING COEFFICIENT)**

m = 1.6671e-14 Kg; **(MASS)**

Y = 73e-3 N/m; **(SURFACE TENSION FOR WATER)**

d = initial separation = 1.5 nm; **(PARTICLE PARAMETER)**

EQUILIBRIUM POINTS

1.0e-008 *

{-0.1711

-0.1504

0.0215}

LINEARIZATION PARAMETERS FOR CHARACTERISTIC MATRIX

1) -A = --1.7813E18;

2) -b = -0.1038;

3) dF1/dx1 = 0;

4) dF1/dx2 = 1;

MATRIX = [3 4; 1 2];

FORCE f = 1e-6; Newton;

r1 = -5.1900e-002 +9.1970e+004i;

r2 = -5.1900e-002 -9.1970e+004i;

w = 9.1970e+003;

a = -1.3614e-023;

c = 1.1942e-016;

c1 = 2.3400e-010 -1.2608e-016i;

c2 = 2.3400e-010 +1.2608e-016i;

The following simulation results were observed when the linearized system was solved utilizing the system information given above. *Figures 2.7.1.1 to 2.7.1.6* illustrate the 3

– D phase, 2 – D phase and time plots for a particle of radius 1 micro meter. The first set of plots *(Figures 2.7.1.1 to 2.7.1.3)* are for a time period ranging from 0 seconds up till 0.1 seconds and the second set of plots *(Figures 2.7.1.4 to 2.7.1.6)* are for a time period from 0 seconds to 1 second (which means more number of cycles to solve).

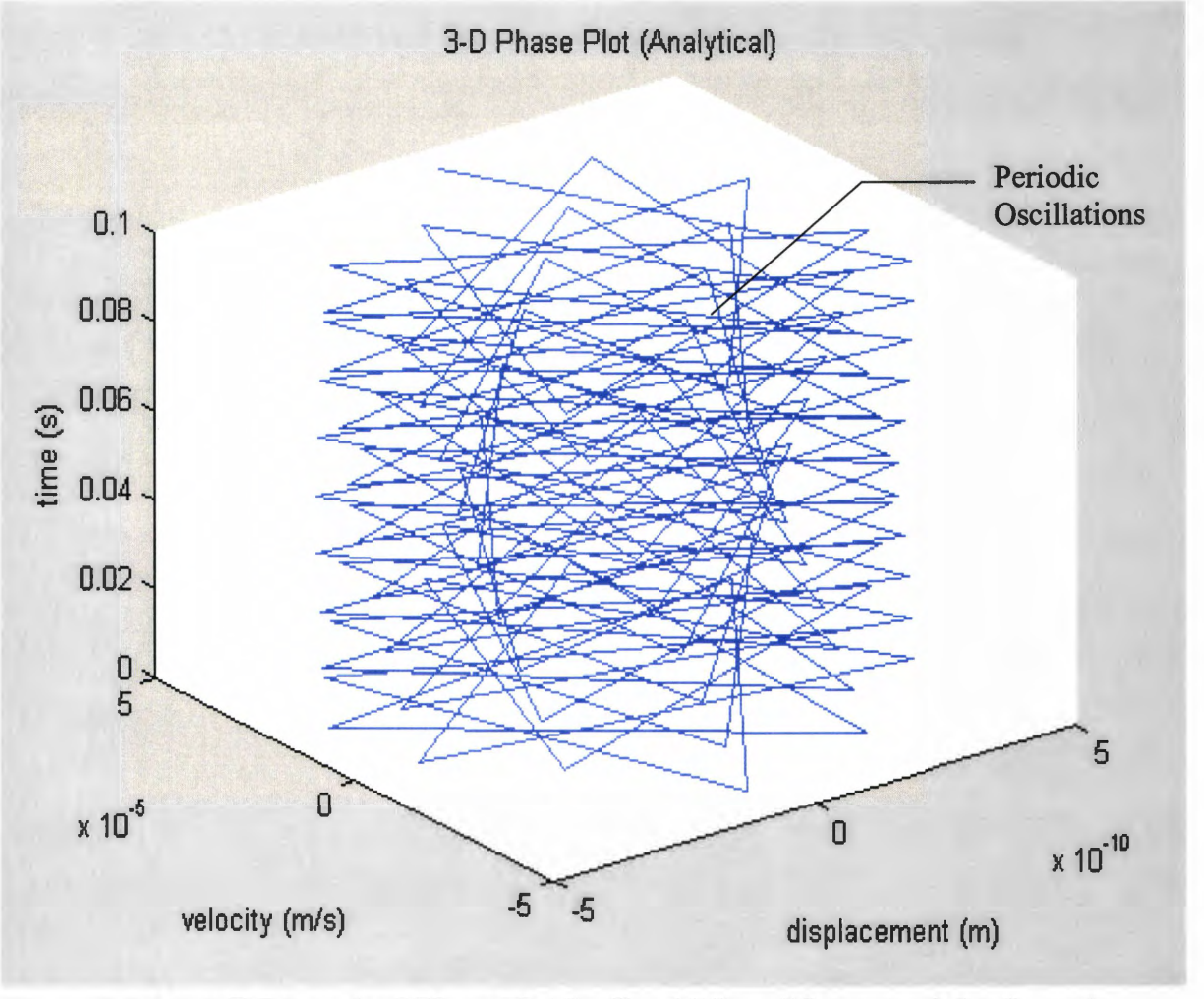

Figure 2.7.1.1: **3-D Linearized Phase Plot for R = 1 Micro Meter, t = 0:0.1 Seconds**

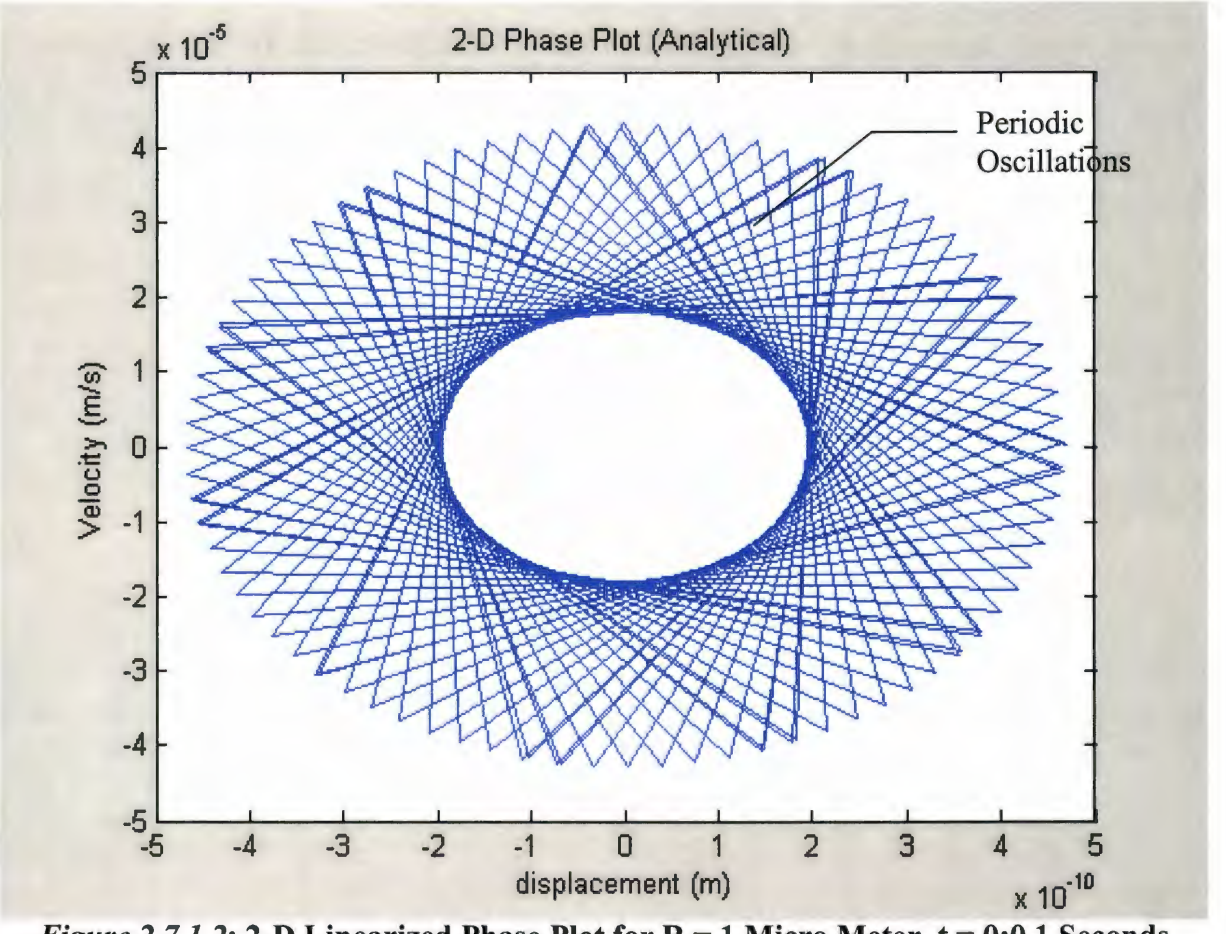

***Figure 2.7.1.2*: 2-D Linearized Phase Plot for R = 1 Micro Meter, t = 0:0.1 Seconds**

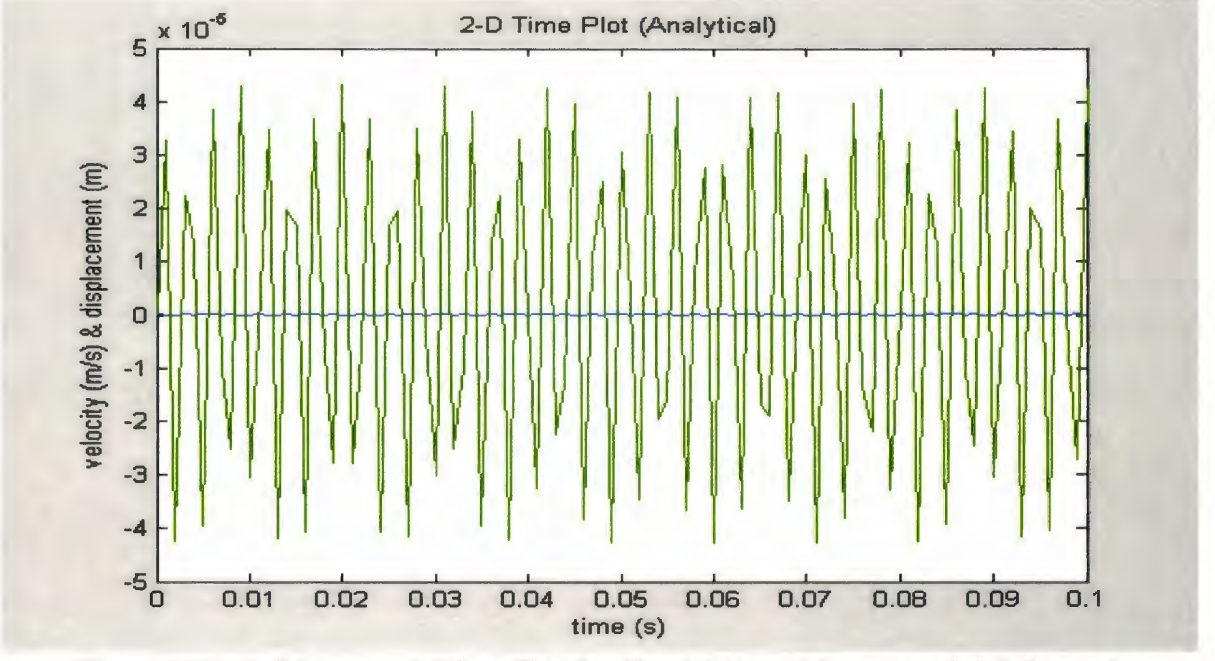

***Figure 2.7.1.3*: Linearized Time Plot for R = 1 Micro Meter, t = 0:0.1 Seconds**

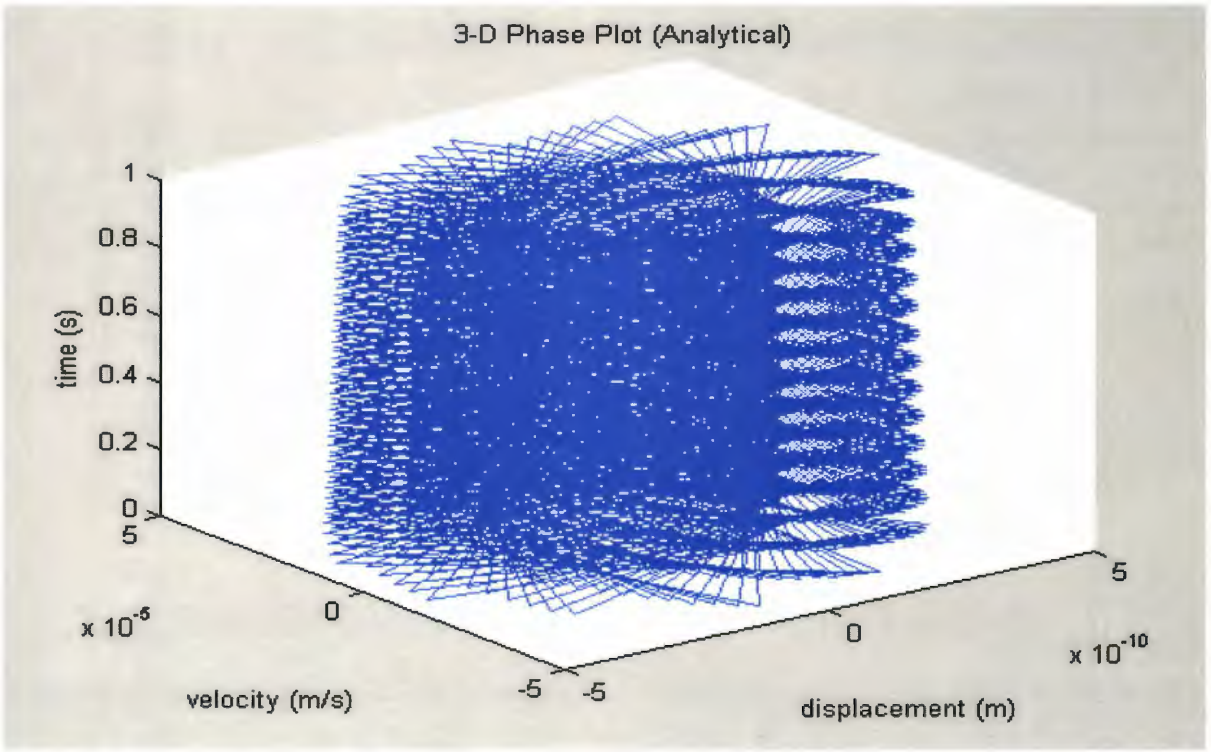

***Figure 2.7.1.4*: 3-D Linearized Phase Plot for R = 1 Micro Meter, t = 0:1 Second**

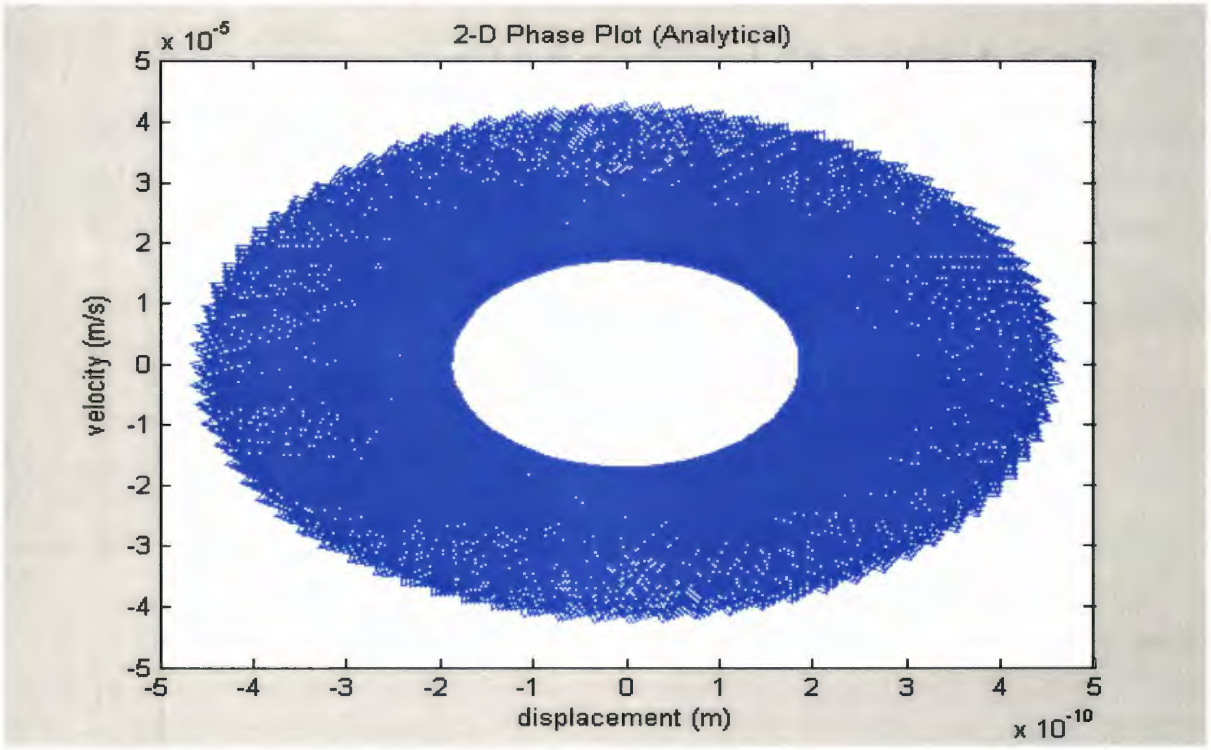

***Figure 2.7.1.5*: 2-D Linearized Phase Plot for R = 1 Micro Meter, t = 0:1 Second**

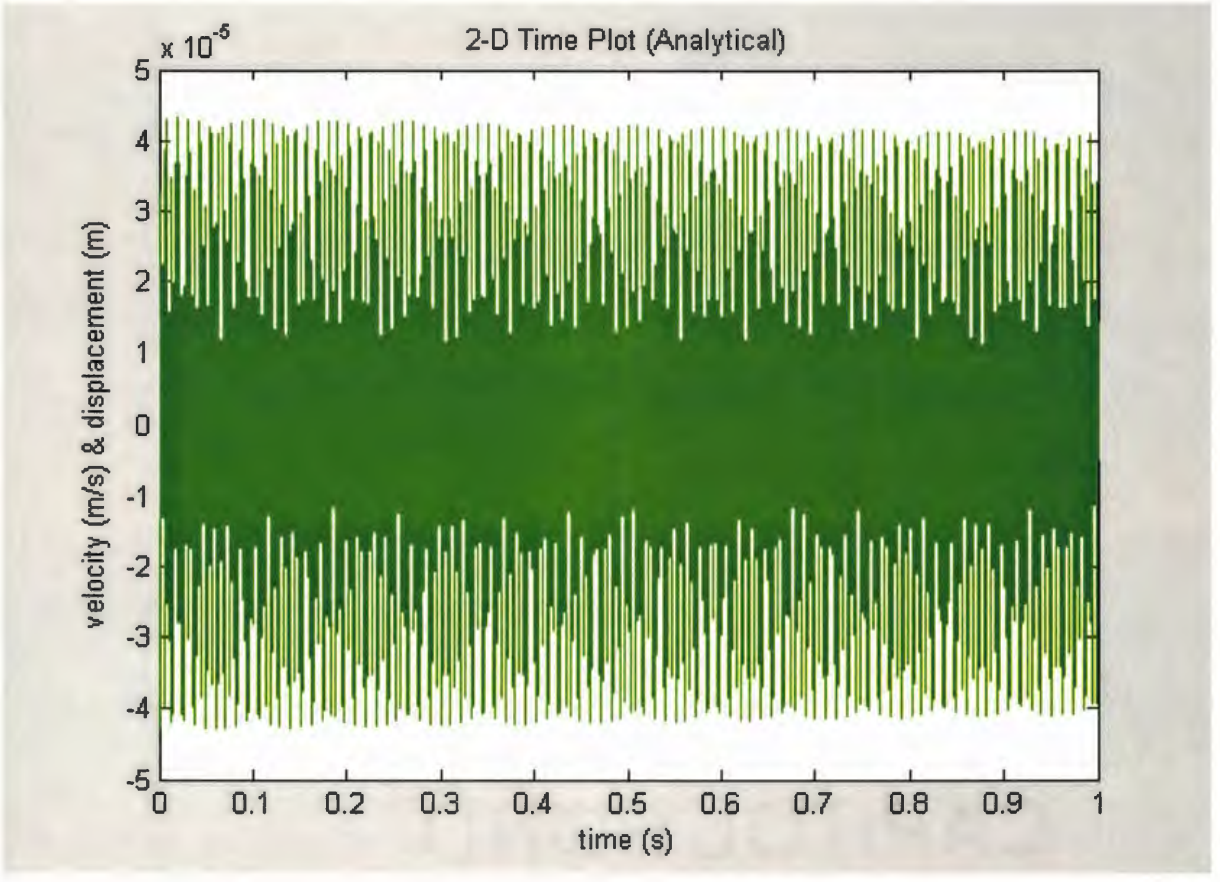

***Figure 2.7.1.6*: Linearized Time Plot for R = 1 Micro Meter, t = 0:1 Second**

The above plots imply that the system is oscillating between the equilibrium point on the positive and negative side. Any region below the equilibrium point is taken to be negative. There will be doubts whether the particle would bang into the system under consideration. But the displacement value at 5 angstroms between the positive and negative side assuages all these fears and concerns. For the above systems, the equilibrium point has been shifted to the origin and hence the oscillations of the system start at the origin (0, 0). The time plots show a predominantly oscillating trend. There is also an occurrence of beat frequency noted. Later when the coupled vibrations are solved, wherein the lateral and longitudinal vibrations are coupled, the beat frequency is found to play an important role in particle separation.

Figures 2.7.1.7 and 2.7.1.8 refer to the numerical simulation of the complete non – linear system. There has been no linearization carried out and the behavior is explained on studying the following plots.

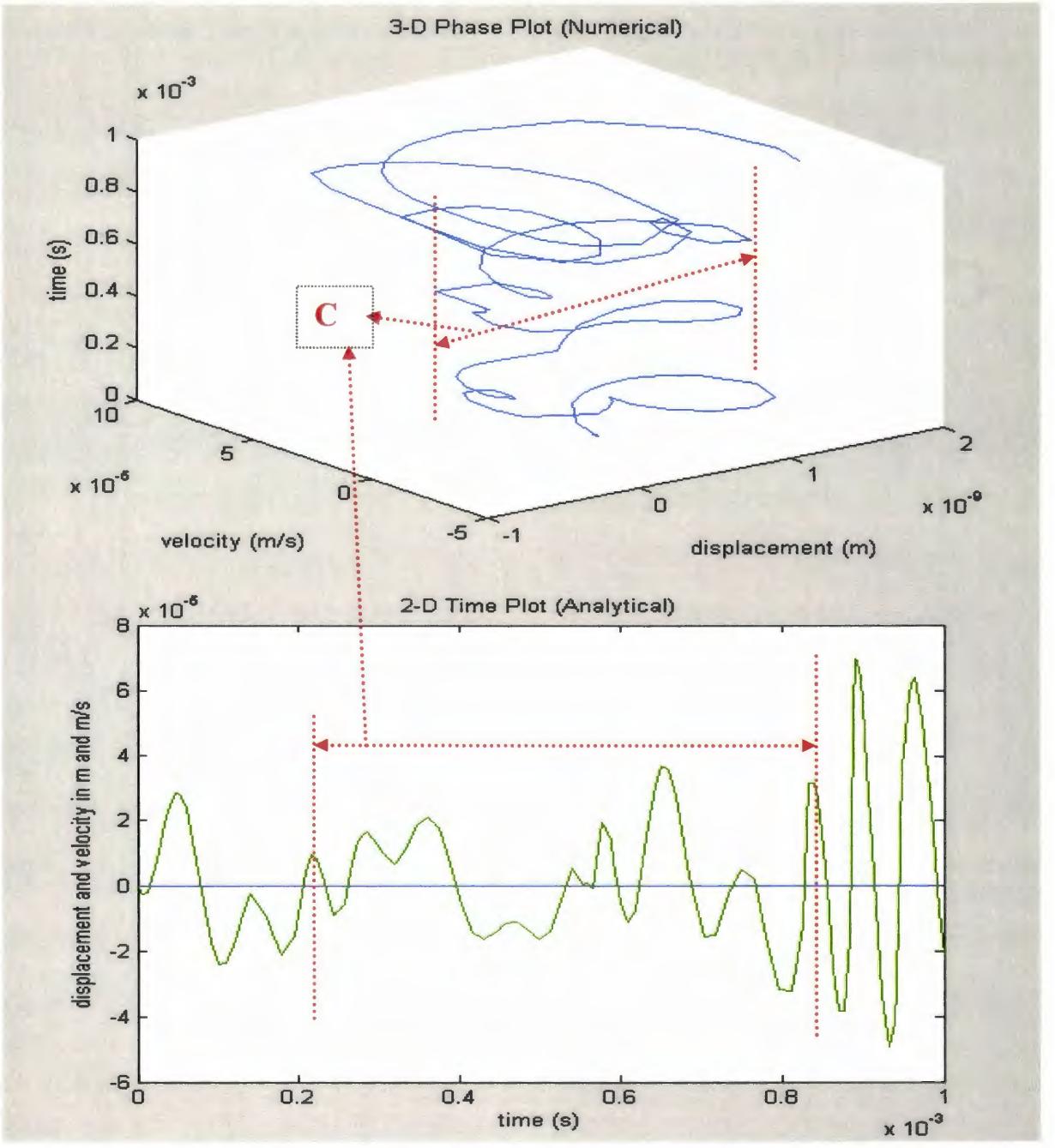

***Figure 2.7.1.7*: 3-D Nonlinear Phase and Time Plot for R = 1 Micro Meter, t = 0:0.001 Second**

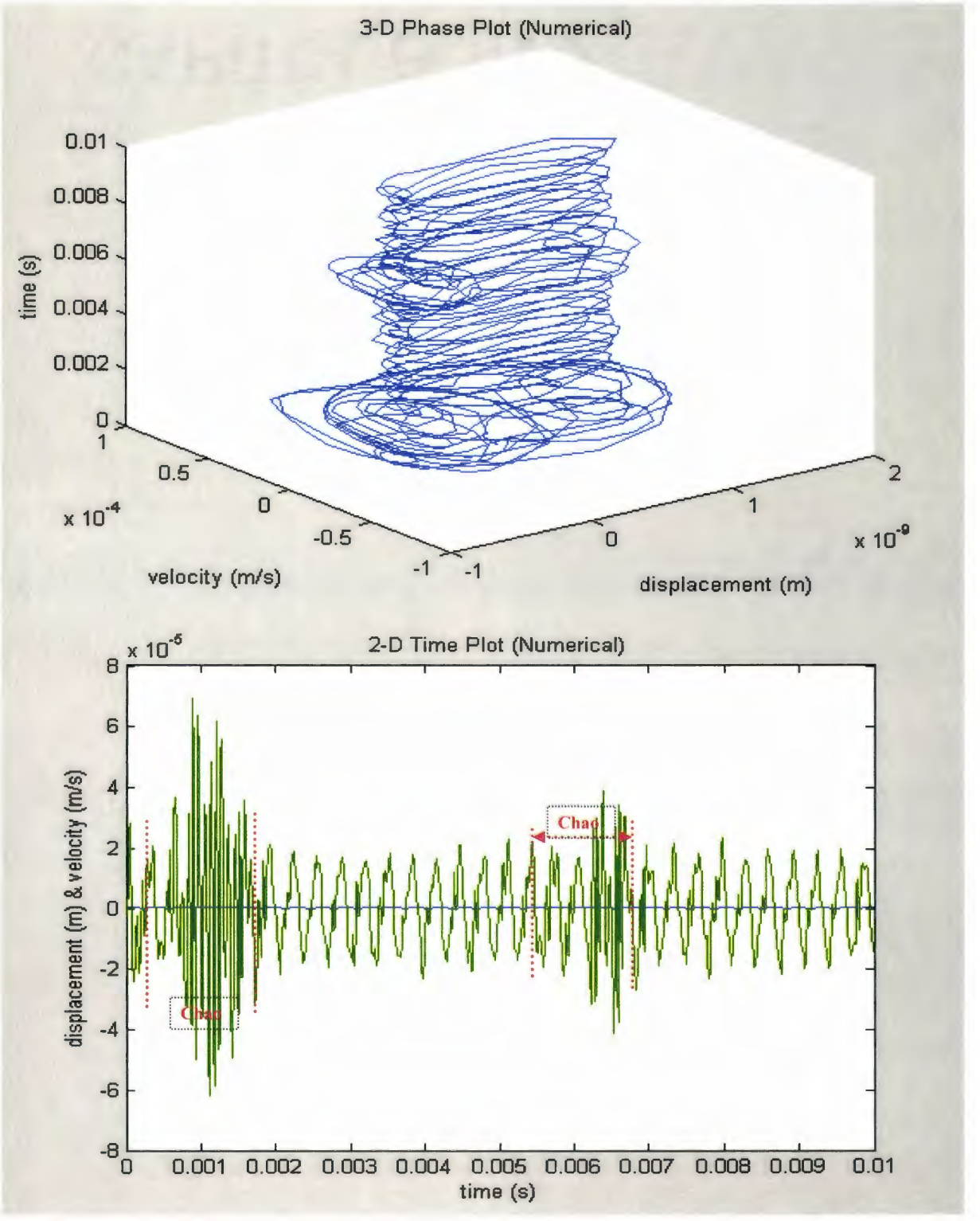

***Figure 2.7.1.8*: Nonlinear 3-D Phase and Time Plot for R = 1 Micro Meter, t = 0:0.01 Seconds**

From the above plots, it is found that the system, in its complete non – linear form, displays some sort of chaotic behavior. This is very difficult to study because all the stability analysis and eigen value analysis carried out, pertain to systems which have been linearized around the equilibrium point. So, in a broad sense, only a small region around the equilibrium point is studied and conclusions are made on the behavior of the system in that sense. But when the whole system in its complete non–linear form is studied, it is found that the time plot shows some sort of a chaotic behavior, wherein there are no observable patterns. There is also some beat frequency phenomenon happening but the significance of that on the system is lost due to the non–linearity.

From all this, an obvious method of particle removal is by inducing negative damping in the system. As explained earlier, a combination of positive and negative damping induces the system into a limit cycle behavior and if this limit cycle becomes unstable, such that all solution curves and trajectories starting nearby the limit cycle, spiral away from it, then the particle is separated from the substrate. The following simulation *(Figure 2.7.1.9)* has been carried out by considering the shift between positive and negative damping. Thus energy is being alternately pumped into the system and keeps getting dissipated. This change in energy scenario promotes limit cycle behavior.

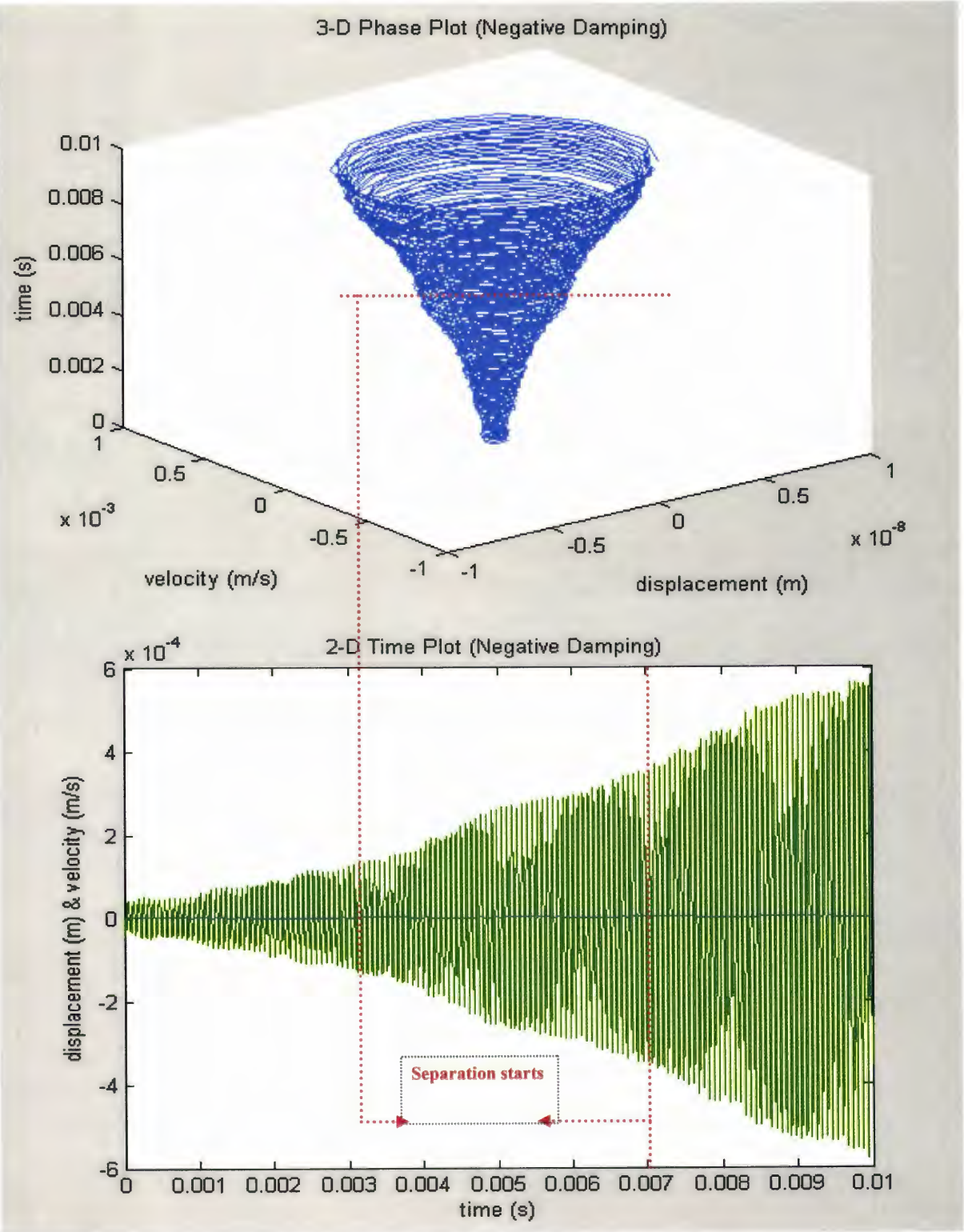

***Figure 2.7.1.9*: Nonlinear 3-D Phase and Time Plot for R = 1 Micro Meter, t = 0:0.01 Seconds with Non-linear damping.**

Thus, it is seen clearly that when there is a shift between positive and negative damping, the time plot shows a divergence and also the phase plot shows a curve growing in nature in the form of limit cycle instability. This curve grows unbounded and goes to infinity as the time period increases and goes to infinity. Thus, negative damping comes across as an effective method for particle removal by longitudinal vibrations.

The aim of this chapter was to theoretically study the phenomenon of stability versus instability as applied to micro/nano systems. There were two types of stability methods studied and the more robust of them was found to be the Lyapunov method of analysis. Simulations carried out, incorporating the stability criterion shows that particle removal is not possible for small frequency of vibration and medium amplitudes. The system is always going to be stable in such a case, as explained by the stability analysis. The complete non – linear system shows a chaotic behavior, which is hard to understand, given the limitations of the stability analysis to linearized dynamics. Better techniques would be to use Floquet analysis (Rand, 2003) for periodic systems or to carry out a study on the bifurcations, which can be seen in the non – linear system. This goes into the realm of chaos and is left as future work to be pursued. The phenomenon of negative damping comes across as an effective method for particle separation. But this is tough to be realized practically, which poses another problem and is left to the experimentalists to prove this technique. Above all, an increase in the amplitude of vibrations along with a large excitation frequency, coupled with negative damping, is sure to cause separation between the particle and substrate.

CHAPTER 3

LATERAL REMOVAL METHODS

3.1 INTRODUCTION

Lateral removal methods focuses on removal of the particle stuck to the substrate by means of utilizing the friction force. Generally, friction is defined as an impediment to motion. But in this case, friction plays an important role because, it aids in removal of the particle. The lateral removal model was first proposed by Busnaina et. al. (Busnaina et. al., 2002) for post CMP cleaning. They utilized brush cleaning methods to roll off the submicron silica or alumina particles stuck on the surface of silicon wafers. There are three different modes of cleaning proposed by them. Non-contact, partial contact and full contact cleaning techniques were found to be effective in particle removal. In the proposed lateral removal method, the aim is to improvise on the existing model and come up with a unique technique that utilizes friction and pull-off forces to separate the particle from the substrate. There will also be other removal techniques postulated, based on the shear stress and also by considering the fluid layer between the particle and the substrate, formed due to capillary condensation as a series of springs.

3.2 LATERAL FORCE MODEL

One of the drawbacks of the longitudinal vibrations method is that, for separation to be induced there is a requirement for large amplitude of vibrations. This might prove to be

detrimental to the system, as large amplitudes might break the fragile micro/nano scale device. Also, another possibility for removal, in the form of negative damping was proposed earlier on, in the longitudinal model. Though the idea sounds interesting, in that the flip between positive and negative damping, produces a limit cycle, wherein energy is dissipated and generated alternatively, the phenomenon of negative damping is difficult to be realized practically. Most of the real world systems do not consider such a possibility at all. Also, it is found that the stability analysis for the longitudinal model comes up with a criterion that depends on the damping coefficient. These drawbacks of the longitudinal model made it necessary to devise a simpler and more effective technique, which can bring about separation without any damage to the system under consideration. The longitudinal model concentrated on the dynamic point of view, while trying to solve the problem of particle adhesion. But the lateral force model will focus on the static point of view. The aim is to come up with an efficient model, without any hassles. Along the way, while developing this model, important conclusions regarding friction and adhesion forces can be formulated and a relationship can be framed between these two forces. The particle is pried loose, in the lateral removal model, by means of rolling. Typically there are two modes of removal, laterally.

1. **Removal by Sliding** -: In this technique, the particle is removed by sliding it off the substrate on which it is stuck. This means that, for the particle to be slid off, the ratio of the removal forces to the adhesion forces must be greater than or equal to 1. Once this is true, then, the particle is easily removed by sliding across the surface of the substrate. Hence for removal by sliding:

$$RS = \frac{\text{Removal Force}}{\text{Adhesion Force}} \geq 1, \quad \textit{(3.2.1)}$$

The removal force is comprised of the lateral force applied at the center of the particle and the adhesion force is comprised of the combination of the Van Der Waal (VDW) and Capillary forces.

2. **Removal by Rolling -:** In this technique, the particle is rolled off the surface of the substrate by means of a rolling moment. Because of elastic deformation between the particle and substrate, at the region of contact, induced by the deformation induced VDW forces, there is an indentation distance δ through which the particle has indented into the substrate, which can be evaluated by means of the Johnson – Kendall – Roberts (1971) theory. In this removal method, when moments are applied at the point at which the particle has indented into the surface, when the removal moment is greater than the adhesion resisting moments, then separation is induced. Thus, for removal by rolling:

$$RM = \frac{\text{Removal Moment}}{\text{Adhesion Resisting Moment}} \geq 1 \text{ , } \textbf{\textit{(3.2.2)}}$$

Generally removal by rolling is preferred to removal by sliding, as it is found that the kinetic energy consumed while rolling is only 5/7ths the kinetic energy consumed while sliding. This can be easily proved as shown below.

Consider a spherical ball, being slid and also rolled. Let the sliding velocity be 'u' and the rolling velocity be 'v' (say). When the ball is struck, it starts motion by sliding. As it travels, the friction between the ball and the ground causes it to start rolling until the rate of rolling is matched to its progress across the ground that is, there is no sliding. It can be easily proved that the kinetic energy of a rolling ball is 5/7ths the kinetic energy of a sliding ball with equal energy. Alternatively this

can be expressed as the velocity of a rolling ball travels at ~84% of the velocity of a sliding ball struck with equal force.

Consider a ball with an initial sliding velocity of *u*. The total energy, E_T , of the ball is solely its kinetic energy, E_K , the energy due to its skidding or sliding velocity. The kinetic energy is given by the following:

$$E_T = E_K = \frac{1}{2} m u^2$$

The mass of the ball is given by *m*. For a rolling ball with linear velocity ***v***, there are two components of energy; the kinetic energy as above and the rotational energy, E_R. The rotational energy for a body is given by the following equation, and the components of it follow.

$$E_R = \frac{1}{2} I \omega^2$$

I is the moment of inertia. For a solid sphere, i.e. the croquet ball, this is given by:

$$I = \frac{2}{5} m r^2$$

Again *m* is the mass of the ball and *r* is its radius. 'w' is the rotational velocity in radians per second:

$$\omega = \frac{v}{r}$$

Thus E_R is:

$$E_R = \frac{1}{2} \cdot \frac{2}{5} m r^2 \cdot \frac{v^2}{r^2} = \frac{1}{5} m v^2$$

For the rolling ball its total energy is the sum of the kinetic and rotational energy:

$$E_T = E_K + E_R$$

$$E_T = \frac{1}{2} m v^2 + \frac{1}{5} m v^2 = \frac{7}{10} m v^2$$

We can now compare the linear velocities of two balls hit with the same energy, one sliding and the other rolling. As E_T is the same,

$$\frac{7}{10} m v^2 = \frac{1}{2} m u^2$$

$$v^2 = \frac{5}{7} u^2$$

At this point, given that kinetic energy is proportional to the square of the velocity, we can see that the kinetic energy of the rolling ball is 5/7 (71.4%) that of a sliding ball.

Taking square roots yields the relative velocities:

$$v = 0.845\, u$$

Or, the rolling velocity is 84.5% of the skidding velocity. Thus, we can easily prove that the force required to remove a particle by rolling is less than the force required by sliding.

Thus, rolling and sliding are important methods and in the proposed method, attention is focused on rolling rather than sliding, for all the obvious reasons explained earlier.

Thus, for a) Removal by Sliding -: $RS = \frac{\text{Removal Force}}{\text{Adhesion Force}} \geq 1$, ***(3.2.3)***

b) Removal by Rolling -: $RM = \frac{\text{Removal Moment}}{\text{Adhesion Resisting Moment}} \geq 1$, ***(3.2.4)***

3.3 FORCES INVOLVED IN THE LATERAL REMOVAL MODEL

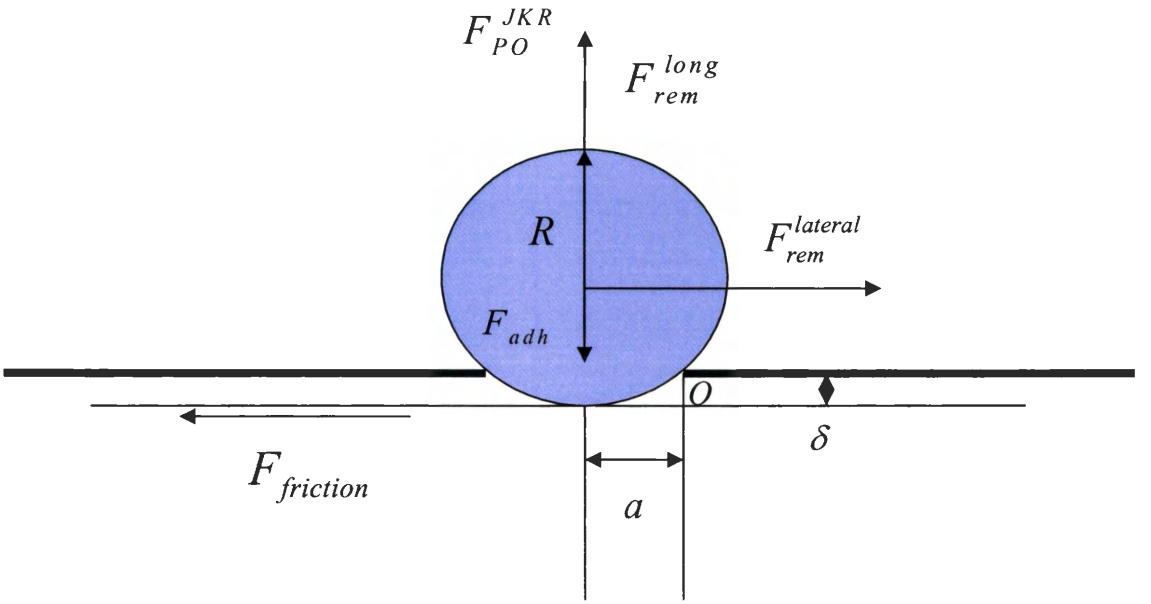

***Figure 3.3.1*: Schematic Diagram Representing the Forces Involved in the Lateral Removal Model**

1) **Adhesion Forces** -: The major contributors to the adhesion force are the VDW and capillary forces. The expressions for the same are as follows. Here, z is the distance between the particle and substrate that change with time. So, z = z (t). z_0 represents the initial separation between the particle and the substrate and so z_0 = 1.5 nano meters (from standard studies, (Israelachvili, 1985)). The particle radius is R and A represents the *Hamaker* constant for interaction between alumina and silicon. The particle is taken to be made of alumina and the substrate is made of silicon. Γ (gamma) represents surface tension of the fluid layer formed due to capillary condensation, between the particle and substrate.

The expression for **VDW** force is given as follows:

$$F_{VDW}^{ADH} = \frac{AR}{6(z+z_0)^2} + \frac{ARa^2}{6(z+z_0)^3}, \textbf{(3.3.1)}$$

The second term in the VDW force, represents the deformation induced Van Der Waal Force. This force is the cause for indentation of the particle into the substrate by elastic deformation.

The **capillary** force is given as follows:

$$F_{CAPS}^{ADH} = \frac{4\pi\gamma R\cos\theta}{\left(1+\frac{z}{z_0}\right)}, \textbf{(3.3.2)}$$

2) **Friction Force** -: The friction force plays a very important role in particle removal by the lateral force method. By evaluating the coefficient of friction between the

particle and substrate, by experimental means, we can get a relationship between the normal force and friction force. The normal force here pertains to the adhesion forces. Hence, there is a coupling between the lateral and longitudinal directions by means of the relationship between the friction and adhesion forces. The following equations hold true for the friction and adhesion forces:

$$F_{friction} = \mu N = \mu F^{ADH}$$

$$\text{But, } F^{ADH} = F_{VDW}^{ADH} + F_{CAPS}^{ADH} = \frac{AR}{6(z+z_0)^2} + \frac{ARa^2}{6(z+z_0)^3} + \frac{4\pi\gamma R\cos\theta}{\left(1+\frac{z}{z_0}\right)}$$

$$\Rightarrow F_{friction} = \mu\left[\frac{AR}{6(z+z_0)^2} + \frac{ARa^2}{6(z+z_0)^3} + \frac{4\pi\gamma R\cos\theta}{\left(1+\frac{z}{z_0}\right)}\right] \qquad \textit{, (3.3.3)}$$

$$\Rightarrow F_{friction} = \frac{AR\mu}{6(z+z_0)^2} + \frac{AR\mu a^2}{6(z+z_0)^3} + \frac{4\pi\gamma\mu R\cos\theta}{\left(1+\frac{z}{z_0}\right)}$$

3) **Repulsive Contact Force -:** Since there is elastic deformation occurring at the region of contact between the particle and substrate, due to the deformation induced VDW force, this deformation is modeled as a repulsive force, at the point of contact. Hence, the pull - off forces are evaluated at zero external load according to the JKR (Johnson – Kendall – Roberts, 1971) theory. Then while taking moments to evaluate the removal forces, this pull – off force can also be accounted for. For this we first need to evaluate the work of adhesion between the particle and

substrate, for a given material (alumina for particle and silicon for the substrate). Hence, the work of adhesion is given as:

$W_a = \frac{A}{12\pi z_0^2}$; where z_0 is the minimum separation between particle and substrate T

he JKR model predicts that the force required to pull – off the particle from the surface is given as:

$$F_{PO}^{JKR} = \frac{3}{4}\pi W_a D \text{ , } \textbf{(3.3.4)}$$

4) **Evaluation of the Indentation Distance -:** The next step is to evaluate the indentation distance, between the particle and surface. To evaluate this, we first need to know the contact radius 'a' and the work of adhesion. Both of them can be found from the JKR theory.

$$a = \left(\frac{3\pi W_a D}{2K}\right);$$

Here, K is the effective Young's Modulus for the particle and substrate. It is given as:

$$K = \frac{4}{3}\left(\frac{1-\nu_1^2}{E_1} + \frac{1-\nu_2^2}{E_2}\right)^{-1} \text{ , } \textbf{(3.3.5)}$$

Here, ν_1 and ν_2 are the Poission's' ratio for the particle and substrate; E_1 and E_2 are the Young's moduli for alumina and silicon (particle and substrate). Hence the indentation distance is given as:

$$\delta = \frac{a^2}{R} - \frac{2}{3}\sqrt{\frac{3\pi W_a a}{K}}, \textbf{(3.3.6)}$$

So, we have the expressions for all forces which can play a part in lateral removal of the particle from substrate. The next step is to evaluate moments at point O, near the point of indentation, at contact between the particle and substrate. Rolling is preferred over sliding as it requires lesser force. Thus if the removal moment ratio is greater than 1, then the particle is removed by rolling.

3.4 MOMENT BALANCE AT 0

Taking moments at O,

1) Clockwise moment due to lateral removal force -: $F_{rem}^{lateral}(R-\delta)$
2) Clockwise moment due to friction force -: $F_{friction}\delta$
3) Counter clockwise moment due to adhesion forces -: $\left(F_{VDW}^{ADH}a + F_{CAPS}^{ADH}a\right)$
4) Clockwise moment due to pull – off force -: $F_{PO}^{JKR}a$

Thus, the removal moments are taken care of, by the lateral removal force, Friction force and the Pull – off force. The adhesion resisting moments are taken care of, by the VDW and Capillary forces. Thus, the removal moment ratio is given as:

$$RM = \frac{F_{rem}^{lateral}(R-\delta) + F_{PO}^{JKR} a + F_{friction}\delta}{a\left(F_{VDW}^{ADH} + F_{CAPS}^{ADH}\right)}, \textbf{(3.4.1)}$$

Thus, when $RM \geq 1$ we get separation. This happens when the removal moment overcomes the adhesion resisting moment.

The next step is to compare the longitudinal removal and lateral removal forces. For separation to occur, through the lateral force model, the removal force is given as:

$$F_{rem}^{lateral} \geq \frac{a\left(F_{VDW}^{ADH} + F_{CAPS}^{ADH}\right) - F_{PO}^{JKR} a - F_{Friction}\delta}{(R-\delta)}, \textbf{(3.4.2)}$$

When we consider the longitudinal removal force, then the expression for the removal force, considering the longitudinal direction is given as:

$$F_{rem}^{long} \geq \frac{a\left(F_{VDW}^{ADH} - F_{CAPS}^{ADH}\right) - F_{PO}^{JKR} a - F_{friction}\delta}{a}, \textbf{(3.4.3)}$$

Hence, comparing the two removal forces, the only change occurs in the denominator. Removal can occur in both the cases, but it can bee seen that, if we have a lower removal force, it is better for the system. Hence comparing the denominator values, for different sized particles, after evaluating the indentation depth and contact radius, it can be established that the denominator in the lateral removal expression is greater than the one in the longitudinal removal expression. This further shows that the lateral removal force has a lower value than the longitudinal removal force. Hence, the lateral removal method is more efficient and not detrimental to the system.

Thus, by the above conclusion, it is obvious that the lateral force model has an edge over the longitudinal method. There are no vibrations which damage the system and there is also no necessity for negative damping. ***Table 3.4.1*** characterizes the particle radius, indentation depth and contact radius and comparison between $(R-\delta)$ and a shows that the former is greater than the contact radius.

***Table 3.4.1*: Comparison between Lateral and Longitudinal Models**

Radius, R (m)	Contact radius, a (m)	Indentation δ (m)	R – δ
1.0000E-03	1.9262E-06	3.5840E-09	1.0000E-03
1.0000E-04	4.1500E-07	1.6638E-09	9.9980E-05
1.0000E-05	8.9408E-08	7.7223E-10	9.9960E-06
1.0000E-06	1.9262E-08	3.5842E-10	9.9440E-07
1.0000E-07	4.1500E-09	1.6638E-10	9.9834E-08

It is obviously clear that column 4 is greater than column 2. The expressions for the indentation depth and contact radius are:

$$a = \left(\frac{3\pi W_a D}{2K} \right), \textbf{(3.4.4)}$$

$$K = \frac{4}{3}\left(\frac{1-\nu_1^2}{E_1} + \frac{1-\nu_2^2}{E_2} \right)^{-1}, \textbf{(3.4.5)}$$

$$\delta = \frac{a^2}{R} - \frac{2}{3}\sqrt{\frac{3\pi W_a a}{K}}, \textbf{(3.4.6)}$$

3.5 REMOVAL BY OPPOSING THE SHEAR FORCE

A second method of removal involves evaluating the shear stress and contact area and putting forth the idea that, removal is possible, if there is a force applied which is greater than the shear force caused by friction. Hence, here too, friction plays an important part. The contact area must be evaluated and since we are considering a circular contact, the contact area can be found out as:

$$A_s = \pi a^2 , \textbf{(3.5.1)}$$

The shear strength is independent of the applied load as well as the repulsive contact occurring between the particle and substrate at the contact point. The only change in the shear strength occurs near pull – off loads for a particular particle size and system parameters.

Thus when the removal force is greater than the shear force, we get separation. In terms of equations:

$$\text{Removal occurs when } F_{removal} > \tau A_s , \textbf{(3.5.2)}$$

3.6 REMOVAL BY CONSIDERING STIFFNESS OF FLUID LAYER

A third method of removal, by means of lateral force and moments, is to consider the fluid layer between the particle and substrate, formed due to capillary condensation, as a series of springs. There is a need to evaluate the stiffness of the springs. After that, a removal moment is applied. This is different from the previous method in that, the previous

method considered the contact stiffness and not the stiffness of the fluid layer. Thus when the applied moment overcomes the resistance offered by the springs, we get removal.

3.6.1 DETERMINATION OF STIFFNESS OF FLUID LAYER

Let the initial height of the fluid layer be 'h'. Then the change in height is given as Δh. This means that the strain is given as $\varepsilon = \frac{\Delta h}{h}$. Now if E is the elasticity of the fluid layer, then the stress is related to the strain by Hooke's law. Which implies that, $\sigma = \varepsilon E$. But the elasticity for water is related to the bulk modulus in the following manner: $E_{fluid} = 3K(1-2\nu)$. Generally Poisson's ratio for water assumed to be incompressible is 0.5. But for our calculations we consider it to be 0.499 because if it were 0.5 and the bulk modulus going to infinity, then the Young's modulus would become indeterminate. Thus:

$$\sigma = \varepsilon E = \frac{3\Delta h K(1-2\nu)}{h}$$

But, $F = k\Delta h \Rightarrow \sigma A = k\Delta h$

Here, A is the contact area = πa^2 , ***(3.6.1.1)***

Thus, $\left(k = \frac{3K(1-2\nu)A}{h} \right)$; where h = z_0 (Initial separation)

We have the stiffness by the above method. Hence if the applied moment is greater than the produce of the stiffness, indentation depth (which gives the deflection force) and the contact radius, separation is induced.

Thus for separation,applied moment $\geq k\delta a$. , ***(3.6.1.2)***

Three removal methods have been postulated. The first one considers rolling moments taken around the point O. The second method relies on the applied removal force being greater than the shear force for removal and the third method evaluates the stiffness of the fluid layer and puts forth the idea that for removal to occur, the applied moment must be greater than the product of the deflection force and contact radius. These removal methods need to be experimentally verified to strengthen their claim on particle removal. All in all, the lateral removal methods are found to be more advantageous than the longitudinal vibration model since the removal force necessary to separate the particle laterally is lower than the one required in the longitudinal direction. Hence damage to the system is reduced by utilizing the lateral removal methods. Future work in this area would involve experimental procedures to prove the theoretical postulates and to study the effectiveness of fluid drag force and mega sonic particle cleaning, in the lateral direction.

CHAPTER 4

REMOVAL BY COUPLED VIBRATIONS

4.1 INTRODUCTION

In the previous chapters (2 and 3), particle removal was made possible by means of longitudinal vibrations and lateral removal models. As seen earlier, the longitudinal model, while being theoretically right, puts forth ideas that may not be realized practically. The lateral removal models have to be proved experimentally, to strengthen their claim on particle removal. In this chapter, the focus is on a coupling between the lateral and longitudinal directions, induced by the relationship between the friction force in the lateral direction and adhesion forces in the longitudinal directions. The aim is to excite the dynamic system and look at the changes in separation between the particle and substrate. So, the idea is to break the fluid bond, by means of lateral forcing, at the same time, utilizing the longitudinal solution and coupling it with the lateral direction. Efforts are made, to provide a displacement or velocity coupling to the lateral model and corresponding change in separation is monitored. Once it is established that the amplitude of displacement is greater than the initial separation distance then the particle is free and detached from the substrate. The first portion of this chapter aims at characterizing a system matrix, based on which certain stability criteria are established. By inputting the stability conditions into the model and simulating it, using ODE solvers, particle removal is made possible. The phenomenon of

beat frequency which arises during simulation is also given due consideration and efforts are made to understand its evolution.

4.2 FORUMLATION OF THE DYNAMIC SYSTEM FOR COUPLED VIBRATIONS

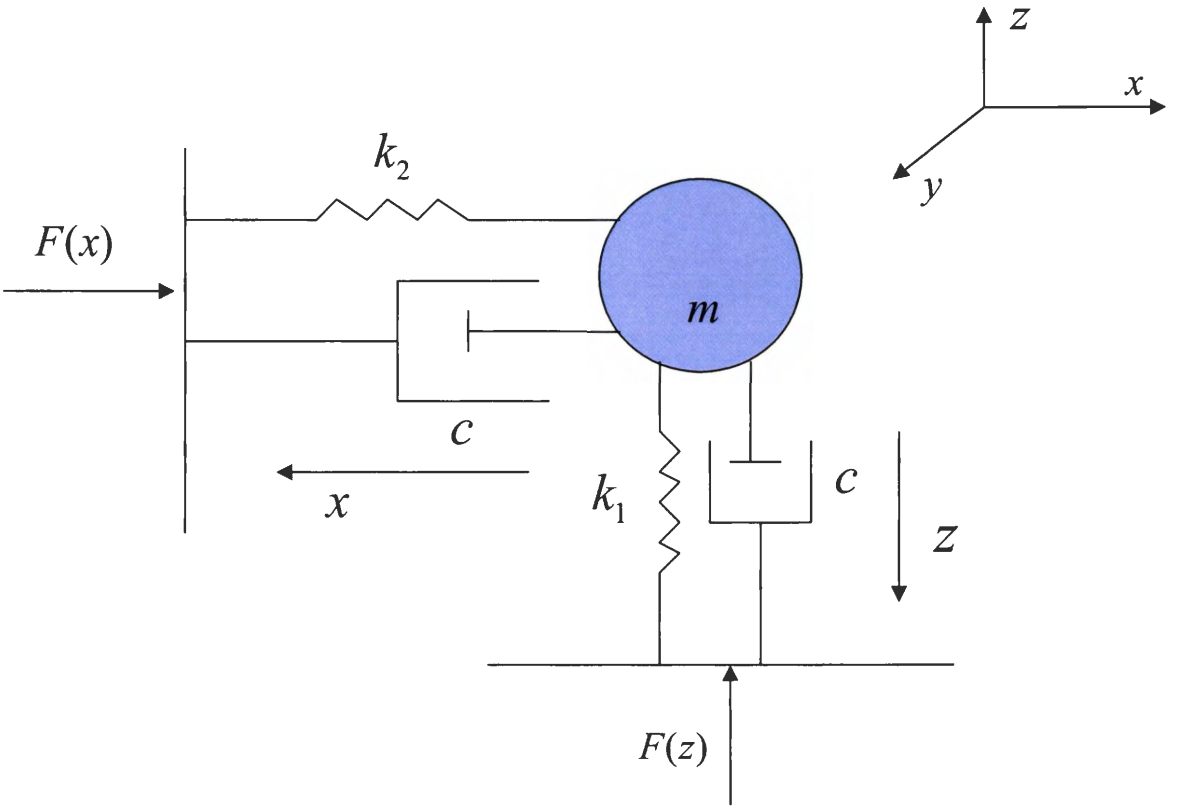

***Figure 4.2.1*: Formulation of the Dynamic System for Coupled Vibrations**

In *Figure 4.2.1*, F (x) and F (z) represent the sinusoidal excitation forces, provided as an input to destabilize the system. X, Y and Z represent the three axes. The axes under consideration will be Z along the longitudinal direction and X along the lateral direction; c is the damping coefficient, due to the fluid layer, formed by capillary condensation; k_1 and k_2 represent the longitudinal and lateral stiffness. The expressions for the same are provided

later on; m represents the mass of the particle, R is the radius of the particle. The stiffness considered here refers to the contact stiffness values. The following are the parameters considered. The particle size is varied and the corresponding parameters are found out from those listed on page 23 in Chapter 2.

1) Mass of the particle = m = $\frac{4}{3}\pi R^3\rho$; (ρ is the density of the particle)

2) Damping Coefficient = c = $6\pi\eta R$; (η is the kinematic viscosity)

3) Static Load = L = $\frac{AR}{6z_0^2} + 4\pi\gamma R\cos\theta$; (Load at t = 0)

4) Contact radius = a = $\sqrt[3]{\frac{3RL}{4E^*}}$

5) Effective Elastic Modulus = $E^* = \left[\frac{1-\nu_1^2}{E_1} + \frac{1-\nu_2^2}{E_2}\right]^{-1}$

6) Effective Bulk Modulus = $G^* = \left[\frac{2-\nu_1}{G_1} + \frac{2-\nu_2}{G_2}\right]^{-1}$

7) Longitudinal Stiffness = $k_1 = 2aE^*$

8) Lateral Stiffness = $k_2 = 8aG^*$

Thus, the different parameters are evaluated using the expressions show above and are charted out for calculations. The next step involves formulation of the dynamic model. As already seen in Chapter 2, the dynamic model is formulated along similar lines and the corresponding system equations are as follows. The system can be forced by sinusoidal vibrations and these vibrations themselves can be coupled together, if needed.

$$mz'' + k_1(z+z_0) + cz' = \frac{AR}{6(z+z_0)^2} + \frac{4\pi\gamma R\cos\theta}{(1+z/z_0)} + \bar{f}\sin(\omega t);\ \omega = k\omega_n;\ k \le 1$$

$$mx'' + k_2(x+x_0) + cx' = \frac{\mu AR}{6(z+z_0)^2} + \frac{4\pi\gamma\mu R\cos\theta}{(1+z/z_0)} + \bar{f}\cos(\omega t);\ \omega = k\omega_n;\ k \le 1 \quad \textit{(4.2.1)}$$

4.3 STABILITY CRITERIA BASED ON STEADY STATE SOLUTIONS OF THE COUPLED VIBRATIONS

A stability criteria, that provides a bound on the equilibrium points as well as the lateral stiffness is characterized here. Since the system equations are nonlinear, a Taylor series expansion is made, around the equilibrium point. The stability criterion can then provide information on the stability of the system as a whole and say whether the particle has separated from the substrate, once they are applied to the system.

Governing equations for the dynamic system are:

$$mz'' + k_1(z+z_0) + cz' = \frac{AR}{6(z+z_0)^2} + \frac{4\pi\gamma R\cos\theta}{(1+z/z_0)} + \bar{f}\sin(\omega t);\ \omega = k\omega_n;\ k \le 1$$

$$mx'' + k_2(x+x_0) + cx' = \frac{\mu AR}{6(z+z_0)^2} + \frac{4\pi\gamma\mu R\cos\theta}{(1+z/z_0)} + \bar{f}\cos(\omega t);\ \omega = k\omega_n;\ k \le 1 \quad \textit{(4.3.1)}$$

Since the VDW and Capillary force terms are nonlinear, we linearize them by Taylor's expansion, around the equilibrium point. Considering the equilibrium point to be Z_1; it is given as $(z, z') = (z_1, 0)$.

Let, $f_1(z) = \dfrac{AR}{6(z+z_0)^2} \equiv \dfrac{\Gamma_1}{(z+z_0)^2} \Rightarrow \Gamma_1 = \dfrac{AR}{6}$

Let, $f_2(z) = \dfrac{4\pi\gamma R\cos\theta}{(1+z/z_0)} \equiv \dfrac{\Gamma_2}{(z+z_0)} \Rightarrow \Gamma_2 = 4\pi\gamma z_0 R\cos\theta$

By evaluating a Taylor's series at the equilibrium point $(z,z') = (z_1,0)$ we get the following

$$\rightarrow f_1(z)_{(z_1,0)} = \frac{\Gamma_1}{(z+z_0)^2}_{(z_1,0)} = \frac{\Gamma_1}{(z_1+z_0)^2} - \frac{2\Gamma_1(z+z_0-z_1)}{(z_1+z_0)^3}$$

$$\rightarrow f_2(z)_{(z_1,0)} = \frac{\Gamma_2}{(z+z_0)}_{(z_1,0)} = \frac{\Gamma_2}{(z_1+z_0)} - \frac{\Gamma_2(z+z_0-z_1)}{(z_1+z_0)^2}$$

Also, let $\dfrac{\Gamma_1}{(z_1+z_0)^2} = \bar{\varepsilon}_1;\ \dfrac{2\Gamma_1}{(z_1+z_0)^3} = \bar{\varepsilon}_2;$

$$\frac{\Gamma_2}{(z_1+z_0)} = \bar{\delta}_1;\ \frac{\Gamma_2}{(z_1+z_0)^2} = \bar{\delta}_2; \qquad , (4.3.2)$$

$(z_0 - z_1) = \xi$

Hence, the dynamic equations for the lateral and longitudinal cases are as follows -:

$$mz'' + k_1(z+z_0) + cz' = \bar{\varepsilon}_1 - \bar{\varepsilon}_2(z+\xi) + \bar{\delta}_1 - \bar{\delta}_2(z+\xi) + F$$

$$\Rightarrow z'' + \omega^2{}_{n1}(z+z_0) + 2bz' = (\varepsilon_1+\delta_1) - (z+\xi)(\varepsilon_2+\delta_2) + F$$

$$\Rightarrow x'' + \omega^2{}_{n2}(x+x_0) + 2bx' = \mu(\varepsilon_1+\delta_1) - \mu(z+\xi)(\varepsilon_2+\delta_2) + F$$

If we consider the homogenous case,

$$z'' + \omega^2{}_{n1}(z+z_0) + 2bz' = (\varepsilon_1+\delta_1) - (z+\xi)(\varepsilon_2+\delta_2)$$

$$\Rightarrow z'' + \omega_{n1}^2 z + \omega_{n1}^2 z_0 + 2bz' = [\varepsilon_1+\delta_1 - \xi(\varepsilon_2+\delta_2)] - z(\varepsilon_2+\delta_2)$$

$$\Rightarrow z'' + 2bz' + z[\omega_{n1}^2 + (\varepsilon_2+\delta_2)] = [\varepsilon_1+\delta_1 - \xi(\varepsilon_2+\delta_2) - \omega_{n1}^2 z_0] \qquad , \textit{(4.3.3)}$$

Let $[\varepsilon_1+\delta_1 - \xi(\varepsilon_2+\delta_2) - \omega_{n1}^2 z_0] = \alpha_1$; $[\omega_{n1}^2 + (\varepsilon_2+\delta_2)] = \beta_1$; (say)

Then, $\Rightarrow \left[z'' + 2bz' + \beta_1 z = \alpha_1\right] \cdots\cdots (1)$

Similarly,

$$x'' + \omega^2{}_{n2}(x + x_0) + 2bx' = \mu(\varepsilon_1 + \delta_1) - \mu(z + \xi)(\varepsilon_2 + \delta_2)$$

$$\Rightarrow x'' + \omega^2{}_{n2}(x + x_0) + 2bx' = [\mu(\varepsilon_1 + \delta_1) - \mu\xi(\varepsilon_2 + \delta_2)] - \mu z(\varepsilon_2 + \delta_2)$$

$$\Rightarrow x'' + 2bx' + x(\omega^2{}_{n2}) + z\mu(\varepsilon_2 + \delta_2) = [\mu(\varepsilon_1 + \delta_1) - \mu\xi(\varepsilon_2 + \delta_2) - \omega^2{}_{n2}x_0] \quad \textbf{(4.3.4)}$$

Let $[\mu(\varepsilon_1 + \delta_1) - \mu\xi(\varepsilon_2 + \delta_2) - \omega^2{}_{n2}x_0] = \alpha_2;\ \mu(\varepsilon_2 + \delta_2) = \beta_2;$ (say)

Then, $\Rightarrow \left[x'' + 2bx' + x(\omega^2{}_{n2}) + \beta_2 z = \alpha_2\right] \cdots\cdots (2)$

Now a sinusoidal forcing function is considered to be acting on the particle in both the longitudinal and lateral directions. Hence,

$$F_{lateral} = f\sin(\omega t)$$
$$F_{longitudinal} = f\cos(\omega t) \quad \textbf{(4.3.5)}$$

Both the forces are normalized by the mass of the particle under scrutiny. The next step involves the assumptions for steady state solutions. The steady state solutions for the two dynamic equations (1) and (2) are assumed to be sinusoidal as well. Therefore, the steady state solutions are:

$$z = z_0\cos(\omega t) \Rightarrow z' = -\omega z_0\sin(\omega t) \Rightarrow z'' = -\omega^2 z_0\cos(\omega t)$$
$$x = x_0\sin(\omega t) \Rightarrow x' = \omega x_0\cos(\omega t) \Rightarrow x'' = -\omega^2 x_0\sin(\omega t) \quad \textbf{(4.3.6)}$$

The steady state solutions along with the forcing functions are substituted into equations (1) and (2) and we arrive at a characteristic matrix. The eigen values are solved for, from the characteristic equations and the stability criteria arrived at. Based on the critical values obtained from solving for the eigen value and applying the condition for stability, it can be easily gauged if the system under consideration is stable or unstable, once it overshoots the bounds provided by the stability analysis. The stability analysis provides with a stability condition for the equilibrium point and lateral stiffness as follows:

$$\left[z'' + 2bz' + \beta_1 z = \alpha_1\right]$$

$$\left[x'' + 2bx' + x(\omega^2{}_{n2}) + \beta_2 z = \alpha_2\right]$$

Substituting the steady state solutions,

$$\left\langle -\omega^2 z_0 \cos(\omega t) - 2b\omega z_0 \sin(\omega t) + \beta_1 z_0 \cos(\omega t) = \alpha_1 + f\cos(\omega t)\right\rangle$$

$$\left\langle -\omega^2 x_0 \sin(\omega t) + 2b\omega x_0 \cos(\omega t) + \omega^2{}_{n2} x_0 \sin(\omega t) + \beta_2 z_0 \cos(\omega t) = \alpha_2 + f\sin(\omega t)\right\rangle \qquad ,(4.3.7)$$

$$\Rightarrow \left\langle z_0 \cos(\omega t)\left(\beta_1 - \omega^2 - \frac{f}{z_0}\right) + z_0 \sin(\omega t)\left(-2b\omega\right) + x_0 \cos(\omega t)(0) + x_0 \sin(\omega t)(0) = \alpha_1\right\rangle$$

$$\Rightarrow \left\langle x_0 \cos(\omega t)\left(2b\omega\right) + x_0 \sin(\omega t)\left(-\omega^2 + \omega^2{}_{n2} - \frac{f}{x_0}\right) + z_0 \cos(\omega t)(\beta_2) + z_0 \sin(\omega t)(0) = \alpha_2\right\rangle$$

Writing this as a matrix form, and then forming the characteristic matrix, we have -:

$$\Rightarrow \begin{pmatrix} \left(\beta_1 - \omega^2 - \frac{f}{z_0}\right) & \left(-2b\omega\right) \\ \beta_2 & 0 \end{pmatrix} \Leftrightarrow \begin{pmatrix} z_0 \cos(\omega t)(EQ1) & z_0 \sin(\omega t)(EQ1) \\ z_0 \cos(\omega t)(EQ2) & z_0 \sin(\omega t)(EQ2) \end{pmatrix}$$

$$\Rightarrow \begin{pmatrix} 0 & 0 \\ 2b\omega & \left(-\omega^2 + \omega^2{}_{n2} - \frac{f}{x_0}\right) \end{pmatrix} \Leftrightarrow \begin{pmatrix} x_0 \cos(\omega t)(EQ1) & x_0 \sin(\omega t)(EQ1) \\ x_0 \cos(\omega t)(EQ2) & x_0 \sin(\omega t)(EQ2) \end{pmatrix}$$

Thus we have the characteristic matrices as shown above.

We then evaluate the eigenvalues from the characteristic matrix formed as shown above.

$$\begin{vmatrix} \lambda - \left(\beta_1 - \omega^2 - \frac{f}{z_0}\right) & \left(\frac{(-2b\omega)}{1}\right) \\ \beta_2 & \lambda - 0 \end{vmatrix} = 0 \qquad , (4.3.8)$$

$$\begin{vmatrix} \frac{\lambda - 0}{1} & 0 \\ \frac{2b\omega}{1} & \lambda - (-\omega^2 + \omega^2{}_{n2} - \frac{f}{x_0}) \end{vmatrix} = 0$$

The characteristic equations are:

$$\lambda^2 - \lambda\left(\beta_1 - \omega^2 - \frac{f}{z_0}\right) + 2b\omega\beta_2 = 0 \text{ (From longitudinal dynamic system)} \cdots\cdots\cdots (3)$$

$$\lambda^2 - \lambda\left(\omega^2{}_{n2} - \omega^2 - \frac{f}{x_0}\right) = 0 \text{ (From lateral dynamic system)} \cdots\cdots\cdots (4)$$

Solving the above equations and by stating that for stability, the eigen values must be lesser than zero, we get the criteria for stability.

From (1), for stability, $\lambda < 0$

$$\Rightarrow \lambda_{1,2} = \frac{\left(\beta_1 - \omega^2 - \frac{f}{z_0}\right) \pm \sqrt{\left(\beta_1 - \omega^2 - \frac{f}{z_0}\right)^2 - 8b\omega\beta_2}}{2}$$

$$\Rightarrow \lambda_1 < 0 \Rightarrow \frac{\left(\beta_1 - \omega^2 - \frac{f}{z_0}\right) + \sqrt{\left(\beta_1 - \omega^2 - \frac{f}{z_0}\right)^2 - 8b\omega\beta_2}}{2} < 0$$

$$\Rightarrow \left(\beta_1 - \omega^2 - \frac{f}{z_0}\right) < -\sqrt{\left(\beta_1 - \omega^2 - \frac{f}{z_0}\right)^2 - 8b\omega\beta_2}$$

$$\Rightarrow \left(4c\omega\beta_2 < 0\right) \cdots\cdots\cdots (a)$$

$\Rightarrow \beta_2 < 0$ (as c and ω are always > 0)

$\Rightarrow \mu(\varepsilon_2 + \delta_2) < 0$

$$\Rightarrow \frac{2\Gamma_1}{(z_1 + z_0)^3} + \frac{\Gamma_2}{(z_1 + z_0)^2} < 0$$

$$\Rightarrow \left\langle z_1 < -\left(\frac{2\Gamma_1}{\Gamma_2} + z_0\right)\right\rangle \cdots\cdots\cdots (a) \qquad \textbf{, (4.3.9)}$$

$$\Gamma_1 = \frac{AR}{6m};\ \Gamma_2 = 4\pi\gamma z_0 R\cos\theta \Rightarrow \frac{2\Gamma_1}{\Gamma_2} = \frac{A}{12\pi\gamma z_0}$$

From (4), we get the following condition -:

$$\omega^2{}_{n2} - \omega^2 - \frac{f}{x_0} < 0 \qquad \text{, (4.3.10)}$$

$$\Rightarrow \left(\omega^2{}_{n2} < \omega^2 + \frac{f}{x_0} \right) \cdots\cdots\cdots (b)$$

From (a) and (b), the condition for stability is arrived at. If the equilibrium point crosses this condition for stability, or if the lateral stiffness exceeds the stability criterion, then the system becomes unstable, which in other words mean that the particle will get separated from the substrate.

4.4 SIMULATION OF THE COUPLED SYSTEM BASED ON THE STABILITY CRITERION

The dynamic system is simulated, by first solving the longitudinal equation. The longitudinal system is linearized around the equilibrium point and the linearized system is solved, using the method of variation of parameters. The solution obtained by this, is input into the lateral system, which is coupled in both the X and Z directions. The idea here is to obtain information on the separation of the particle laterally, whether it breaks the liquid bridge, when the lateral system, coupled with the longitudinal solution, is forced sinusoidally. In the longitudinal direction, the dynamic system is as shown below:

$$\text{Problem -: } mz'' + k_1(z + z_0) + cz' = \frac{AR}{6(z + z_0)^2} + \frac{4\pi\gamma R z_0}{(z + z_0)} + f\sin(\omega t)\text{ , } \textbf{(4.4.1)}$$

The equilibrium point is solved for, in the first place. When the dynamic system is solved, there will be four equilibrium points, corresponding to the four roots of the equation. For

finding the equilibrium point, the velocity and acceleration are both equated to zero and the corresponding equation obtained, is solved for and roots are found.

After linearization, the system has the form, as show below

$z_1' = z_2$

$z_2' = -Az_1 - bz_2$, where $-A = -\frac{k_1}{m} - \frac{2AR}{6m(z+z_0)^3} - \frac{4\pi\gamma R z_0}{m(z+z_0)^2}$; $-b = -\frac{c}{m}$

Thus, $z'' + bz' + Az = 0 \rightarrow (Homogenous)$

General solution for the linearized equation -:

Let, $z = e^{rt} \rightarrow z' = re^{rt}; z'' = r^2 e^{rt}$

So, $e^{rt}(r^2 + br + A) = 0 \rightarrow r = \frac{-b \pm \sqrt{b^2 - 4A}}{2}$

Thus, $z = c_1 e^{r_1 t} + c_2 e^{r_2 t}$, where $r_1 = \frac{-b + \sqrt{b^2 - 4A}}{2}$; $r_2 = \frac{-b - \sqrt{b^2 - 4A}}{2}$

c_1 and c_2 can be found out from the initial conditions.

When we input a forcing function, scaled by the mass of the system, then we need to find the particular solution for the system.

Thus, $z'' + bz' + Az = f\sin(\omega t)$

So, we choose $z = a\cos(\omega t) + c\sin(\omega t)$, as the particular solution, with a and c being constants. We then substitute it into the main equation, and by equating the coefficients of cosine and sine on both sides, we can find out what a and b are. After that we take the initial conditions into account and find out the value of c_1 and c_2

Thus, the solution for the longitudinal dynamic system is given as follows -:

$$\left(z(t) = c_1 e^{r_1 t} + c_2 e^{r_2 t} + a\cos(\omega t) + b\sin(\omega t)\right)$$

Where,

$$c_1 = -\frac{[cw + r_2(z_0 - a)]}{[r_1 - r_2]}$$

$$c_2 = \frac{[cw + r_1(z_0 - a)]}{[r_1 - r_2]}, \textbf{(4.4.2)}$$

$$r_1 = \frac{-b + \sqrt{b^2 - 4A}}{2}$$

$$r_2 = \frac{-b - \sqrt{b^2 - 4A}}{2}$$

$$a = -\frac{fb\omega}{[(A - \omega^2)^2 + (b\omega)^2]}, \textbf{(4.4.3)}$$

$$c = \frac{f(A - \omega^2)}{[(A - \omega^2)^2 + (b\omega)^2]}$$

$$\omega = l\omega_n;\ l \le 1$$

This is the solution to the equation:

$$z'' + bz' + Az = f\sin(\omega t), \textbf{(4.4.4)}$$

The dynamic equation for the lateral system is as follows:

$$mx'' + k_2(x + x_0) + cx' = \frac{\mu AR}{6(z + z_0)^2} + \frac{4\pi\gamma\mu R\cos\theta}{(1 + z/z_0)} + \bar{f}\cos(\omega t);\ \omega = \mathrm{L}\omega_n;\ \mathrm{L} \le 1, \textbf{(4.4.5)}$$

Hence, the solution obtained for z(t) can be substituted into the above equation and the dynamic system can be simulated using the ODE45 solver in Matlab.

Writing the above system as a sequence of first order systems,

$x_1' = x_2$

$$x_2' = -\frac{k_2}{m}(x_1 + x_0) - \frac{c}{m}x_2 + \frac{\mu AR}{6(z + z_0)^2} + \frac{4\pi\gamma\mu R\cos\theta}{(1 + z/z_0)} + f\cos(\omega t), \textbf{(4.4.6)}$$

Hence,

$$\begin{bmatrix} x' \\ x_2' \end{bmatrix} = \begin{pmatrix} 0 & 1 \\ -\frac{k_2}{m} & \frac{c}{m} \end{pmatrix} \begin{pmatrix} x_1 \\ x_2 \end{pmatrix} + \begin{pmatrix} 0 \\ \frac{\mu AR}{6(z + z_0)^2} + \frac{4\pi\gamma\mu R\cos\theta}{(1 + z/z_0)} \end{pmatrix} + \begin{pmatrix} 0 \\ f\cos(\omega t) \end{pmatrix}$$

The initial conditions are as follows -:

z(0)=1.5nm (thickness of condensed fluid film); z′(0)=0; , ***(4.4.7)***

x(0)='a' (contact radius); x′(0)=0

The equilibrium points for various particle sizes are as shown below. After applying the stability criterion for the equilibrium point, it is found that the equilibrium point value must be lesser than the following-:

By Stability Analysis

$$z_1 < -\left(\frac{2\Gamma_1}{\Gamma_2} + z_0\right) = -\left(\frac{A}{12\pi\gamma z_0} + z_0\right), \textbf{(4.4.8)}$$

$$\Rightarrow z_1 < -(1.52e-9)m$$

Thus, in the set of equilibrium points evaluated, those points which do not satisfy the above condition are discarded and the stable equilibrium points are taken into consideration.

4.5 EQUILIBRIUM POINTS FOR VARIOUS PARTICLE SIZES

The following are the various equilibrium points for particle size ranging from one milli meter to one hundred nano meters.

Radius = 1 mm (*1e-08)	**Radius = 100 µm (*1e-08)**	**Radius = 10 µm (*1e-08)**	**Radius = 1 µm (*1e-08)**	**Radius = 100 nm (*1e-08)**
-0.4307 (Unstable)	**-0.3755 (Unstable)**	**-0.3414 (Unstable)**	**-0.3214 (Unstable)**	**-0.3106 (Unstable)**
-0.1510 (Stable)	**-0.1514 (Stable)**	**-0.1521 (Stable)**	**-0.1529 (Stable)**	**-0.1535 (Stable)**
-0.0172 (Stable)	**-0.0716 (Stable)**	**-0.1044 (Stable)**	**-0.1227 (Stable)**	**-0.1325 9Stable)**

4.6 SIMULATIONS FOR THE LATERAL SYSTEM, THROUGH STABLE AND UNSTABLE EQUILIBRIUM POINTS

The idea here is to utilize the stable equilibrium points and simulate the system. What is expected here is stable behavior, in the sense of a stable spiral or focus and also the time plot against displacement and velocity, showing sinusoidal or converging behavior (when energy is dissipated due to damping). All these plots go to show that the stability analysis was carried out right and that the particle though it oscillates about its mean position by a large magnitude, it still is not enough to bring about separation. For separation, the unstable equilibrium points will have to be considered while simulating the system. In the following plots, velocity and displacements are measured in meters per second (m/s) and meters (m). Time is measured in seconds (s).

The ODE45 solver from Matlab gives the following plots *(Figures 4.6.1 to 4.6.6)* for the Phase Space portrait and also the time plot against velocity.

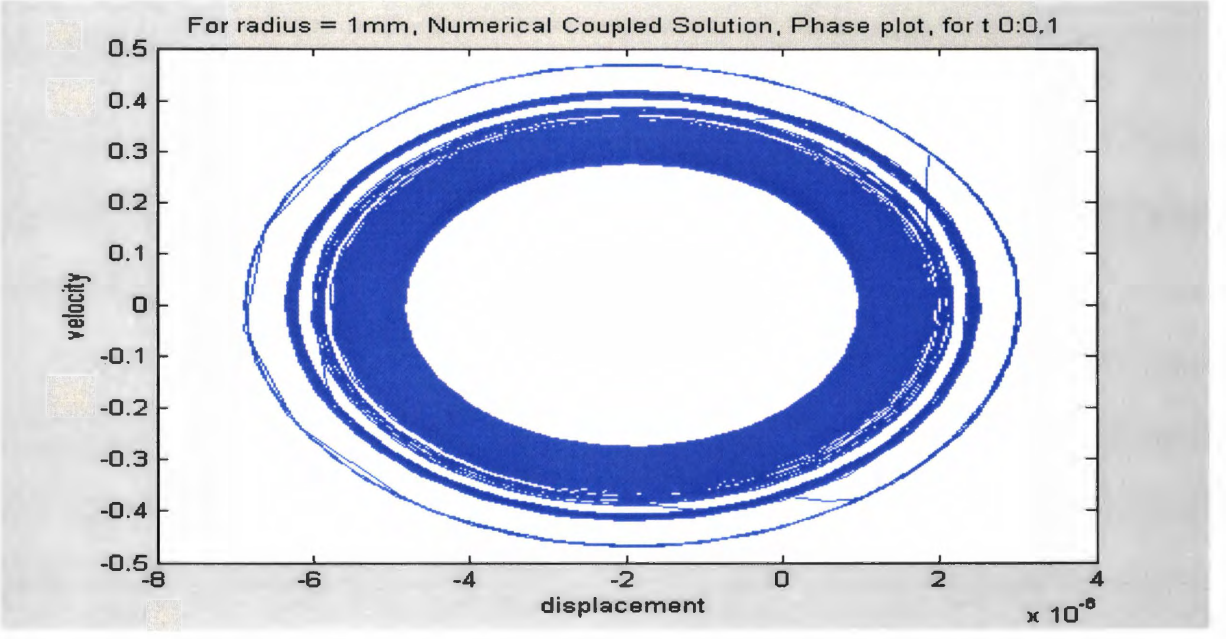

***Figure 4.6.1*: 2-D Linearized Phase Plot for Particle of R = 1mm, t = 0:0.01 seconds**

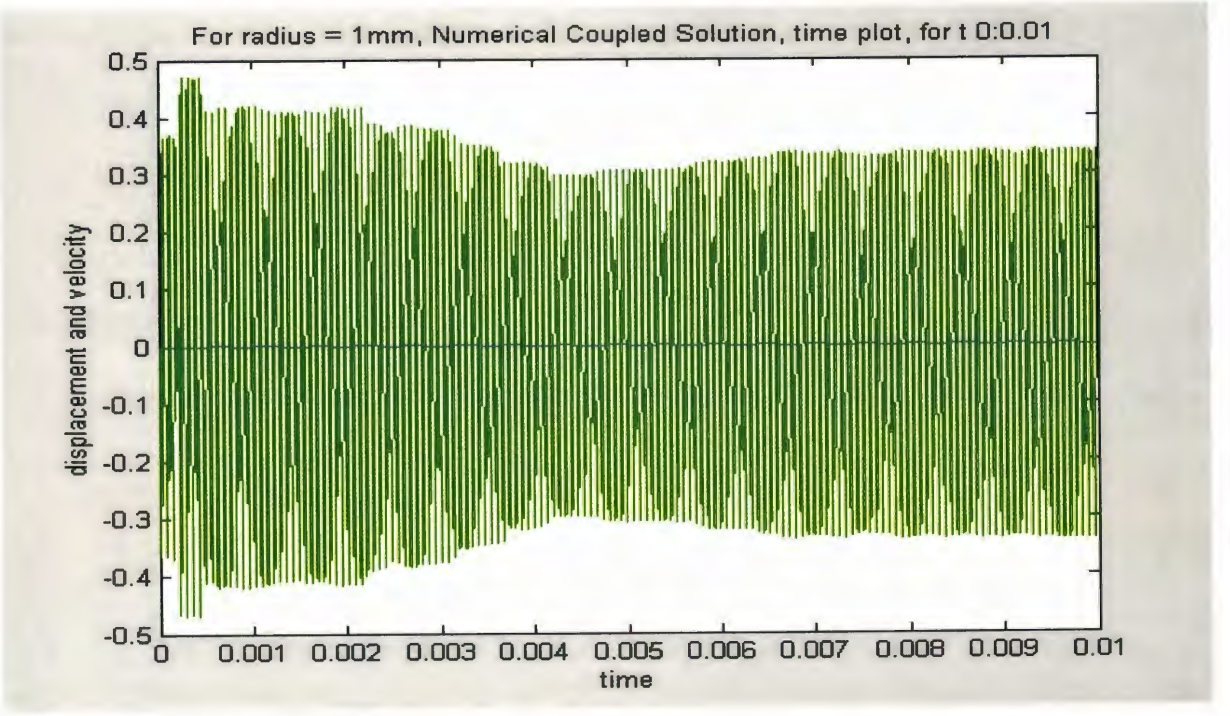

***Figure 4.6.2*: Linearized Time Plot for Particle of R = 1mm, t = 0:0.01 seconds**

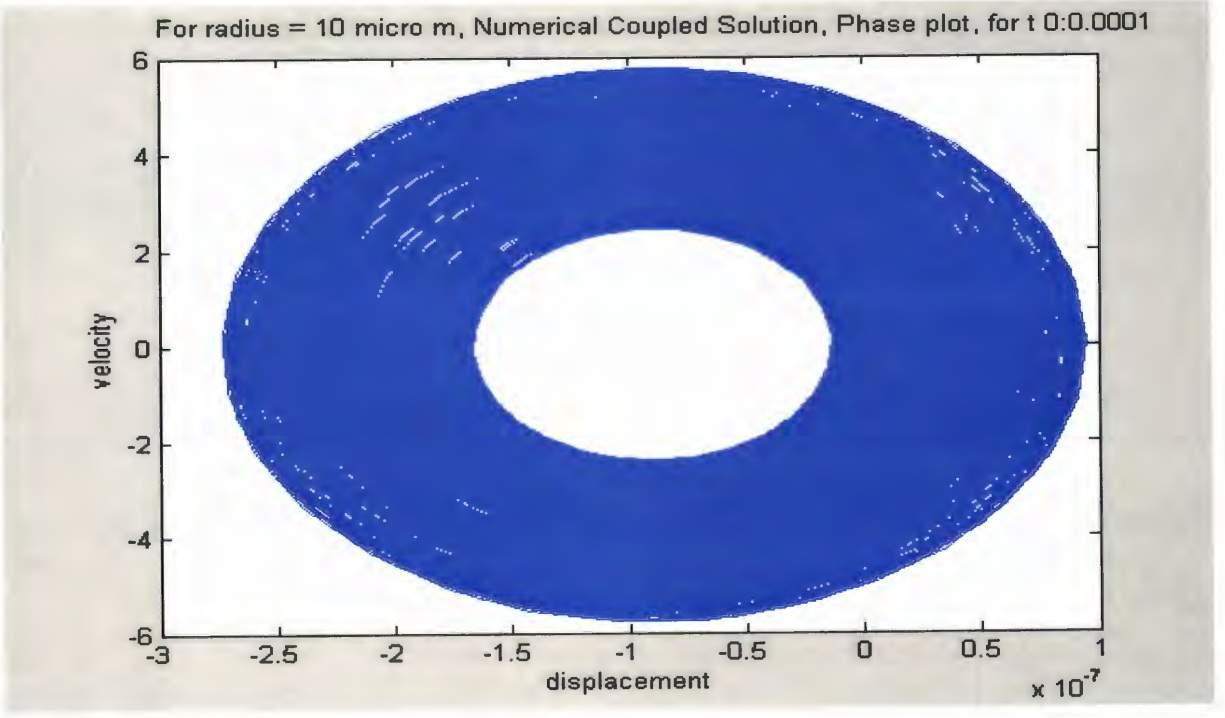

***Figure 4.6.3*: 2-D Linearized Phase Plot for Particle of R = 10 μm, t = 0:0.001s**

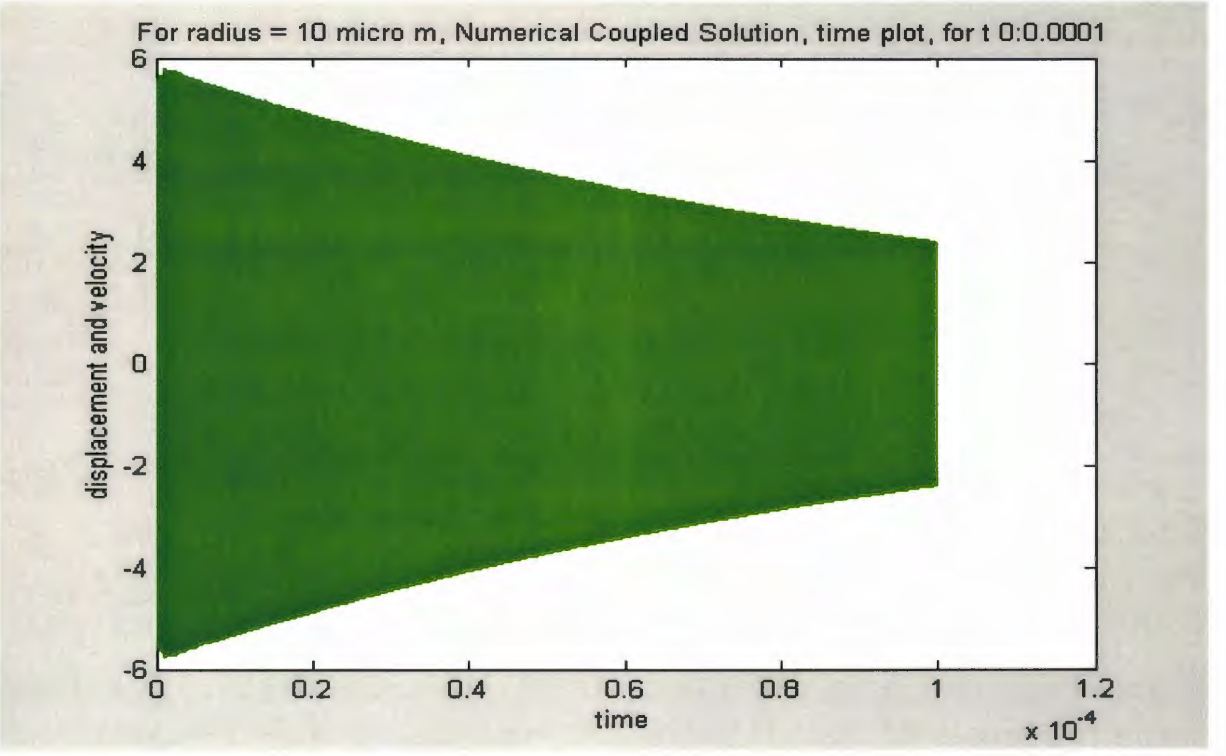

***Figure 4.6.4*: Linearized Time Plot for Particle of R = 10 μm, t = 0:0.0001 seconds**

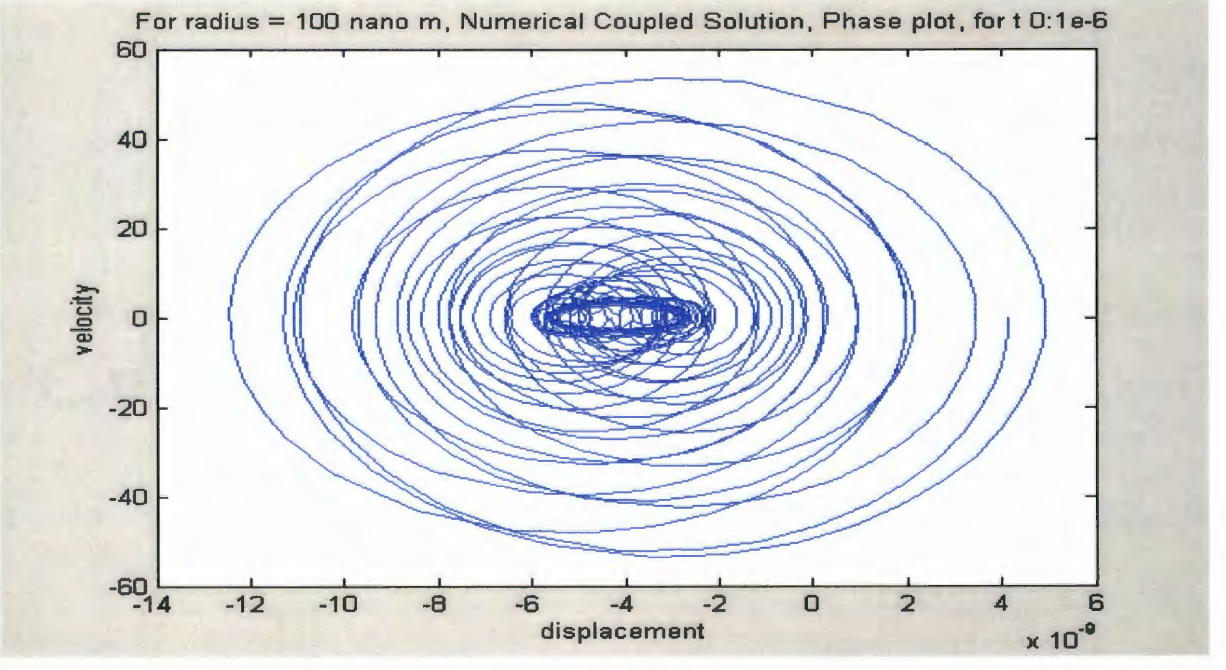

***Figure 4.6.5*: 2-D Linearized Phase Plot for Particle of R = 100 nm, t = 0:1e-6 s**

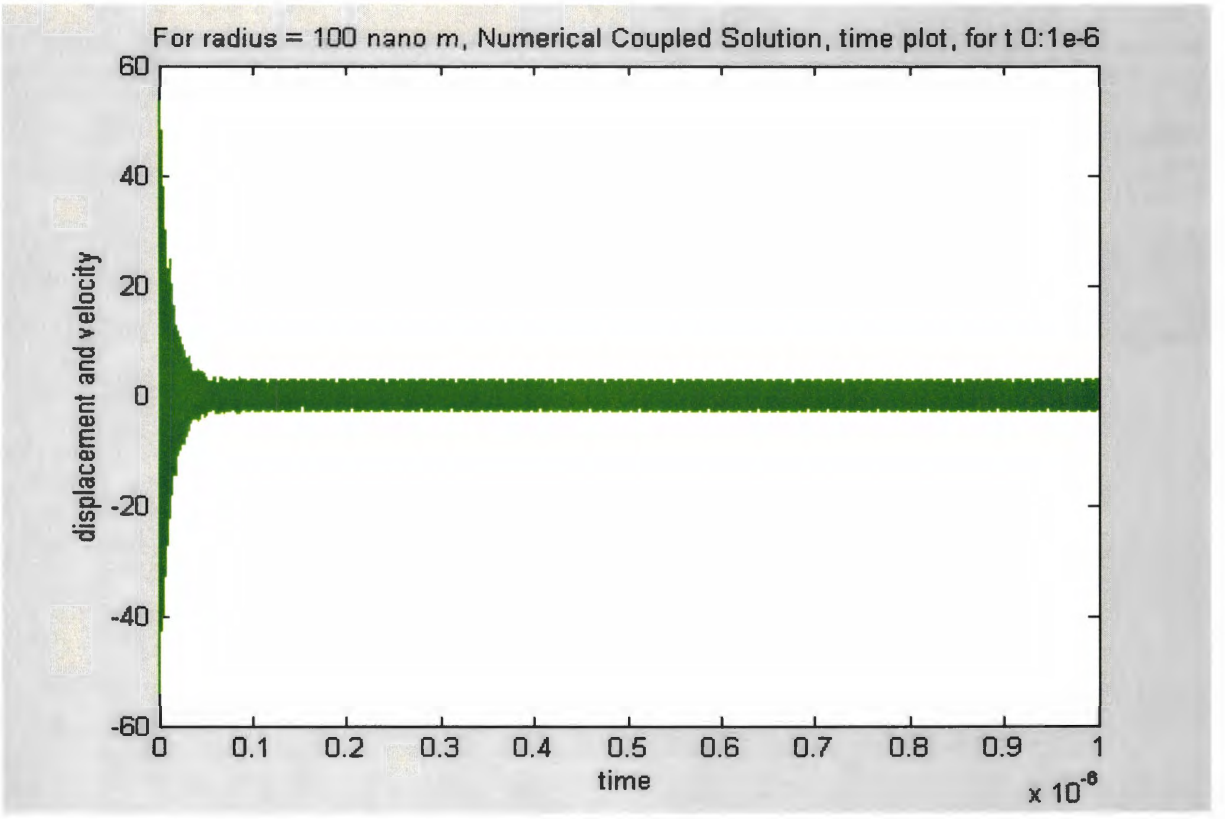

***Figure 4.6.6*: Linearized Time Plot for Particle of R = 1mm, t = 0:1e-6 seconds**

4.7 PHENOMENON OF BEAT FREQUENCY

It is seen that there is this phenomenon of beat frequency occurring. Beat frequency is mainly due to the constructive or destructive interference of the waves in the time plot, due to the sinusoidal excitation function. The underlying fact that needs to be unearthed is whether this beat frequency is a function of the system or a characteristic of the input parameters. By input parameters, we mean the excitation frequency (mainly) and also the amplitude of vibrations. The idea here is to add the beat frequency onto the already existing forcing function, so that the combined effect of these two can bring about separation, when the stable equilibrium points are considered.

The system, before application of the beat frequency looks as shown below:

$$mz'' + k_1(z+z_0) + cz' = \frac{AR}{6(z+z_0)^2} + \frac{4\pi\gamma R\cos\theta}{(1+z/z_0)} + \bar{f}\sin(\omega t);\ \omega = k\omega_n;\ k \le 1$$
$$mx'' + k_2(x+x_0) + cx' = \frac{\mu AR}{6(z+z_0)^2} + \frac{4\pi\gamma\mu R\cos\theta}{(1+z/z_0)} + \bar{f}\cos(\omega t);\ \omega = k\omega_n;\ k \le 1 \quad \textit{(4.7.1)}$$

The system after combining the beat frequency ω_0 along with the excitation frequency is as shown:

$$mz'' + k_1(z+z_0) + cz' = \frac{AR}{6(z+z_0)^2} + \frac{4\pi\gamma R\cos\theta}{(1+z/z_0)} + \bar{f}\sin(\omega t) + \bar{f}\sin(\omega_0 t);$$
$$mx'' + k_2(x+x_0) + cx' = \frac{\mu AR}{6(z+z_0)^2} + \frac{4\pi\gamma\mu R\cos\theta}{(1+z/z_0)} + \bar{f}\cos(\omega t) + \bar{f}\cos(\omega_0 t); \quad \textit{(4.7.2)}$$

The plan of action then, is to consider a particular system (fixed radius, mass, stiffness and damping) and vary the input parameters such as excitation frequency and amplitude of vibrations. Of particular significance is the variation in the excitation frequency as a function of the natural frequency of the system. Once this is done, the time plots are scrutinized and the beat frequency calculated. Thus, for a particular system, the variation of the beat frequency with respect to the input parameters is studied. The next step would be to ape this for varying system parameters. Thus we first fix the system parameters and study the influence of input parameters on the beat frequency. The next step is to vary the system parameters themselves and study the change in the beat frequency for different systems. The following graphs *(Figures 4.7.1 to 4.7.4)* will make the phenomenon of beat frequency more clear. The graphs are plots of velocity versus time wherein velocity is measured in meters per second (m/s) and time is measured in seconds (s). They exhibit the beating frequency pattern, as seen explicitly in the figure.

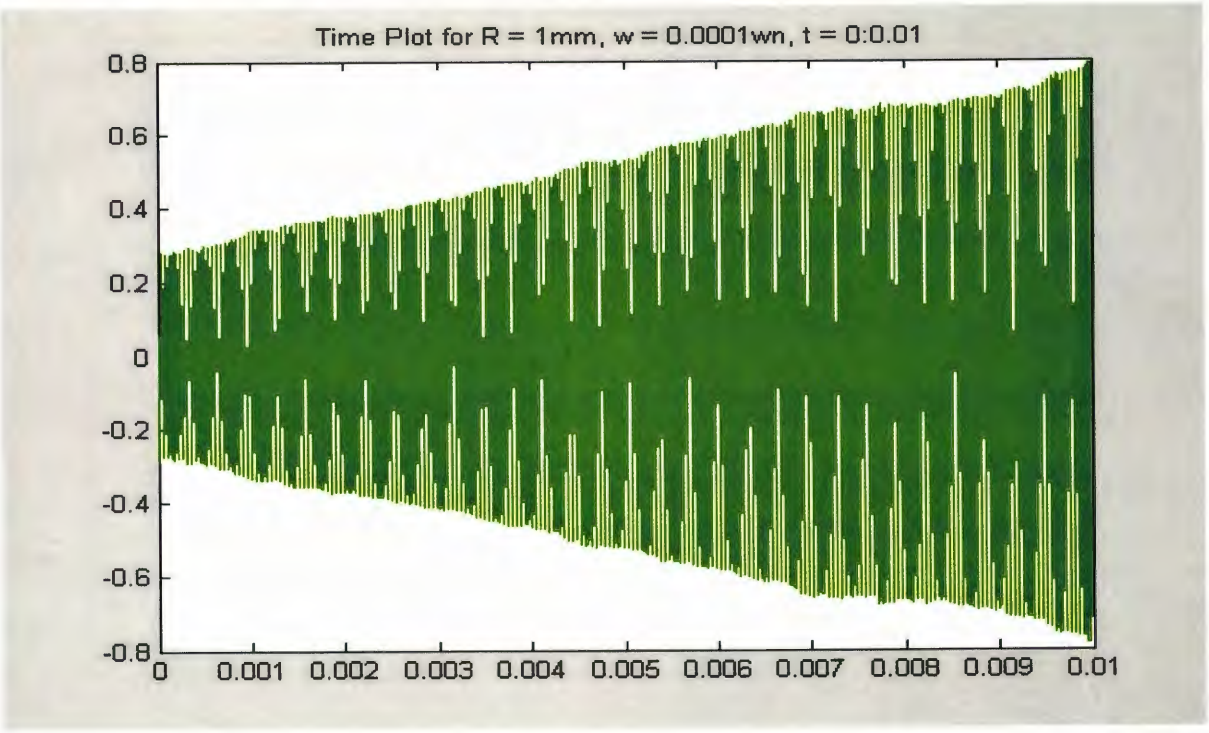

***Figure 4.7.1*: Time plot for R = 1mm, w = 0.0001 w_n, t = 0:0.01**

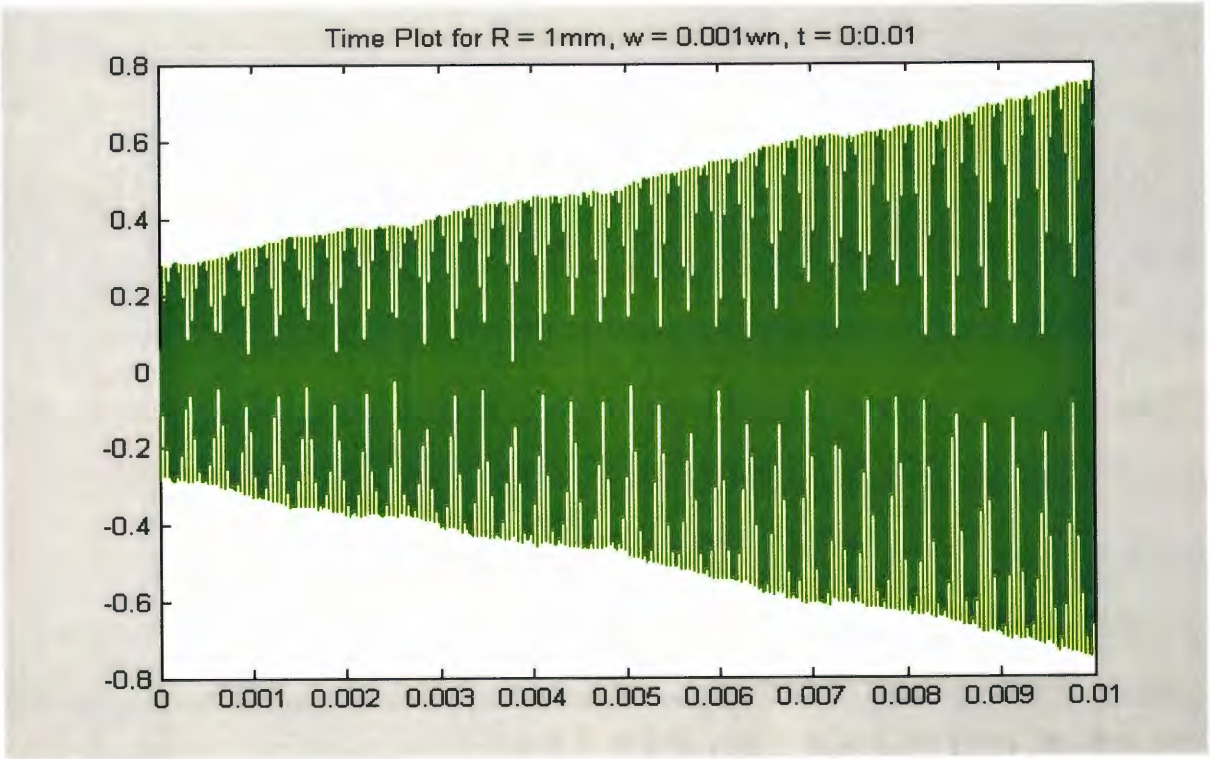

***Figure 4.7.2*: Time plot for R = 1mm, w = 0.001 w_n, t = 0:0.01**

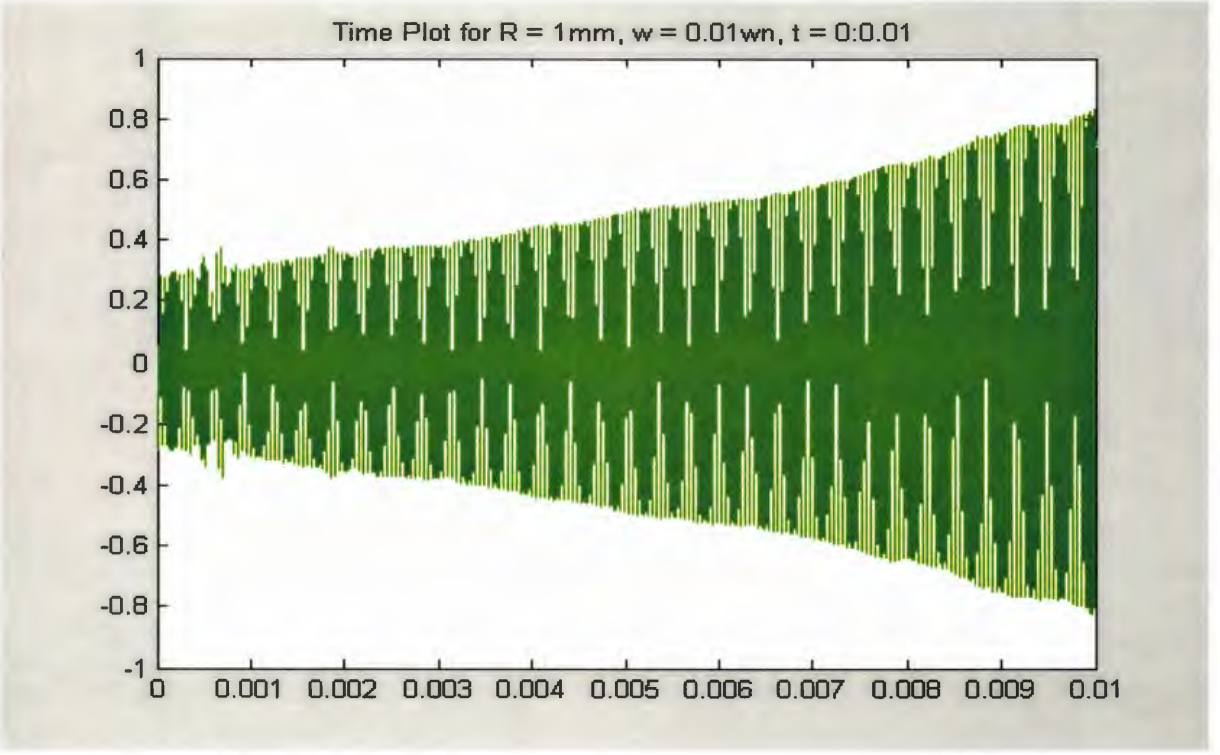

Figure 4.7.3: **Time plot for R = 1mm, w = 0.01 w_n, t = 0:0.01**

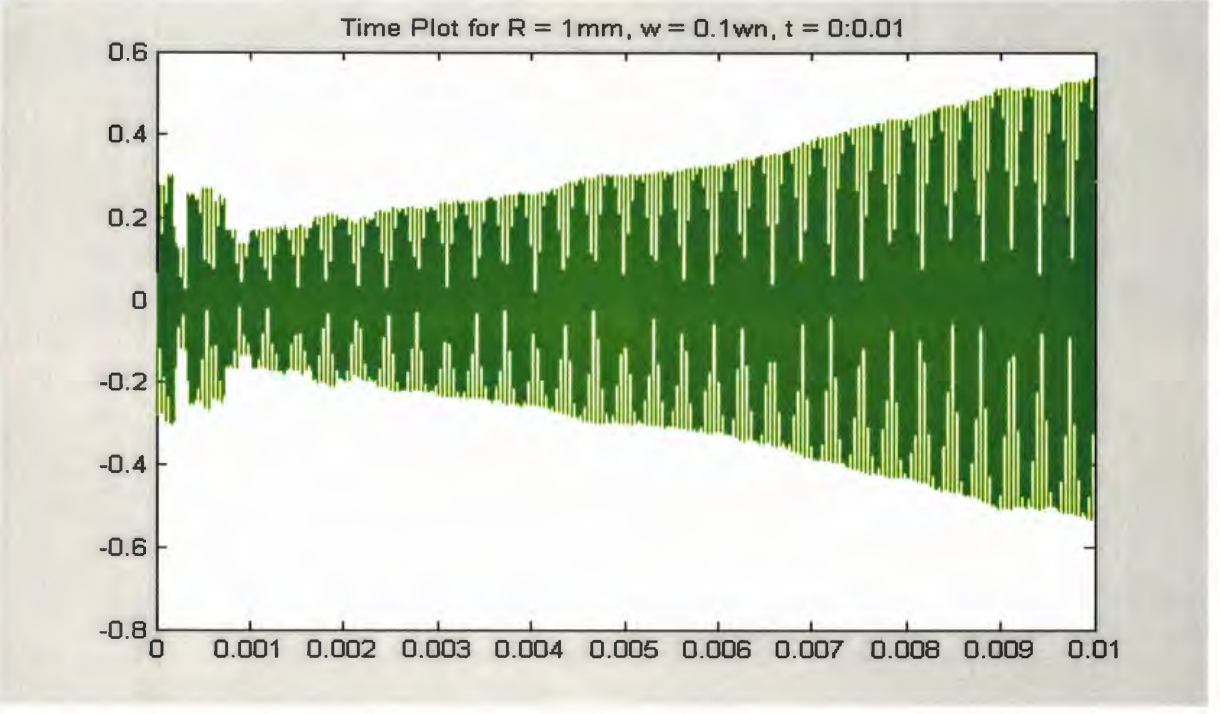

Figure 4.7.4: **Time plot for R = 1mm, w = 0.1 w_n, t = 0:0.01**

***Table 4.7.1*: Beat Frequency Calculations for Several Particle Sizes**

	0.1*ω	0.01*ω	0.001*ω	0.0001*ω
R = 1mm	BF1 = 1.5152e3 BF2 = 1.4925e3	BF1 = 1.4286e3 BF2 = 1.5152e3	BF1 = 1.4286e3 BF2 = 1.5152e3	BF1 = 1.4286e3 BF2 = 1.5152e3
R = 10 μm	BF1 = 5.00e5 BF2 = 5.00e5	BF1 = 5.00e5 BF2 = 5.00e5	BF1 = 5.00e5 BF2 = 5.00e5	BF1 = 5.00e5 BF2 = 5.00e5
R = 100 μm	BF1 = 4.00e4 BF2 = 4.00e4	BF1 = 4.00e4 BF2 = 4.00e4	BF1 = 4.00e4 BF2 = 4.00e4	BF1 = 4.00e4 BF2 = 4.00e4

Table 4.7.1 summarizes the occurrence of beat frequency. The aim now is to excite the system at a combination of the beating and excitation frequency. Also, an increase in amplitude is aimed at, so that the particle can be separated, when working with the stable equilibrium point itself. The obvious conclusion in working with the unstable equilibrium point is that separation will certainly occur otherwise. The time frames for calculating the beat frequency is given below. When we take the inverse of the time differences, we get the beat frequency.

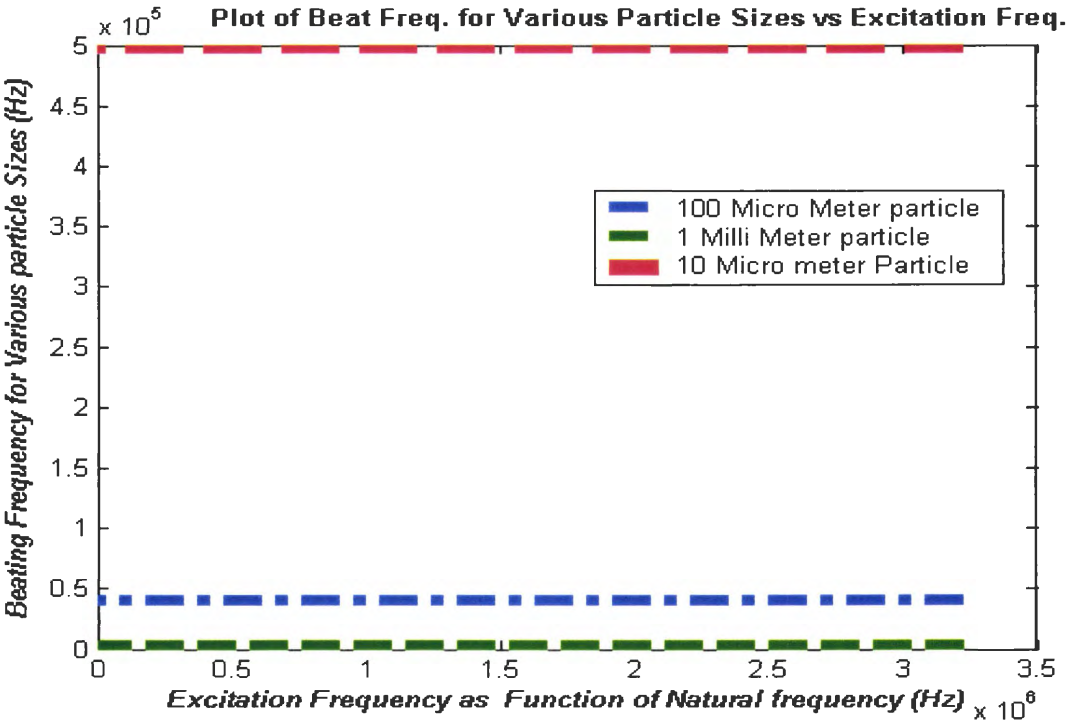

The conclusions that can be drawn from the study of beating frequency are:

1) The beat frequency is not found to change with the input parameters (more specifically with the excitation frequency). For a particle of radius one milli meter, the beating frequency is found to lie in the range between 1.42e3 and 1.52e3. For particles of radius ten micro and 100 micro meters, the beating frequency is found to remain constant.
2) The beating frequency is found to change with the system parameters. As the radius and other system parameters are varied, the beating frequency is also found to vary.
3) There seems to be a strange relationship between the natural frequency and beating frequency for varying system parameters. For a particle of radius one milli meter, the ratio of natural to beating frequency is found to be 100. As we decrease the particle size and go further below, the ratio reduces to 75 for one hundred micro and 50 for a

ten micro meter sized particle. The significance of this result is a mystery as it is found not to play any role in the dynamic simulations.

Thus, a combination of the beating and excitation frequency is tried out at the stable equilibrium point to see if there is any change wrought in the adhesion problem. The following graphs *(Figures 4.7.5 to 4.7.8)* plot the phase portrait and time plots for various particle sizes wherein velocity, displacement and time are in meters per second, meters and seconds, respectively.

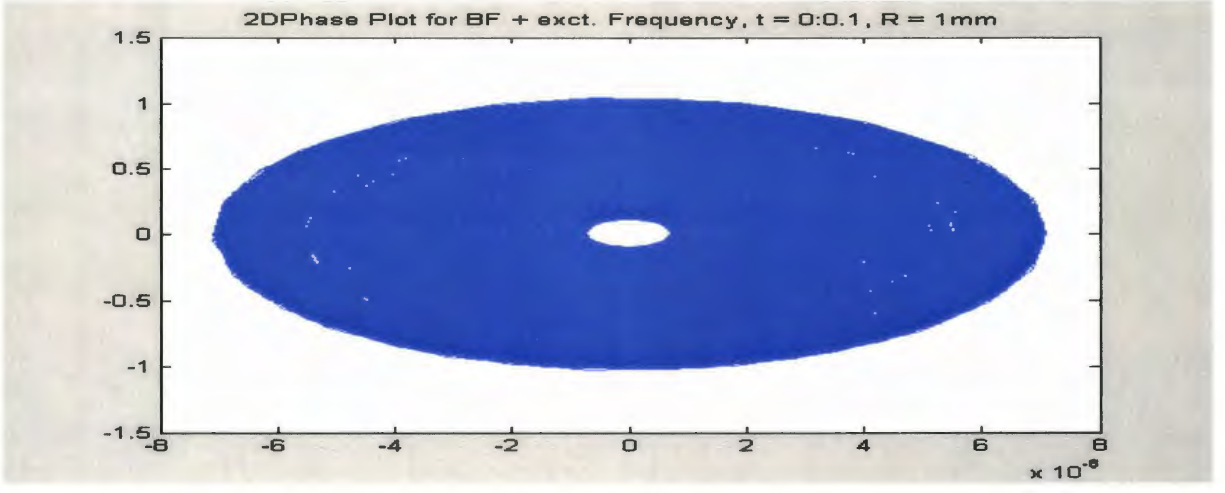

***Figure 4.7.5*: Phase plot for R = 1mm, Beat Frq. + Excit. Frq. t = 0:0.1 s**

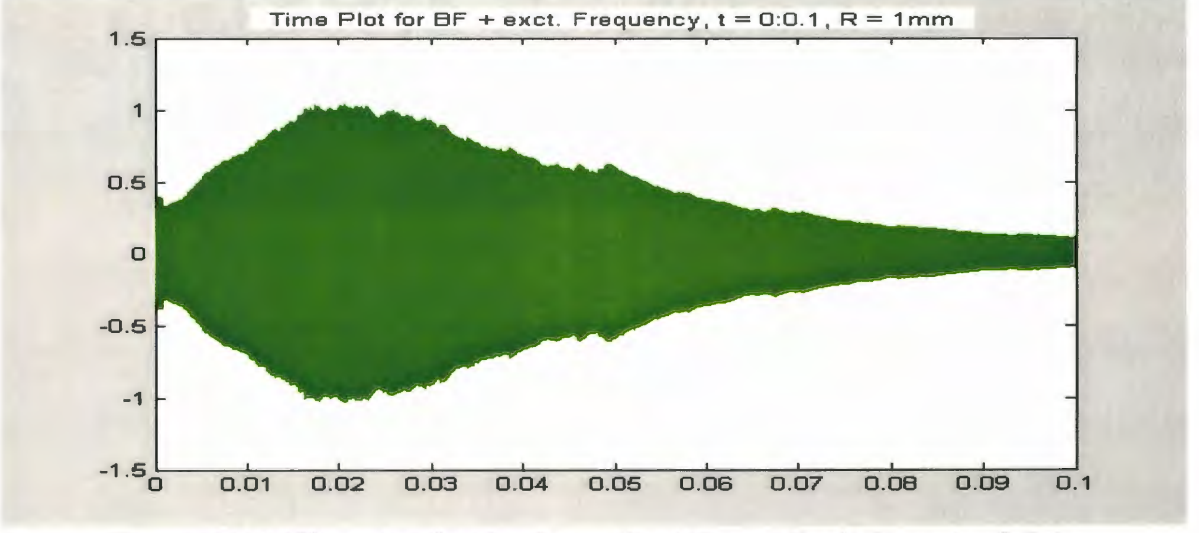

***Figure 4.7.6*: Time plot for R = 1mm, Beat Frq. + Excit. Frq. t = 0:0.1 s**

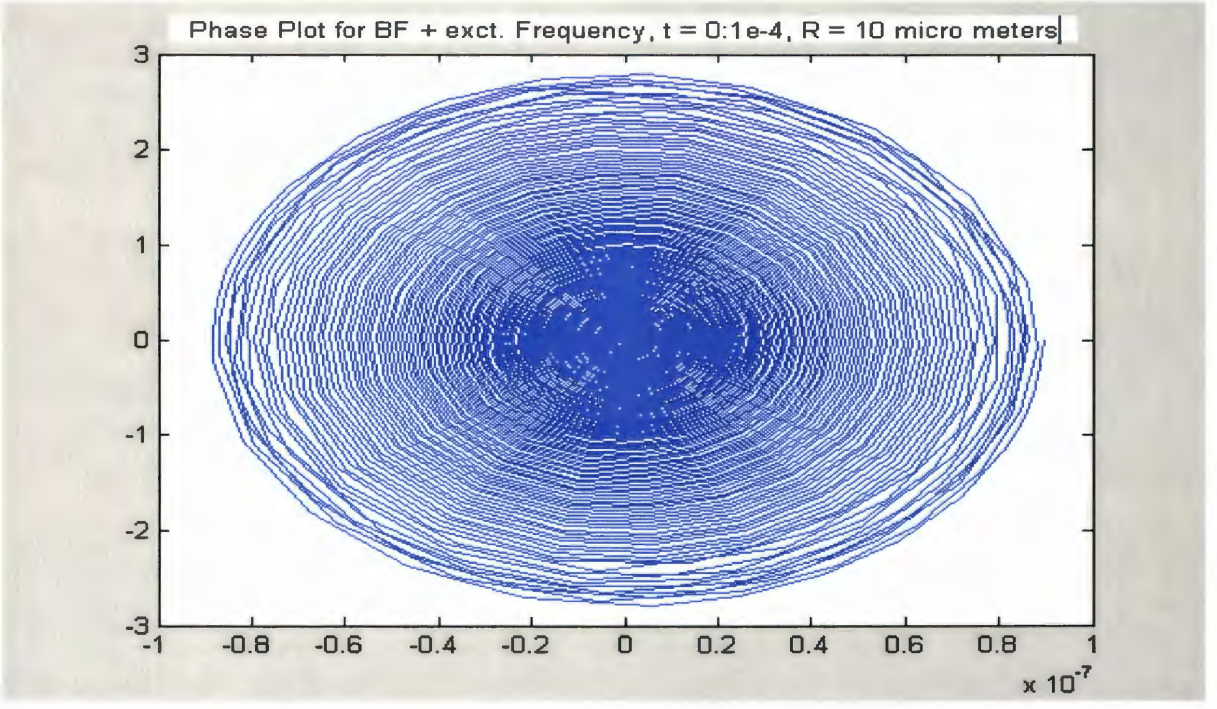

***Figure 4.7.7*: Phase plot for R = 10 μm, Beat Frq. + Excit. Frq. t = 0:1e-4 s**

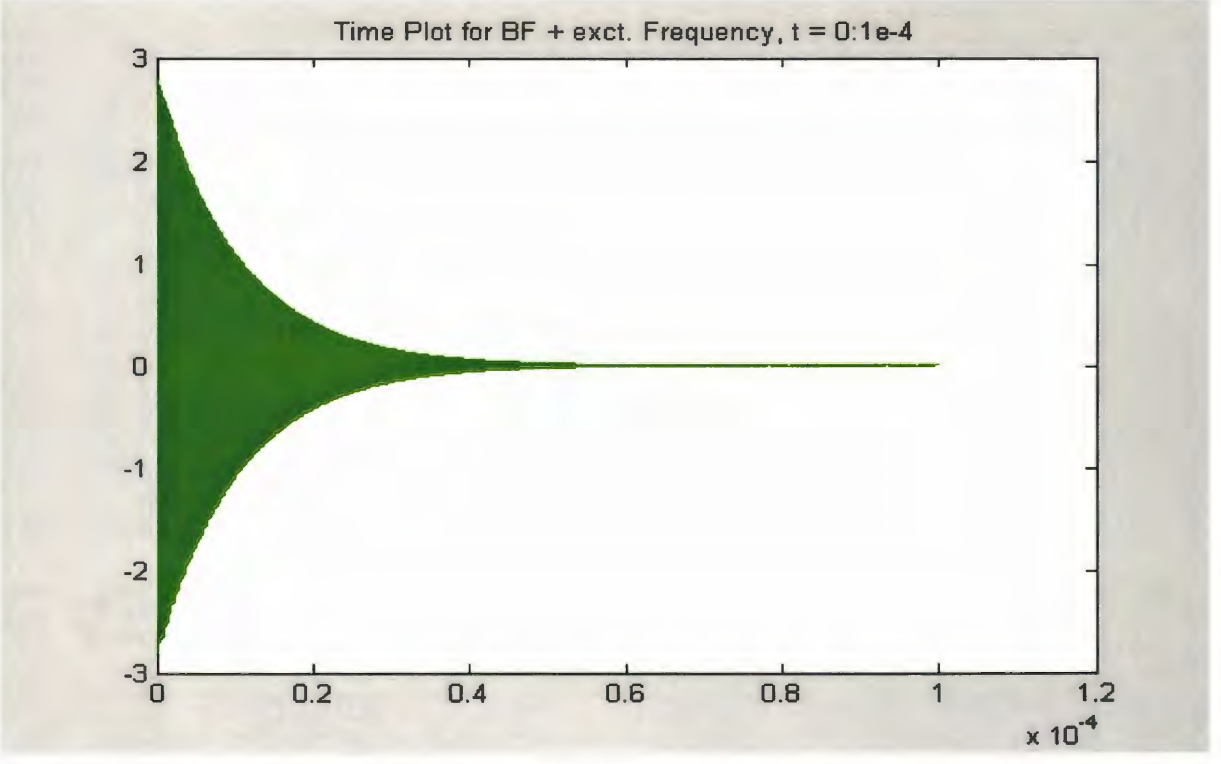

***Figure 4.7.8*: Time plot for R = 10 μm, Beat Frq. + Excit. Frq. t = 0:1e-4 s**

What we see above is, when an early time period is considered, the there is a divergence pattern obtained in the time plot. This can be clearly seen in the time plot for a particle of radius 1 milli meter, between t = 0.01 and 0.03. The same pattern is also seen in the next time plot, for a particle of radius 10 micro meters, but only that the time period is so small that it cannot be discerned in the plot shown above. What this means is that, when the system is excited at a combination of the beating and excitation frequency, separation is induced in an early time period. The large amplitude of oscillation (in the phase plots), says that this is a reasonable argument. Thus separation is enhanced by the addition of beating frequency to the system, for small time scales.

The next step would be to see the effect of increase in amplitude along with beating and excitation frequency. The amplitude of excitation was one micro Newton for all the particle sizes considered. Here, the amplitude is upped to about 0.1 milli Newton, a rather drastic increase. The following plots ***(Figures 4.7.9 and 4.7.10)*** show the effect of increase in amplitude on the dynamic system:

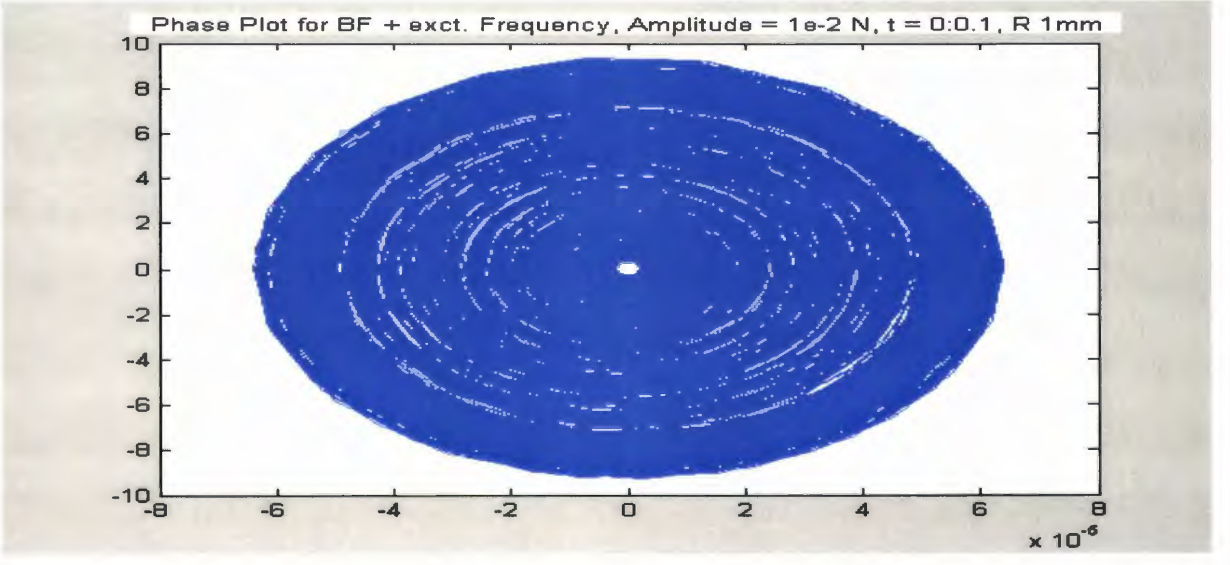

***Figure 4.7.9*: Phase plot for R = 1mm, Beat Frq. + Excit. Frq. + Amplitude Increase**

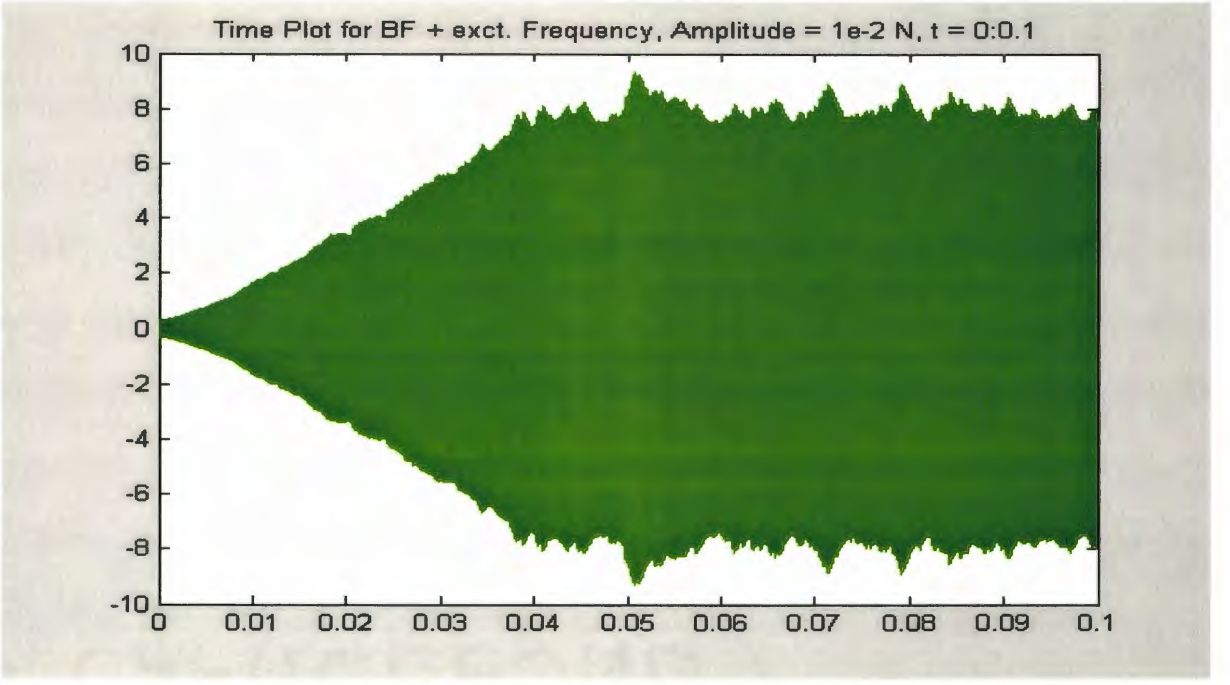

***Figure 4.7.10*: Time plot for R = 1mm, Beat Frq. + Excit. Frq. + Amplitude Increase**

Thus, we see that an increase in amplitude of the excitation function, along with a combination of the beating frequency, gives separation, which is rather obvious from the plots above. But this also means that there is a danger of the system getting damaged due to the large oscillations. These oscillations are in the lateral direction and separation here indicates the break in the fluid bond between the particle and substrate.

There are different other techniques that can be tried as future work, in the area of coupled vibrations. Velocity and displacement coupling are two of them. By velocity and displacement coupling, we mean equations that are as shown below. As usual, the longitudinal system is solved at first. The solution obtained therein, z (t) is the plugged into the lateral system as an input term, either in the form of a displacement or in the form of velocity, scaled by suitable constants and the lateral system is hence forced. This can lead to

more complex dynamics, but it looks promising, in that the coupling is capable of inducing separation between the particle and substrate.

$$mz'' + k_1(z + z_0) + cz' = \frac{AR}{6(z + z_0)^2} + \frac{4\pi\gamma R\cos\theta}{(1 + z/z_0)} + \bar{f}\sin(\omega t);\ \omega = k\omega_n;\ k \le 1$$

Displacement Coupling involves the following equation -:

$$mx'' + k_2(x + x_0) + cx' = \frac{\mu AR}{6(z + z_0)^2} + \frac{4\pi\gamma\mu R\cos\theta}{(1 + z/z_0)} + Xz(t);\ \text{X is a scaled constant}\ ,\ \textbf{\textit{(4.7.3)}}$$

Velocity Coupling involves the following changes in the equation -:

$$mx'' + k_2(x + x_0) + cx' = \frac{\mu AR}{6(z + z_0)^2} + \frac{4\pi\gamma\mu R\cos\theta}{(1 + z/z_0)} + Az'(t);\ \text{A is a scaled constant}$$

Thus, the aim of this chapter was to put forth new ideas on coupled vibrations. The uniqueness of this idea is that, different directions can be coupled and separation can be thought of, using the same system dynamics. In the beginning of the chapter, a system characteristic matrix was formed, wherein the eigen values give the stability criterion. The stability criterion affects the equilibrium points as well as the lateral stiffness. So, the point of focus was to separate the particle, while working around the stable equilibrium point. Simulations of the coupled system threw light on interesting phenomena such as limit cycles and beating frequency. The beat frequency was studied extensively and conclusions were drawn regarding its nature (its variation with the system and not input parameters). The dynamic system was excited at a combination of the beating and excitation frequency and separation was induced at early time periods. Also, the amplitude of excitation was increased and this gives separation too, which is rather an intuitive idea. All in all, coupled vibrations come across, as a moderately successful method for particle removal.

CHAPTER 5

DISCUSSION AND CONCLUSIONS

5.1 INTRODUCTION

This chapter is divided into three parts. Part one discusses the longitudinal vibrations model and concludes by stating the effectiveness of particle removal utilizing longitudinal vibrations. Part two explains the lateral removal model. This section carries out detailed discussions about and comparisons with, existing theories and finally concludes by stating obvious advantages over the longitudinal removal method. The third part involves particle removal by coupled vibrations. The coupled model is discussed in detail and the section concludes by comparing the efficacy of the various theories proposed in this thesis.

5.2 LONGITUDUNAL VIBRATIONS MODEL

Longitudinal vibrations were dealt with in Chapter 2. The obvious aim of this model was to induce separation between the particle and surface. The forces of adhesion were evaluated at the beginning and the major contributors to adhesion force were found to be the Van Der Waal and capillary Forces. A stability analysis was carried out by characterizing the eigenvalues and also from the point of view of Lyapunov's direct method for non – autonomous systems. After the stability analysis, numerical and analytical simulations of the dynamic system were carried out, first by linearizing the system and also by taking into

account the complete non – linear system. The following points illustrate the importance of the longitudinal model, along with its limitations.

1. It is found that there are three equilibrium points or rest points for a particle of given radius. Out of these three points, two of them will be stable and the third is assumed to be unstable, as its value is found to be greater than the thickness of the fluid film. For example, for a particle of radius 1 micro meter, made of alumina, resting on a silica surface, the initial separation between the particle and surface which is nothing but the thickness of the fluid film due to capillary condensation is found to be 1.5 nano meters. If the system dynamics are formulated and the equilibrium points evaluated, we get the following values -:

   $x_1(1) = -1.711e-9\ m$

   $x_1(2) = -1.504e-9\ m$, ***(5.2.1)***

   $x_1(3) = 2.15e-10\ m$

   Out of these, the second and third values are almost equal and smaller than the fluid film thickness. Typically the particle will be oscillating between its mean or equilibrium position. If the equilibrium point is below the fluid film thickness, then the particle might bang into the substrate and can get damaged. Hence this is thought of as an unstable equilibrium point. The corresponding stability analyses show this in a different way.

2. On carrying out the eigenvalue analysis, it is found that, irrespective of the equilibrium point under consideration, as the Jacobian is evaluated and the eigenvalues calculated, the system shows a stable focus or stable spiral behavior. This is because the eigenvalues have the form $\lambda_{1,2} = -\mu \pm i\eta$, which only implies stability,

as the real part of the eigen value is negative in connotation. The eigen value analysis is carried out without considering the forcing function. Hence we are dealing with autonomous systems. It is not clear, if the forcing function causes any distinction, when included. But through an intuitive idea, the eigen value analysis seems inadequate. The reason for this is that, large amplitude of vibration or large excitation frequency would certainly jeopardize stability and cause the particle to come unstuck, from the substrate. This limitation of the eigen value analysis is addressed in Lyapunov's direct method which takes the forcing function into consideration during the analysis.

3. Lyapunov's stability criterion comes as a strong counter argument to answer the shortcomings shown by the eigen value analysis. In this analysis, the system is considered in its non – autonomous form; which means dependence on the forcing function is taken into account. A scalar potential function depending on the energy of the dynamic system is chosen as a Lyapunov function candidate and the analysis is centered on it. The conclusion that can be drawn from this is that, when the system is forced by a forcing function with moderate amplitude, comparable to the static force on the system and excitation frequency, which is a fraction of the natural frequency of the system, the system shows a stable behavior, which is expected and so, true. But when the idea of negative damping comes into question, the system shows an unstable behavior. This is because a combination of positive and negative damping induces the system trajectory to show limit cycle behavior. If the limit cycle is unstable, such the nearby solution curves, starting at the initial condition, swerve away from the limit cycle then the system is deemed unstable. Hence, the particle can

be separated from the substrate by alternately pumping energy in the form of negative damping and dissipating energy in the form of positive damping into the system.

4. Thus, particle separation is possible in the longitudinal model if there are means to pump in energy into the system and create the scenario of negative damping. Also, a sufficiently large amplitude and excitation frequency will be capable of bringing about separation.
5. The previous conclusions come as limitations to this model. Negative damping is difficult to be realized practically. Large amplitude of vibration would potentially damage the system and may not be an effective way of inducing separation. Also, stability analyses are only necessary criteria and not sufficient in any manner. For any scalar potential function chosen as a candidate for Lyapunov's analysis and showing stable behavior, there can be another scalar potential function which can model unstable behavior. This results in the conclusion, about negative damping causing separation.
6. The longitudinal vibrations model proves to be a robust method, which can bring about particle separation, after a sufficiently significant fight against the adhesion forces. This may not be the most efficient method, when compared to the lateral or coupled vibrations, but nevertheless is very simple and intuitive. Experimental verifications are necessary to realize such a theoretical model in practice.

5.3 LATERAL REMOVAL MODEL

The lateral removal model proposes a simple and effective way of separating particles from the substrate, by means of moment balance. First proposed by Busnaina et. al. (Busnaina, 2003), the idea of this model is to remove particles either by rolling or sliding them away from the substrate. It has been explained in Chapter three that rolling consumes lesser kinetic energy than sliding and hence, rolling is a more efficient method of separating particles from the substrate. There is also a third method, called lifting or pull – off. This is not very popular, as it might damage the particle, when being lifted off, by a tweezer. For particle removal by rolling, the rolling ratio is given as the ratio of the removal moment to the adhesion resisting moment. Once the rolling ratio becomes greater then or equal to one, then the particle will be rolled off, the substrate. For removal by sliding, the sliding ratio is given as the ratio of the removal force to the adhesion force. Once this becomes greater than one, then the particle is removed by sliding. There have also been two other techniques proposed in this thesis, which looks at particle removal in the lateral direction by considering the stiffness of the fluid layer and also the shear stress induced by the friction forces. The following are the conclusions that can be derived from the model.

1. Friction is found to play an important role in the lateral particle removal model. In case of the longitudinal model, friction is never considered in the scheme of things. But from the expression for the removal moment that is given in Chapter 3 it is found that friction actually aids in particle removal. This is one of the advantages of the current model over the one proposed by Busnaina (Busnaina, 2003). Also, the pull – off forces induced due to repulsive elastic contact between the particle and substrate

and modeled using the JKR theory, is considered. The effects of friction and pull – off forces are not considered by Busnaina in his post – CMP particle removal model.

2. A comparison of the lateral removal method versus the longitudinal method as explained in Chapter three reveals that the lateral method utilizes a lower removal force than the longitudinal model. This is because, the comparison of the removal moment for the lateral and longitudinal models show that the denominator for the lateral removal model, which is the difference between particle radius and indentation depth (ref. Chap.3) is greater than the denominator for the longitudinal case, which is the contact radius. Thus the efficiency of the lateral removal method is higher than that for the longitudinal method. A lower removal force only means that the damage to the system would be reduced substantially. Thus, this is more advantageous, when we consider the static conditions for the system. The dynamic motions along the lateral direction are explained in the coupled vibrations model (Chap. 4).
3. The removal method, in which the stiffness of the fluid layer is calculated and multiplied with the indentation depth and contact radius to gain the moment, is something which would need experimental facts to be proven. Since the fluid thickness between the particle and substrate is a very small value, the stiffness would be very high, posing problems, as the assumptions would be improbable, in such a case.
4. The third removal method proposed, in which the shear force plays an important role is also good method. Shear stress can be easily evaluated between the particle and substrate and the contact area can be found out, utilizing information about the

contact radius. Hence, this can become a powerful method for separation, if its worthiness is proved experimentally.

5.4 COUPLED VIBRATIONS MODEL

Chapter 4 deals with the coupled vibrations model. The idea here is to couple vibrations along the lateral and longitudinal directions. While, Chapters 2 and 3 looked at longitudinal and lateral vibrations separately, Chapter 4 combines them, so as to increase the effectiveness. The initial step was to formulate a system matrix or a characteristic matrix, to come up with a stability criterion. The stability criterion dealing with the equilibrium point as well as the lateral stiffness is given below -:

1. $\left\langle z_1 < -\left(\frac{2\Gamma_1}{\Gamma_2} + z_0 \right) \right\rangle$: The equilibrium point condition, ***(5.4.1)***

2. $\left(\omega^2{}_{n2} < \omega^2 + \frac{f}{x_0} \right)$: Condition pertaining to the lateral stiffness, ***(5.4.2)***

The idea of formulating a characteristic matrix was taken from a paper written by Marui et. al. (Marui et. al., 1988), who applied the idea of extracting a stability criterion by utilizing the steady state solutions in a spindle – work piece, under chatter vibrations. Thus the system matrix was first formed by substituting the steady state solutions into the dynamic system for particle separation. Then the eigen values were found and after applying the condition that the eigen values must be lesser than zero for stability, the stability conditions are obtained. The longitudinal system is then linearized and solved analytically. The solution obtained is plugged into the lateral system, and numerical simulations are carried out to ascertain the stability factors. The following refer to the important facets of the coupled model -:

1. Among the values of the equilibrium points obtained, some of them are found to be unstable and the rest stable, based on the stability criterion obtained. Hence, if the system were forced around the unstable equilibrium point, then it would lead to particle separation from the substrate. This shows the effectiveness of the stability analysis, in deciding how unstable a system can be. Lateral stiffness also plays an important role in defining the stability. If the value of the lateral stiffness is more than that prescribed in the criterion, then the system goes unstable.
2. The system being forced around the stable equilibrium points, show stable behavior. The time plot shows a convergence (ref. Chap. 4), which means that after lateral excitations, the particle will come to rest at the center or equilibrium position. This is true of any particle size, when forced at a stable equilibrium point and with a lateral stiffness well below the unstable region.
3. During the numerical simulations, a beating frequency pattern is observed. It was first not clear if the beating frequency was a function of the system parameters such as radius, mass, damping or stiffness, or if it were a function of the input parameters such as excitation frequency and amplitude of vibrations. So, there was a need for closer observation. A particular system was chosen, by fixing the system parameters, and the input parameters, (more importantly the excitation frequency was varied as a function of the natural frequency of the system) were varied. This was repeated for several systems. The results show that the beating frequency remains constant for a given system. But as the system parameters are changed, the beating frequency also changes, with an increase in beat frequency observed, as the size of the particle gets reduced. Also, there was a fixed ration between the beating frequency and natural

frequency, for a given system, and this ratio was found to decrease as the particle size decreased. The significance of this ratio is not known, and is left as future work.

4. The next step was to force the system at a combination of the beating and excitation frequency. Suitable changes were observed in the behavior of the system. As the frequency was increased along with the beating frequency, separation became a possibility. Also, the amplitude of vibrations was increased. This certainly brought about a change in the system pattern. The time plot showed a divergence and the phase plot showed an unstable limit cycle, which only means that the particle must have separated from the substrate, laterally.
5. Thus, separation is possible, by arriving at a judicious combination of the beating and excitation frequency. Moreover, an increase in the amplitude also brings about separation. Care must be taken as to avoid damage to the system, when the frequency and amplitude are increased beyond the safe limits for operating on micro/nano devices. Coupled vibrations come off, as a suitable method for particle removal. There are still a lot of variations, which need to be ironed out. A suitable experimental design to verify the theoretical model would come a long way in proving the effectiveness of this mode of particle removal.

5.5 FUTURE WORK

Several types of particle removal methods have been postulated in the preceding chapters. These are all theoretical models, with numerical simulations to prove their effectiveness. The following can be done to improve the effectiveness of the proposed models, as future work.

1. Experiments must be designed to prove the longitudinal vibration model. This will be a tough assignment as the system cannot be captured in all its non – linearity, during experimentation.
2. A study of the bifurcations occurring in the Phase Plots of the longitudinal and coupled vibrations case, when the complete non – linear system is simulated, could lead to interesting conclusions on the stability of the system.
3. A simple experiment to ascertain particle removal from substrate would be to assemble a vibrating stage, which can move along the lateral and longitudinal directions. By carrying out vibrations in a particular direction alone, particle separation can be observed, by using CCD cameras to capture the motion. Or else, the entire stage must be fitted onto the viewing area of an optical microscope. The stage must be subject to vibrations so, as to observe the motion of the particles. It would be very difficult to capture the exact displacement and velocity of the particles, but an approximation within range of operations would be good enough. The entire idea can be summarized as follows -: Basically, micro/nano sized particles (spherical silica/alumina particles of radius between 1 milli meter and 100 nano meters) are to be placed on a vibrating tray or plate and mounted beneath an optical microscope. The tray/plate must be vibrated over a range of frequencies, lesser or at the most equal to the natural frequency of the system under consideration. The experiment must be carried out at a relatively high humidity environment, so as to ascertain the participation of the Capillary forces, due to fluid film condensation between the particle and substrate. The tray/plate must be vibrated along the lateral and longitudinal directions (not necessarily simultaneous). By carrying out this

experiment, and by capturing information about the displacement change from initial values, the simulation results can be verified. This comes as a good experimental means of verifying the proposed theoretical model. Coupled vibrations can also be carried out through the same experimental set up.

4. In the coupled vibrations scheme, the significance of the relationship between the beating and natural frequency is not known. Further investigation in this area would lead to interesting results. Also, study of bifurcations during the complete non – linear diagnosis of the several systems along the lateral and longitudinal directions can lead to interesting results bordering on chaos and fractal theories.

REFERENCES CITED

Ashhab, M., Salapaka, M., Dahleh, M., Mezic, I. (1999), "Melnikov Based Dynamical analysis of Microcantilevers in Scanning Probe Microscopy", *Nonlinear Dynamics*, **20**: 197 – 200.

Bowling, Allen. R. (1988), "A Theoretical Review of Particle Adhesion", Chapter in "*Particles on Surfaces*", Mittal, K.L., ed., Plenum Press, New York.

Burnham, N.A. and Kulik, A.J. (1997), "Surface forces and adhesion", Chapter in "*Handbook of Micro/Nanotribology*", Bushan, B., ed., CRC Press, Boca Raton, FL.

Busnaina, A.A., Hong Lin, Naim Moumen, Jiang-wei Feng and Jack Taylor (2002), "Particle Adhesion and Removal Mechanisms in Post CMP Cleaning Processes", *IEEE Transactions on Semiconductor Manufacturing*, **Vol.15**, No.4, November 2002.

Horacio Marquez, (2003), *"Nonlinear Control Systems – Analysis and Design"*, Wiley Interscience, Boston, MA.

Hutter, J.L. and Bechhoefer, J. (1993), "Calibration of atomic force microscope tips", *Review of scientific instruments* **64** (7), 1993, 1868 – 1873.

Israleachvili, J. N. (1985), "*Intermolecular and Surface Forces*", Academic Press, Boston, MA.

Junno, T., Deppert, K., Montelius, L., Samuelson, L (1995), "Controlled Manipulation of Nanoparticles with an AFM", *Applied Physics Letters*, **66** (26), 26th June, 1995.

Marui, E., Kato. S., Hashimoto, M., Yamada, T. (1988), "The Mechanism of Chatter Vibration in a Spindle – Work piece System – Parts 1, 2 and 3", *Transactions of the ASME*, **236**/Vol. 110, August 1988.

Rand, R.H. (2003), *"Lecture Notes on Nonlinear Vibrations"*, Cornell University, Ithaca, NY.